

Recent developments in symmetry-adapted perturbation theory

Konrad Patkowski 

Department of Chemistry and Biochemistry, Auburn University, Auburn, Alabama

Correspondence

Konrad Patkowski, Department of Chemistry and Biochemistry, Auburn University, Auburn, Alabama 36849.
 Email: kjp0013@auburn.edu

Funding information

U.S. National Science Foundation CAREER, Grant/Award Number: CHE-1351978

Abstract

Symmetry-adapted perturbation theory (SAPT) is a well-established method to compute accurate intermolecular interaction energies in terms of physical effects such as electrostatics, induction (polarization), dispersion, and exchange. With many theory levels and variants, and several computer implementations available, closed-shell SAPT has been applied to produce numerous intermolecular potential energy surfaces for complexes of experimental interest, and to elucidate the interactions in various complexes relevant to catalysis, organic synthesis, and biochemistry. In contrast, the development of SAPT for general open-shell complexes is still a work in progress. In the last decade, new developments from several research groups, including the author's, have greatly enhanced the capabilities of SAPT. The new and emerging approaches are designed to make SAPT more *widely applicable* (including interactions involving multireference systems, complexes in arbitrary spin states, and intramolecular noncovalent interactions), more *accurate* (enhanced description of intramolecular correlation, a better account of exchange effects, relativistic SAPT, and explicitly correlated SAPT), and more *efficient* (enhanced density-fitted implementations, linear-scaling variants, empirical dispersion, and an implementation on graphics processing units). The new developments open up avenues for SAPT applications to an unprecedented variety of weakly interacting complexes.

This article is categorized under:

Electronic Structure Theory > Ab Initio Electronic Structure Methods

Electronic Structure Theory > Density Functional Theory

Molecular and Statistical Mechanics > Molecular Interactions

KEY WORDS

dispersion, electrostatics, induction, noncovalent interactions, symmetry-adapted perturbation theory

1 | INTRODUCTION

Noncovalent interactions exist between any two (or more) molecules and exhibit impressive diversity in their strength and directionality. These interactions are so numerous that they do not need to be large to have a profound influence on the properties of matter. For example, two helium atoms experience a very weak attraction due to van der Waals

dispersion forces: the energy of a helium dimer at its van der Waals minimum is lower than the energy of two separated helium atoms by only 0.02 kcal/mol.¹ However, this tiny attraction is the very reason helium becomes liquid below 4 Kelvin! The strength of typical intermolecular attraction is on the order of 1 kcal/mol, but it can reach 100 kcal/mol and more for large supramolecular complexes.² Noncovalent interactions are not only ubiquitous, but they are also absolutely necessary to describe many physical, chemical, and biochemical phenomena, ranging from thermodynamics of nonideal gases to spectroscopy and scattering cross sections of interstellar complexes to the performance and selectivity (including enantioselectivity) of molecular catalysts to the secondary, tertiary, and quaternary structure of proteins, the double-helix structure of DNA, and the interaction between enzymes and their substrates (or inhibitors). Thus, theoretical and experimental investigations of noncovalent interactions are published in very large quantities, and various aspects of these interactions have been reviewed in this journal^{3–15} and elsewhere.^{16–32}

From the theoretical standpoint, the interaction energy E_{int} between two subsystems A and B is usually computed within the *supermolecular approach*³³:

$$E_{\text{int}} = E_{\text{AB}} - E_{\text{A}} - E_{\text{B}}, \quad (1)$$

where E_X is the total energy of system X computed, for a given geometry of the complex, at some particular level of electronic structure theory and basis set. For weakly interacting systems, E_{int} is several orders of magnitude smaller than E_{AB} , E_{A} , and E_{B} , and the success of the supermolecular approach hinges on a cancellation of errors between the three total energies. In order to facilitate this cancellation, the electronic structure approach used to compute E_{AB} , E_{A} , and E_{B} must be the same, correct at long range (in particular, it needs to be *size consistent* which means that E_{AB} approaches $E_{\text{A}} + E_{\text{B}}$ as the intersystem separation increases), and as accurate as possible so that the individual errors are small to start with. Thanks to a multi-decade, tireless benchmarking effort from many computational chemistry groups, we understand quite well what methods and basis sets are suitable for computing E_{int} to a desired accuracy using Equation (1). For most simple complexes, highest interaction energy accuracy can be attained using methods from the coupled-cluster (CC) family,³⁴ in particular, the CC approach with single, double, and noniterative triple excitations, CCSD(T).³⁵ The supermolecular CCSD(T) treatment in a basis set that is sufficiently converged to the complete basis set (CBS) limit has been termed the *gold standard* of interaction energy calculations. Moreover, higher-accuracy (platinum) and lower-accuracy (silver) standards have also been designated and thoroughly benchmarked, and these standards are also based on the CC methodology.^{31,36}

Besides the requirement of error cancellation, the supermolecular approach has one other significant shortcoming: all that Equation (1) provides is a single number that says nothing about the underlying nature of interaction. Thus, there is a need for an alternative approach which gives reasonably accurate total energies but also provides an *interaction energy decomposition* into physically meaningful terms. Symmetry-adapted perturbation theory (SAPT) fulfills both of these requirements. With a sufficiently high-level treatment of intramolecular electron correlation (which will be discussed in more detail in Sections 2.2–2.3), the accuracy of SAPT interaction energies comes close to the CCSD(T) gold standard, and the overall result is obtained as a sum of distinct perturbation theory corrections that have separate physical interpretations. On the fundamental level, SAPT decomposes the intermolecular interaction energy into four contributions:

Electrostatics: The Coulomb interaction between the charge densities of isolated molecules (monomers). Each charge density contains discrete nuclear charges and a continuous electron density. At large separation, electrostatics gives rise to interactions between the permanent multipole moments (charge, dipole, quadrupole, ...) of the monomers: at short range, the *charge penetration* effects resulting from the overlap of electron densities are also included.

Induction: The energetic effect of mutual polarization between the two molecules. The leading-order induction term arises due to the electric field from an isolated molecule A polarizing molecule B and vice versa, and some higher-order induction contributions will be described in Section 2.2. At long range, induction primarily contains interactions between permanent multipole moments on one molecule with the induced multipole moments on the other, with the latter depending on static polarizabilities and hyperpolarizabilities.

Dispersion: The effect of intermonomer electron correlation, usually explained in terms of correlated fluctuations of electron density on both molecules. Dispersion is an attractive effect that provides weak binding between any two systems, even nonpolar molecules and rare gas atoms. At long range, dispersion energy relates to dynamic polarizabilities of the two molecules evaluated at imaginary frequencies.

Exchange: A short-range repulsive force that is a consequence of the Pauli exclusion principle. Exchange vanishes exponentially with distance just like the overlap of two electron densities, and it provides the primary source

of short-range repulsion between molecules. Exchange also provides short-range quenching of the induction and dispersion effects. While this review concerns only SAPT, it is appropriate to mention that SAPT is not the only framework in which noncovalent (and sometimes covalent) interaction energies can be decomposed and physically interpreted.³⁷ Other popular approaches include the Kitaura-Morokuma energy decomposition analysis (EDA),^{38–40} EDA based on natural bond orbitals,⁴¹ the interacting quantum atoms framework,⁴² the effective fragment potential methods,^{43,44} the decomposition based on absolutely localized molecular orbitals,^{45–47} and the partitioning that employs the local pair natural orbital CCSD(T) approach.^{15,48} Each decomposition scheme provides useful chemical information in the form of a slightly different set of interaction energy contributions, and several schemes have been compared to SAPT term by term,^{48–51} obtaining a similar qualitative assignment of the interactions but differing in the quantitative contributions. For more information on these alternative decomposition schemes, the reader is referred to the original and review works cited above.

2 | THE SAPT FORMALISM

2.1 | Fundamentals of the SAPT theory

The perturbation expansion in SAPT proceeds in orders of the intermolecular interaction operator

$$V = \sum_{A \in A, B \in B} \frac{Z_A Z_B}{R_{AB}} - \sum_{i \in A, B \in B} \frac{Z_B}{R_{iB}} - \sum_{A \in A, j \in B} \frac{Z_A}{R_{Aj}} + \sum_{i \in A, j \in B} \frac{1}{R_{ij}}, \quad (2)$$

where the indices i, j run over electrons, and indices A, B over nuclei of the respective monomer, Z_X is the atomic number of nucleus X , and R_{XY} is the distance between the particles X and Y . Atomic units have been assumed in Equation (2) and throughout the rest of this text. The choice of the zeroth-order (noninteracting) Hamiltonian and wavefunction merits more discussion and I will revisit it in Section 2.2. Here, I will assume that the electronic Schrödinger equations for isolated (unperturbed) monomers A and B can be solved exactly, that is, that SAPT is used to compute the interaction energy between two systems described by their full configuration interaction (FCI) wavefunctions. This SAPT(FCI) variant leads to a formalism that is conceptually and mathematically clearest and I adopt it here for educational purposes. In practice, SAPT(FCI) can only be applied to interactions between few-electron systems, and all studies of high-order perturbation theory convergence for model complexes such as $\text{He}\cdots\text{He}$,^{52,53} $\text{He}\cdots\text{H}$,^{54,55} and $\text{Li}\cdots\text{H}$ ^{56–58} have indeed used the SAPT(FCI) approach.

In the SAPT(FCI) formalism, the zeroth-order Hamiltonian $H_0 = H_A + H_B$ is the sum of the Hamiltonians for the noninteracting monomers, and the zeroth-order wavefunction and energy are the product and sum, respectively, of the respective isolated monomer quantities:

$$H_A \Psi_A^{(0)} = E_A^{(0)} \Psi_A^{(0)} \quad H_B \Psi_B^{(0)} = E_B^{(0)} \Psi_B^{(0)} \quad \Psi^{(0)} = \Psi_A^{(0)} \Psi_B^{(0)} \quad E^{(0)} = E_A^{(0)} + E_B^{(0)}. \quad (3)$$

Let N_A and N_B be the number of electrons in the isolated subsystems A and B, respectively. It should be noted that Equation (3) treats electrons $1, \dots, N_A$ initially assigned to monomer A (on which H_A acts) as distinguishable from electrons $N_A + 1, \dots, N_A + N_B$ initially assigned to monomer B (on which H_B acts). Thus, the zeroth-order function $\Psi^{(0)}$, which is more precisely written (in terms of the spatial and spin coordinates of each electron) as

$$\Psi^{(0)}(1, \dots, N_A + N_B) = \Psi_A^{(0)}(1, \dots, N_A) \cdot \Psi_B^{(0)}(N_A + 1, \dots, N_A + N_B), \quad (4)$$

is antisymmetric with respect to interchanges of electrons within monomers but not between monomers. Therefore, the intermolecular Pauli exclusion principle is not enforced in $\Psi^{(0)}$, and exchange contributions to interaction energy will not be recovered until such an enforcement is performed by a suitable permutational *symmetry adaptation*. Inter-molecular perturbation theory without any symmetry adaptation, that is, the ordinary Rayleigh-Schrödinger (RS) expansion⁵⁹ with the unperturbed Hamiltonian $H_0 = H_A + H_B$ and the perturbation of Equation (2), is known as

the *polarization approximation*.⁶⁰ The polarization series diverges whenever one of the monomers has three or more electrons,^{56,61,62} however, its low-order truncations are highly useful; in particular, they provide the correct leading-order terms in the asymptotic expansion of the intermolecular interaction energy.⁶³

When one is interested in the ground state of the interacting complex, the first- and second-order energy corrections in the polarization approximation are given by standard RS perturbation theory formulas:

$$E_{\text{RS}}^{(1)} = \left\langle \Psi_A^{(0)} \Psi_B^{(0)} | V | \Psi_A^{(0)} \Psi_B^{(0)} \right\rangle, \quad (5)$$

$$E_{\text{RS}}^{(2)} = \sum_{i \neq 0} \frac{\left| \left\langle \Psi_A^{(0)} \Psi_B^{(0)} | V | \Psi_A^{(i)} \Psi_B^{(0)} \right\rangle \right|^2}{E_A^{(0)} - E_A^{(i)}} + \sum_{j \neq 0} \frac{\left| \left\langle \Psi_A^{(0)} \Psi_B^{(0)} | V | \Psi_A^{(0)} \Psi_B^{(j)} \right\rangle \right|^2}{E_B^{(0)} - E_B^{(j)}} + \sum_{i, j \neq 0} \frac{\left| \left\langle \Psi_A^{(0)} \Psi_B^{(0)} | V | \Psi_A^{(i)} \Psi_B^{(j)} \right\rangle \right|^2}{E_A^{(0)} + E_B^{(0)} - E_A^{(i)} - E_B^{(j)}}, \quad (6)$$

where $(\Psi_A^{(i)}, E_A^{(i)})$ and $(\Psi_B^{(j)}, E_B^{(j)})$, $i, j = 1, 2, \dots$, are the excited eigenfunctions and eigenvalues of the operators H_A and H_B , respectively.

Equations (5) and (6) form the basis for the physical interpretation of different energy terms in the polarization approximation. The $E_{\text{RS}}^{(1)}$ term is just the expectation value of the intermolecular interaction operator over the unperturbed product wavefunction $\Psi_A^{(0)} \Psi_B^{(0)}$. Thus, this term expresses the electrostatic interaction between the charge densities $\rho_A^{(0)}, \rho_B^{(0)}$ for the unperturbed monomers, consisting of the (positive) discrete nuclear charges and (negative) continuous electron density:

$$\rho_A^{(0)}(\mathbf{r}_1) = \sum_{A \in A} Z_A \delta(\mathbf{r}_1 - \mathbf{R}_A) - N_A \sum_{\sigma_1} \int \Psi_A^{(0)*}(1, 2, \dots, N_A) \Psi_A^{(0)}(1, 2, \dots, N_A) d\tau'_1, \quad (7)$$

where the notation $d\tau'_1$ signifies the integration over the space and spin coordinates of all electrons but the first one, and this integration is accompanied by the summation over the possible spins σ_1 of electron 1. An analogous definition holds for $\rho_B^{(0)}$. Then,

$$E_{\text{RS}}^{(1)} \equiv E_{\text{elst}}^{(1)} = \iint \rho_A^{(0)}(\mathbf{r}_1) \frac{1}{|\mathbf{r}_1 - \mathbf{r}_2|} \rho_B^{(0)}(\mathbf{r}_2) d\mathbf{r}_1 d\mathbf{r}_2, \quad (8)$$

When the densities $\rho_A^{(0)}(\mathbf{r})$ and $\rho_B^{(0)}(\mathbf{r})$ do not overlap, the electrostatic potentials that they generate can be represented by multipole expansions, and $E_{\text{elst}}^{(1)}$ becomes a sum of terms expressing the interaction between a permanent multipole moment on A and a permanent multipole moment on B.⁶⁴ For example, when A and B are electrically neutral but polar molecules (e.g., in the water dimer), the leading long-range contribution to $E_{\text{elst}}^{(1)}$ is the dipole–dipole interaction that vanishes with distance like R^{-3} . When A and B are nonpolar molecules possessing a quadrupole moment (e.g., in the carbon dioxide dimer), the leading $E_{\text{elst}}^{(1)}$ contribution is the quadrupole–quadrupole term which vanishes like R^{-5} . The electrostatic energy can be negative or positive depending on a favorable or unfavorable alignment of the multipole moments on A and B. Importantly, Equation (8) is much more general than the multipole expansion and can be used for overlapping as well as nonoverlapping monomer charge densities. In the former case, the multipole–multipole contributions to $E_{\text{elst}}^{(1)}$ are augmented by the overlap-dependent *charge penetration* terms that vanish exponentially with R . Charge penetration effects can substantially enhance the intermolecular attraction and lead to negative interaction energies despite a positive (unfavorable) multipolar contribution.⁶⁵ In fact, these effects are strong enough to be explored as a potential driving force in the design of materials with desired properties.⁶⁶

The second-order perturbation theory formula, Equation (6), contains a summation over all excited states of the unperturbed system, that is, $\Psi_A^{(i)} \Psi_B^{(j)}$ with i, j not simultaneously equal zero. This sum has been broken down into three terms to facilitate physical interpretation. The first term in Equation (6) involves the electrostatic potential from the unperturbed density $\rho_B^{(0)}$ causing an excitation from $\Psi_A^{(0)}$ to $\Psi_A^{(i)}$. This term represents the polarization of molecule A due to the electric field generated by molecule B and can thus be termed $E_{\text{ind}, B \rightarrow A}^{(2)}$, the part of induction energy resulting

from the field of B shifting the charge density of A. Likewise, the second term can be attributed to $E_{\text{ind},A \rightarrow B}^{(2)}$, where the electric field of A polarizes B. The last term in Equation (6) couples an excitation (instantaneous polarization) of A with a similar excitation on B and thus can be interpreted as dispersion energy $E_{\text{disp}}^{(2)}$. The form of Equation (6) makes clear that all three terms are negative (favorable): the induction and dispersion interactions are always attractive in the ground state of the complex. At long range, the leading induction energy contributions vanish like R^{-4} (charge-induced dipole) for charged systems and like R^{-6} (dipole-induced dipole) for electrically neutral but polar ones. As predicted long ago by the London formula,⁶⁷ dispersion energy vanishes as R^{-6} .⁶⁴

The second-order dispersion energy, the last term in Equation (6), can be written in an alternative form known as the *generalized Casimir-Polder equation*^{68,69}

$$E_{\text{disp}}^{(2)} = -\frac{1}{2\pi} \int_0^\infty \iiint \alpha_A(\mathbf{r}_1, \mathbf{r}'_1 | iu) \alpha_B(\mathbf{r}_2, \mathbf{r}'_2 | iu) \frac{d\mathbf{r}_1 d\mathbf{r}_2 d\mathbf{r}'_1 d\mathbf{r}'_2}{|\mathbf{r}_1 - \mathbf{r}_2| |\mathbf{r}'_1 - \mathbf{r}'_2|} du, \quad (9)$$

where

$$\alpha_X(\mathbf{r}, \mathbf{r}' | \omega) = 2 \sum_{m \neq 0} \frac{E_X^{(m)} - E_X^{(0)}}{\left(E_X^{(m)} - E_X^{(0)}\right)^2 - \omega^2} \langle \Psi_X^{(0)} | \hat{\rho}(\mathbf{r}) | \Psi_X^{(m)} \rangle \langle \Psi_X^{(m)} | \hat{\rho}(\mathbf{r}') | \Psi_X^{(0)} \rangle, \quad (10)$$

is the linear response function that, for a real ω , would describe a response of the electron density at \mathbf{r} to a one-electron perturbation at \mathbf{r}' oscillating with a frequency ω . This specific response function is often called frequency-dependent density susceptibility (FDDS).⁷⁰ In Equation (10), $\hat{\rho}(\mathbf{r}) = \sum_i \delta(\mathbf{r} - \mathbf{r}_i)$ is the electron density operator. Equation (9) can be viewed as the extension of the well-known Casimir-Polder formula,^{64,71} expressing the asymptotic dispersion energy in terms of the monomer dynamic polarizabilities at imaginary frequencies, to finite distances where the electron densities of A and B overlap and the multipole approximation is not valid.

Let me now go beyond the polarization approximation and apply symmetry adaptation which gives rise to the exchange corrections in SAPT. The adaptation is accomplished by inserting the $(N_A + N_B)$ -electron antisymmetrizer A into the perturbation expressions. This *symmetry forcing* process is not unique and there exists a variety of different SAPT formulations employing both weak symmetry forcing (where only energy expressions are antisymmetrized) and strong symmetry forcing (where A enters the expressions for wavefunction corrections)—see Reference 72 for a review. However, all practical, system-independent formulations and implementations of SAPT employ the simplest weak symmetry forcing, the symmetrized Rayleigh-Schrödinger (SRS) approach.⁷³ The SRS wavefunction corrections are taken straight from the unsymmetrized RS theory so that the nonexchange corrections are still given by Equations (5), (6), and analogous formulas in higher orders. After the wavefunction corrections are computed through the desired order, the SRS energy terms are obtained from suitable antisymmetrized expressions. In the first two orders of perturbation theory, the complete SRS energy contributions $E_{\text{SRS}}^{(n)} = E_{\text{RS}}^{(n)} + E_{\text{exch}}^{(n)}$ are computed as

$$E_{\text{SRS}}^{(1)} = \frac{\langle \Psi_A^{(0)} \Psi_B^{(0)} | V A | \Psi_A^{(0)} \Psi_B^{(0)} \rangle}{\langle \Psi_A^{(0)} \Psi_B^{(0)} | A | \Psi_A^{(0)} \Psi_B^{(0)} \rangle}, \quad (11)$$

$$E_{\text{SRS}}^{(2)} = \frac{\langle \Psi_A^{(0)} \Psi_B^{(0)} | \left(V - E_{\text{SRS}}^{(1)} \right) A \Psi_{\text{RS}}^{(1)} \rangle}{\langle \Psi_A^{(0)} \Psi_B^{(0)} | A | \Psi_A^{(0)} \Psi_B^{(0)} \rangle}, \quad (12)$$

where the first-order function

$$\Psi_{\text{RS}}^{(1)} = \Psi_{\text{ind}}^{(1)} + \Psi_{\text{disp}}^{(1)} \quad (13)$$

is split into the induction and dispersion parts in accordance with the partitioning of Equation (6):

$$\Psi_{\text{ind}}^{(1)} = \sum_{i \neq 0} \frac{\langle \Psi_A^{(0)} \Psi_B^{(0)} | V | \Psi_A^{(i)} \Psi_B^{(0)} \rangle}{E_A^{(0)} - E_A^{(i)}} \Psi_A^{(i)} \Psi_B^{(0)} + \sum_{j \neq 0} \frac{\langle \Psi_A^{(0)} \Psi_B^{(0)} | V | \Psi_A^{(0)} \Psi_B^{(j)} \rangle}{E_B^{(0)} - E_B^{(j)}} \Psi_A^{(0)} \Psi_B^{(j)}, \quad (14)$$

$$\Psi_{\text{disp}}^{(1)} = \sum_{i, j \neq 0} \frac{\langle \Psi_A^{(0)} \Psi_B^{(0)} | V | \Psi_A^{(i)} \Psi_B^{(j)} \rangle}{E_A^{(0)} + E_B^{(0)} - E_A^{(i)} - E_B^{(j)}} \Psi_A^{(i)} \Psi_B^{(j)}. \quad (15)$$

The first-order SRS correction, Equation (11), is a sum of $E_{\text{RS}}^{(1)}$ and the first-order exchange energy $E_{\text{exch}}^{(1)}$ which is positive for the interaction of two closed-shell systems. At short range, $E_{\text{exch}}^{(1)}$ provides the primary source of repulsion between any two molecules—the electrons from A and B are discouraged from occupying the same space as the Pauli exclusion principle prevents all of them to reside in the same orbital. $E_{\text{exch}}^{(1)}$, like all other exchange terms in SAPT, is a short-range quantity that does not alter the R^{-n} asymptotics of the polarization corrections. More specifically, $E_{\text{exch}}^{(1)}$ decays exponentially with R , with the rate dependent on the overlap of electron density tails of A and B, which in turn is dependent on the ionization potentials I_A and I_B .^{74,75} In the model case of two identical one-electron atoms ($I_A = I_B = I$), it has been proven⁷⁶ that the asymptotic decay of $E_{\text{exch}}^{(1)}$ is proportional to $R^{(7/2\alpha)-1} e^{-2\alpha R}$ with $\alpha = \sqrt{2I}$.

The splitting of $\Psi_{\text{RS}}^{(1)}$ into induction ($B \rightarrow A$), induction ($A \rightarrow B$), and dispersion parts, as defined by the consecutive terms in Equations (14)–(15), inserted into Equation (12), leads to an analogous splitting of the second-order exchange energy:

$$E_{\text{exch}}^{(2)} = E_{\text{SRS}}^{(2)} - E_{\text{RS}}^{(2)} = E_{\text{exch-ind}, B \rightarrow A}^{(2)} + E_{\text{exch-ind}, A \rightarrow B}^{(2)} + E_{\text{exch-disp}}^{(2)}. \quad (16)$$

All three resulting terms are repulsive in the ground state: they provide appropriate short-range quenching of the attractive induction and dispersion contributions due to the Pauli exclusion principle. Practical calculations show that the exchange quenching of $E_{\text{disp}}^{(2)}$ is fairly minor (of the order of 10% at the van der Waals minimum separation), but the quenching of $E_{\text{ind}}^{(2)}$ is more substantial: the sum $E_{\text{ind}}^{(2)} + E_{\text{exch-ind}}^{(2)}$ is often much smaller in magnitude than either $E_{\text{ind}}^{(2)}$ or $E_{\text{exch-ind}}^{(2)}$, making the short-range description of induction quite difficult.

2.2 | Many-body SAPT and its levels

The SAPT theory introduced in Section 2.1, while conceptually simple and attractive, is not practical as it requires FCI calculations for isolated monomers to provide an exact account of the intramolecular electron correlation. For real systems, one has to settle for a simpler zeroth-order Hamiltonian and forgo, at least initially, some or all intramolecular correlation effects. The natural choice is setting $H_0 = F_A + F_B$, where F_X is the Fock operator of monomer X—note that the preceding Hartree-Fock (HF) calculation for X produces the ground state $\Phi_X^{(0)}$ as well as the entire spectrum of excited states $\Phi_X^{(k)}$, required, for example, for the evaluation of Equation (6). Now, a perturbation theory employing $F_A + F_B$ as the zeroth-order Hamiltonian and V as the perturbation can take into account intermolecular electron correlation (for example, second-order dispersion and exchange dispersion) but misses intramolecular correlation effects on interaction energies completely. Such an approximation is very often too crude and several techniques have been developed to bring intramonomer correlation back into SAPT. In this section, I will present in detail the first and most established of these techniques, the *many-body* (that is, many-electron) SAPT, in which intramolecular correlation is included via a second perturbation expansion involving the Møller-Plesset (MP) fluctuation potential:

$$H = F_A + F_B + \xi(W_A + W_B) + \lambda V, \quad (17)$$

$$W_X = H_X - F_X, \quad (18)$$

where ξ and λ are parameters of the two perturbation expansions. The resulting many-body SAPT corrections $E_{\text{SAPT}}^{(mn)}$ have two indices, with $m = 1, 2, \dots$ denoting the order in V and $n = 0, 1, 2, \dots$ the order in $W = W_A + W_B$. Most of the

available $E_{\text{SAPT}}^{(mn)}$ terms have been developed in the early 1990s—see References 77–80 for original work, References 6 and 81 to 83 for reviews, and⁸⁴ for an erratum of some originally published formulas.

The simplest many-body SAPT approximation that gives reasonable total interaction energies is the SAPT0 method. In this approximation, the intramonomer correlation is completely neglected:

$$E_{\text{int}}^{\text{SAPT0}} = E_{\text{elst}}^{(10)} + E_{\text{exch}}^{(10)} + E_{\text{ind,resp}}^{(20)} + E_{\text{exch-ind,resp}}^{(20)} + E_{\text{disp}}^{(20)} + E_{\text{exch-disp}}^{(20)} + \delta E_{\text{HF}}^{(2)}. \quad (19)$$

The first two terms in $E_{\text{int}}^{\text{SAPT0}}$ are the electrostatic interaction of HF-level monomer charge densities and the exchange repulsion which results from the symmetry adaptation of a product of monomer HF determinants, cf. Equation (11). The next two terms, describing the second order induction energy and its exchange counterpart, are computed including the relaxation of monomer HF orbitals in response to the electrostatic potential of the other monomer. This response, signified by the additional subscript “resp”, requires solving the coupled perturbed Hartree-Fock (CPHF) equations⁸⁵ for each monomer. The $E_{\text{disp}}^{(20)}$ and $E_{\text{exch-disp}}^{(20)}$ terms are the only ones in SAPT0 that contain true electron correlation, providing the simplest approximation to the van der Waals dispersion forces and their exchange quenching. Finally, the $\delta E_{\text{HF}}^{(2)}$ term approximately accounts for the third- and higher-order induction and exchange induction effects via a supermolecular (Equation (1)) HF calculation^{86,87}:

$$\delta E_{\text{HF}}^{(2)} = E_{\text{int}}^{\text{HF}} - E_{\text{elst}}^{(10)} - E_{\text{exch}}^{(10)} - E_{\text{ind,resp}}^{(20)} - E_{\text{exch-ind,resp}}^{(20)}. \quad (20)$$

Combining Equations (19) and (20) leads to

$$E_{\text{int}}^{\text{SAPT0}} = E_{\text{int}}^{\text{HF}} + E_{\text{disp}}^{(20)} + E_{\text{exch-disp}}^{(20)}. \quad (21)$$

Thus, total SAPT0 interaction energies are analogous to the Hartree-Fock plus dispersion (HFD) method⁸⁸ except that the dispersion and exchange dispersion terms are computed ab initio rather than from a damped asymptotic expansion. However, the true utility of SAPT0 lies in the energy decomposition provided by Equation (19). Consequently, one of the primary applications of SAPT0 is the classification of different weakly interacting complexes into interaction types such as hydrogen-bonded, dispersion dominated, or mixed influence.⁸⁹ This classification is made more precise by the ternary diagrams^{36,90,91} that graphically represent the relative strength of the three possibly attractive contributions to intermolecular binding, electrostatics, induction, and dispersion.

A consistent improvement to the accuracy of SAPT0 interaction energies requires a consideration of several double perturbation corrections at once, both including the effects of intramolecular correlation W on SAPT0-level corrections and taking into account higher-order effects of the intermolecular interaction V . The available selection of many-body SAPT corrections is rooted in the considerations of both expected improvement in accuracy and formal and computational complexity. The corrections of similar complexity are typically introduced together, and extensive benchmarking has led to a hierarchy of many-body SAPT approximations from the simplest (SAPT0) to the highest currently available level, SAPT2+3⁹²:

$$E_{\text{int}}^{\text{SAPT2}} = E_{\text{int}}^{\text{SAPT0}} + E_{\text{elst,resp}}^{(12)} + E_{\text{exch}}^{(11)} + E_{\text{exch}}^{(12)} + {}^t E_{\text{ind}}^{(22)} + {}^t E_{\text{exch-ind}}^{(22)}, \quad (22)$$

$$E_{\text{int}}^{\text{SAPT2}+} = E_{\text{int}}^{\text{SAPT2}} + E_{\text{disp}}^{(21)} + E_{\text{disp}}^{(22)}, \quad (23)$$

$$E_{\text{int}}^{\text{SAPT2}+(3)} = E_{\text{int}}^{\text{SAPT2}+} + E_{\text{elst,resp}}^{(13)} + E_{\text{disp}}^{(30)}, \quad (24)$$

$$E_{\text{int}}^{\text{SAPT2}+3} = E_{\text{int}}^{\text{SAPT2}+(3)} + E_{\text{exch-disp}}^{(30)} + E_{\text{ind-disp}}^{(30)} + E_{\text{exch-ind-disp}}^{(30)}. \quad (25)$$

The many-body SAPT terms included at each level of theory as well as their common grouping into the overall electrostatic, exchange, induction, and dispersion energies are illustrated in Figure 1. It should be noted that similar

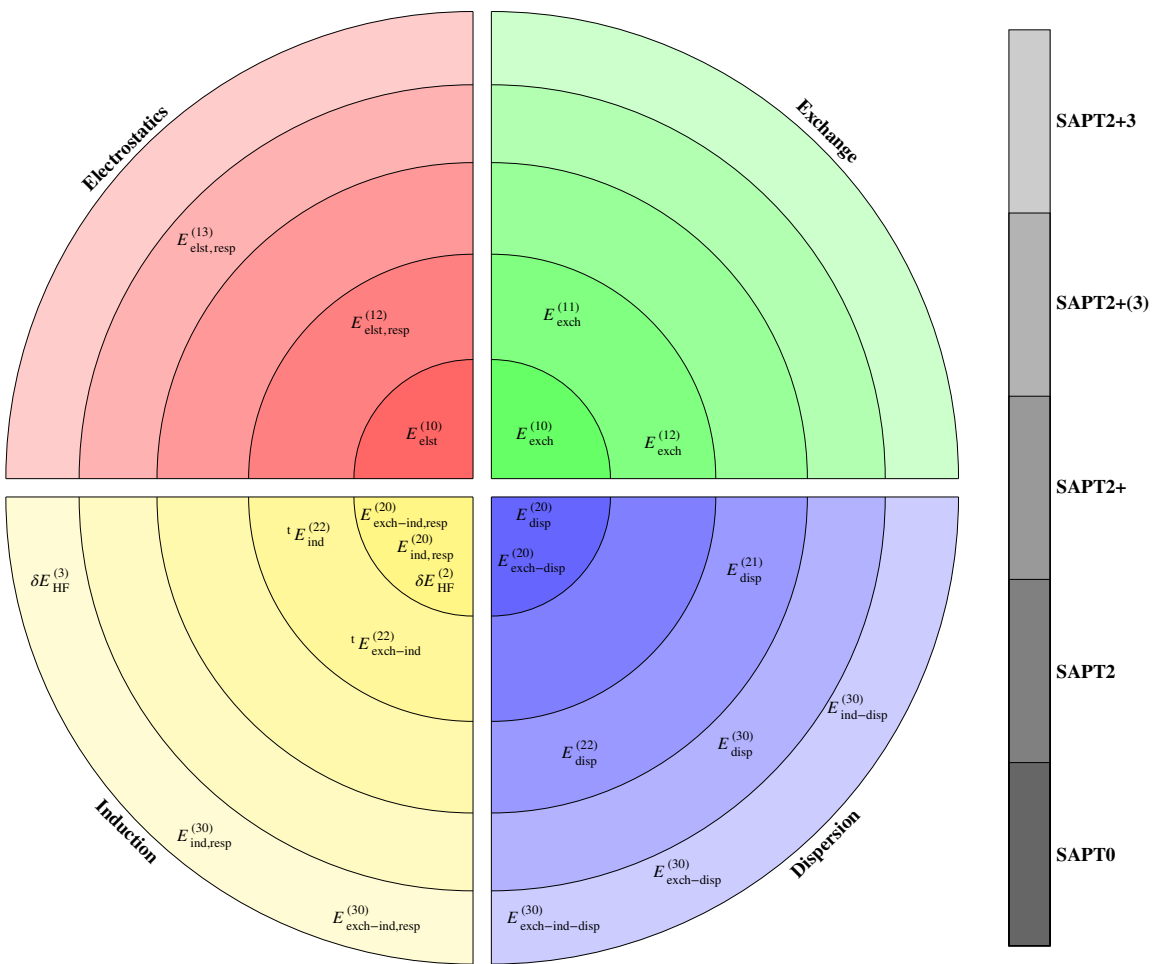


FIGURE 1 The groupings of available many-body symmetry-adapted perturbation theory corrections into the SAPT0, SAPT2, ... levels of theory (concentric shaded circles) and into the overall electrostatic, exchange, induction, and dispersion contributions (pie slices of different colors), as designated in Reference 92

truncations of the double perturbation expansion were used long before the benchmark study of Reference 92, and the SAPT2 level was first defined in Reference 93. A few terms in Equations (22)–(25) merit additional explanation. The inclusion of orbital relaxation in the electrostatic corrections $E_{\text{elst,resp}}^{(12)}$, $E_{\text{elst,resp}}^{(13)}$ requires the same CPHF coefficients as for $E_{\text{ind,resp}}^{(20)}$ and $E_{\text{exch-ind,resp}}^{(20)}$. In the context of electrostatics, orbital relaxation means that the correlated charge densities in Equation (8) are obtained from a finite-field-like MP n expansion in the presence of the perturbing density.^{78,94} The $tE_{\text{ind}}^{(22)}$ term⁸³ denotes the “true” second-order correlation to induction energy, that is, the part of $E_{\text{ind}}^{(22)}$ that does not constitute the “apparent correlation” present already in $E_{\text{ind,resp}}^{(20)}$. The corresponding exchange correction is not computed explicitly, but approximated by scaling:

$${}^tE_{\text{exch-ind}}^{(22)} \approx {}^tE_{\text{ind}}^{(22)} \cdot \frac{E_{\text{exch-ind,resp}}^{(20)}}{E_{\text{ind,resp}}^{(20)}}. \quad (26)$$

Finally, Equations (24) and (25) contain explicitly four of the six parts of the complete SAPT third-order correction computed without intramolecular correlation:

$$E_{\text{SRS}}^{(30)} = E_{\text{ind}}^{(30)} + E_{\text{exch-ind}}^{(30)} + E_{\text{ind-disp}}^{(30)} + E_{\text{exch-ind-disp}}^{(30)} + E_{\text{disp}}^{(30)} + E_{\text{exch-disp}}^{(30)}. \quad (27)$$

The relaxed versions of the pure third-order induction and exchange-induction corrections, $E_{\text{ind},\text{resp}}^{(30)}$ and $E_{\text{exch-ind},\text{resp}}^{(30)}$, form a part of the supermolecular HF interaction energy.⁹⁵ At the SAPT2+3 level, these terms are taken out of $E_{\text{int}}^{\text{HF}}$ and computed explicitly, leading to a modified Hartree-Fock delta term, now approximately accounting for the fourth- and higher-order induction and exchange induction effects:

$$\delta E_{\text{HF}}^{(3)} = E_{\text{int}}^{\text{HF}} - E_{\text{elst}}^{(10)} - E_{\text{exch}}^{(10)} - E_{\text{ind},\text{resp}}^{(20)} - E_{\text{exch-ind},\text{resp}}^{(20)} - E_{\text{ind},\text{resp}}^{(30)} - E_{\text{exch-ind},\text{resp}}^{(30)}. \quad (28)$$

One should note that the explicit computation of the $E_{\text{ind},\text{resp}}^{(30)}$ and $E_{\text{exch-ind},\text{resp}}^{(30)}$ effects does not change either the total SAPT2+3 interaction energy in Equation (25) or the overall assignment of the four SAPT2+3 contributions in Figure 1, as these effects are canceled by the difference between $\delta E_{\text{HF}}^{(3)}$ and $\delta E_{\text{HF}}^{(2)}$ that is also attributed to induction. Interestingly, the third-order induction energy $E_{\text{ind}}^{(30)}$ is not a sum of the $B \rightarrow A$ and $A \rightarrow B$ (hyper)polarization contributions, but contains also a mixed term which can be interpreted as the Coulomb interaction of the electron density of A polarized by the unperturbed electric field of B with the electron density of B polarized by the unperturbed electric field of A. The mixed induction-dispersion term $E_{\text{ind-disp}}^{(30)}$ is in turn a sum of the $B \rightarrow A$ and $A \rightarrow B$ contributions, expressing the dispersion interaction between a polarized monomer and an unperturbed one. Both $E_{\text{ind}}^{(30)}$ and $E_{\text{ind-disp}}^{(30)}$ can be expressed by the linear and quadratic polarization propagators (density response functions) of the individual monomers.^{82,96} The remaining component of $E_{\text{RS}}^{(30)}$, the pure dispersion $E_{\text{disp}}^{(30)}$ term, has long evaded a direct relation to monomer properties, but in 2009 it was expressed through the quadratic monomer propagators and pseudopropagators⁹⁷ (the latter cannot be interpreted in terms of physical properties of monomers but can be computed by any propagator code with a trivial modification). The $E_{\text{disp}}^{(30)}$ term is typically small but repulsive, canceling a small fraction of $E_{\text{disp}}^{(20)}$. Accordingly, its exchange counterpart $E_{\text{exch-disp}}^{(30)}$ is negative unlike all other $E_{\text{exch}}^{(n0)}$ corrections discussed so far. The three parts of $E_{\text{RS}}^{(30)}$ have been derived and implemented in Reference 77 and their exchange counterparts were introduced in Reference 98. The relaxed $E_{\text{ind},\text{resp}}^{(30)}$ correction was proposed in Reference 95. An explicit formula for its relaxed exchange counterpart is not available yet; instead, this term is approximated by scaling

$$E_{\text{exch-ind},\text{resp}}^{(30)} \approx E_{\text{exch-ind}}^{(30)} \cdot \frac{E_{\text{ind},\text{resp}}^{(30)}}{E_{\text{ind}}^{(30)}}. \quad (29)$$

The derivation and implementation of exchange corrections in many-body SAPT merits additional discussion. The matrix elements involving the full antisymmetrizer A , such as those present in Equations (11) and (12), can be expressed through the determinant and cofactors of the matrix \mathbf{S} of overlap integrals involving occupied orbitals on both monomers, χ_i^A and χ_j^B ,

$$\mathbf{S} = \begin{bmatrix} \mathbf{1} & \mathbf{S}_{AB} \\ (\mathbf{S}_{AB})^T & \mathbf{1} \end{bmatrix}, \quad (30)$$

with the intermolecular overlap matrix \mathbf{S}_{AB} having the elements $\langle \chi_i^A | \chi_j^B \rangle$. However, the practical formulas for the resulting SAPT corrections are quite hard to derive and quickly become more complicated as the order of perturbation theory grows. Therefore, in most practical SAPT calculations, only the lowest-order exchange correction $E_{\text{exch}}^{(10)}$ is computed using the full form of A and the formulas introduced in Reference 99. All other exchange terms invoke the *single exchange approximation* to the full ($N_A + N_B$)-electron antisymmetrizer⁸²:

$$A_{N_A + N_B} \approx \frac{N_A! N_B!}{(N_A + N_B)!} A_{N_A} A_{N_B} (1 + P), \quad (31)$$

where the operator $P = - \sum_{i \in A} \sum_{j \in B} P_{ij}$ collects all transpositions of a single pair of electrons between monomers. The application of the single exchange approximation considerably simplifies the resulting formulas as no cofactor algebra is

needed anymore. The resulting expressions for $E_{\text{exch}}^{(mn)}$ retain all terms that are quadratic in the intermolecular overlap integrals but neglect terms that are quartic or higher; thus the alternative name *S^2 approximation*. The single exchange approximation is typically highly accurate around the van der Waals minimum separation and at larger distances, however, it breaks down at shorter intermonomer separations. The breakdown becomes more dramatic in higher orders of perturbation theory and for interactions involving ions.^{100,101} Recent efforts to combat the breakdown of the S^2 approximation will be presented in detail in Section 4.2.

The programmable expressions for different many-body polarization corrections are derived from a perturbative expansion of the Schrödinger equation in its CC form,⁷⁷ which has the benefit that the disconnected terms (which would break size consistency) do not appear at all, instead of having to be canceled term by term as in the conventional MP expansion. The derivation proceeds using standard second quantization techniques except that two sets of creation and annihilation operators have to be considered, one for A and one for B. The same second-quantization techniques can be applied to the exchange corrections,⁸⁰ but only in the case of a *dimer-centered basis set* when the same set of one-electron basis functions is used to expand the (occupied and virtual) orbitals of monomers A and B.¹⁰² Otherwise, the single-exchange operator P (Equation (31)) takes $\Psi_A^{(0)}\Psi_B^{(0)}$ out of the Hilbert space in which the perturbation equations are solved, and consequently does not have a proper second-quantized representation. An alternative approach to SAPT exchange corrections, valid in both dimer- and monomer-centered basis sets, employs the first-quantized representation of P and the one- and two-particle density matrices and transition density matrices of A and B.^{79,98} The final orbital expressions for $E_{\text{exch}}^{(mn)}$ arising from both formalisms are completely different and even exhibit different scaling with the system and basis set sizes. For example, assuming for simplicity an interaction of two identical molecules with o occupied and v virtual orbitals each, the computation of the simplest exchange correction $E_{\text{exch}}^{(10)}$ in the S^2 approximation scales like o^4 for the density-matrix approach and o^2v^2 for the second-quantized one. However, the latter approach requires fewer types of integrals to be transformed from the atomic-orbital (AO) to the molecular-orbital (MO) basis. Both formalisms give identical numerical results as long as a dimer-centered basis set is employed (but not otherwise, when only the density-matrix formulas are correct). Overall, SAPT0 scales like MP2 (N^5), SAPT2 like CCSD (N^6 albeit with a lower prefactor as no iterations are needed), and SAPT2+, SAPT2+(3), and SAPT2+3—like CCSD(T) (N^7) with the system size. The N^7 “triples” terms occur in $E_{\text{disp}}^{(22)}$ and $E_{\text{exch-disp}}^{(30)}$. The formal and practical scaling of SAPT can be improved by the introduction of techniques such as density fitting and virtual space truncations—I will revisit this issue in Section 5.1.

Expressions (19) and (22)–(25) are far from the only options available for computing SAPT total interaction energies, as several modifications are possible stemming from the use of different CC intermediates, hybrid SAPT plus supermolecular approaches, and empirical scaling. First, various many-body SAPT expressions, for example $E_{\text{exch}}^{(11)}$ and $E_{\text{exch}}^{(12)}$, contain as intermediates the singles and doubles amplitudes from the first two iterations of a monomer CCSD calculation (the first iteration simply produces MP2 doubles amplitudes). It has been proposed⁸⁰ to replace these amplitudes by the corresponding quantities from a converged monomer CCSD calculation, thus replacing the sum $E_{\text{exch}}^{(10)} + E_{\text{exch}}^{(11)} + E_{\text{exch}}^{(12)}$ by a term denoted $E_{\text{exch}}^{(1)}$ (CCSD), where the absence of the second subscript signifies that the intramolecular correlation effects have been partially summed over to infinite order using the monomer CCSD amplitudes. A somewhat similar, although more computationally involved, partial infinite-order summation is possible for the second-order dispersion energy.^{103,104} Here, an iterative solution of coupled equations for different coupled cluster doubles (CCD)-like amplitudes produces dispersion energy at the CCD level, and the converged CCD amplitudes can be inserted into the expressions for the singles and triples part of $E_{\text{disp}}^{(22)}$ to produce a dispersion energy approximation termed $E_{\text{disp}}^{(2)}$ [CCD+ST(CCD)]. It was diagrammatically shown¹⁰⁴ that this approximation is legitimate (does not introduce any double counting or spurious terms absent in the MP series) and exact through the third order in W . Second, the SAPT levels of Equations (19) and (22)–(25) all contain the supermolecular HF term; such variants are sometimes referred to as *hybrid SAPT*⁹⁸ as opposed to pure SAPT where the entire interaction energy is accounted for by perturbative corrections. Comparing to benchmark calculations for a limited set of complexes, Reference 98 observed that pure SAPT through third order in V (essentially SAPT2+3) is more accurate than hybrid SAPT for the complexes of nonpolar monomers, while hybrid SAPT remains more accurate for systems composed of polar molecules. On the other hand, in addition to $\delta E_{\text{HF}}^{(2)}$, a second correction can be added to form a “doubly hybrid” SAPT: the δE_{MP2} term coming from a supermolecular MP2 calculation,⁹²

$$\delta E_{\text{MP2}} = E_{\text{int}}^{\text{MP2}} - E_{\text{int}}^{\text{SAPT2}}. \quad (32)$$

The δE_{MP2} term primarily accounts for the third- and higher-order coupling between induction and dispersion and often improves the overall SAPT accuracy for electrostatically bound systems. Thus, a calculation at the SAPT2+3 level requires a modified definition of the δE_{MP2} term to avoid a double counting of $E_{\text{ind-disp}}^{(30)}$ and $E_{\text{exch-ind-disp}}^{(30)}$. Finally, the residual inaccuracies of the S^2 approximation, Equation (31), can be approximately accounted for by a scaling of exchange terms. The underlying assumption is usually that the post- S^2 effects constitute a constant fraction of each exchange correction including $E_{\text{exch}}^{(10)}$ where this fraction can be computed. In other words, a scale factor p_{EX} is defined as^{92,100,105}

$$p_{\text{EX}}(\alpha) = \left(\frac{E_{\text{exch}}^{(10)}}{E_{\text{exch}}^{(10)}(S^2)} \right)^{\alpha}, \quad (33)$$

where the parameter α is nearly always taken equal to one. Now, all exchange corrections in SAPT except for $E_{\text{exch}}^{(10)}$ can be multiplied by p_{EX} to approximate the effect of multiple electron exchanges. Such a scaling, with $\alpha = 1$, is performed by definition at all SAPT0–SAPT2+3 levels of theory, Equations (19) and (22)–(25), as defined in Reference 92 (note, however, that the effects of this scaling on the overall SAPT interaction energy are strongly reduced by the addition of $\delta E_{\text{HF}}^{(2)}$ or δE_{MP2}). Taking this scaling a step further, an empirically corrected scaled SAPT0 (sSAPT0) variant is defined as⁹²

$$E_{\text{int}}^{\text{sSAPT0}} = E_{\text{elst}}^{(10)} + E_{\text{exch}}^{(10)} + E_{\text{ind,resp}}^{(20)} + p_{\text{EX}}(3.0)E_{\text{exch-ind,resp}}^{(20)}(S^2) + E_{\text{disp}}^{(20)} + p_{\text{EX}}(3.0)E_{\text{exch-disp}}^{(20)}(S^2) + \delta E_{\text{HF}}^{(2,p_{\text{EX}}(1.0))}. \quad (34)$$

Note that Equation (34) breaks the cancellation of scaling effects between the SAPT corrections and $\delta E_{\text{HF}}^{(2)}$: the $E_{\text{exch-ind,resp}}^{(20)}(S^2)$ term included from SAPT is scaled by the $p_{\text{EX}}(3.0)$ factor but the same term subtracted as part of $\delta E_{\text{HF}}^{(2)}$ is scaled by the $p_{\text{EX}}(1.0)$ factor as indicated in the notation of the last term in Equation (34). The net result is that the sSAPT0 interaction energy is always more positive than the SAPT0 one, empirically correcting some of the overbinding of the latter at short range. The recent derivation and implementation of the complete, nonapproximated $E_{\text{exch-ind,resp}}^{(20)}$ ¹⁰⁶ and $E_{\text{exch-disp}}^{(20)}$ ¹⁰⁷ corrections makes it possible to compute the entire SAPT0 interaction energy, Equation (19), without the single exchange approximation and to assess the adequacy of the scaling factors of Equation (33) for different choices of the parameter α ; I will discuss these developments in more detail in Section 4.2.

One of the most extensive assessments of the accuracy of different many-body SAPT interaction energies was performed by Parker et al.,⁹² comparing the SAPT values to “gold standard” supermolecular CCSD(T) data for 345 diverse noncovalent complexes from several popular databases. The mean absolute errors (MAE) of different SAPT approximations were computed in a range of Dunning basis sets, completely or partially augmented by diffuse functions.^{108–110} Interestingly, the SAPT0 interaction energies actually became less accurate as the basis set was increased, with the MAE increasing from 0.86 kcal/mol for jun-cc-pVDZ to 1.73 kcal/mol for aug-cc-pVDZ and 2.54 kcal/mol for aug-cc-pV5Z. The reason for this behavior is the systematic overbinding present at the SAPT0 level, which becomes progressively worse as the $E_{\text{disp}}^{(20)}$ correction, the slowest-converging one in SAPT0, grows more and more negative on its approach to the CBS limit. The dispersion correction is at the same time one of the primary reasons for the overbinding itself: the simplest $E_{\text{disp}}^{(20)}$ picture tends to overestimate the intermolecular correlation, just like supermolecular MP2 (which includes dispersion at the $E_{\text{disp}}^{(20)}$ level^{111,112}) severely overestimates the binding between, for example, aromatic molecules.³ There are two consequences of this overbinding that are important for the utility of inexpensive SAPT estimates. First, the success of SAPT0 relies on an error cancellation between the overestimation of intermolecular binding by the method and the underestimation of dispersion by a finite basis set. Therefore, converging SAPT0 to CBS is not a good idea: instead, one should look for a “sweet spot” in the basis set hierarchy to maximize the error cancellation. The numerical evidence of Reference 92, and of others, suggests the “calendar” basis set jun-cc-pVDZ¹¹⁰ as such a sweet spot. Second, the sSAPT0 approach of Equation (34), designed to make the interaction energy less negative, consistently overperforms SAPT0. The MAE value for the sSAPT0/jun-cc-pVDZ approach obtained in Reference 92 is just 0.49 kcal/

mol, a truly remarkable accuracy for a simple and inexpensive model that provides both total interaction energy and its physical decomposition. Another large-scale assessment of the accuracy of many-body SAPT at all levels was performed by Gilson and coworkers.¹¹³

Further improvement to the accuracy of SAPT total energies requires including some intramolecular correlation. In particular, an inclusion of dispersion energy beyond the $E_{\text{disp}}^{(20)}$ level is vital: without it, the SAPT2 level provides only modest improvement over SAPT0, with the lowest MAE of 0.74 kcal/mol obtained in the jun-cc-pVTZ basis set.⁹² Note that all post-SAPT0 levels of theory lose the systematic error cancellation between theory and basis set incompleteness effects and usually become more accurate as the basis set is enlarged. A notable (and practically important) exception is the SAPT2+ level which exhibits the highest accuracy (a MAE of 0.30 kcal/mol) when paired with the aug-cc-pVDZ orbital basis, suggesting an attractive route to an accurate SAPT energy decomposition at an intermediate cost. Finally, the highest-level many-body SAPT approximations, paired with suitably large basis sets, can deliver impressive accuracy (albeit with substantial computational cost). According to the calculations of Reference 92, the particularly successful high-level SAPT treatments are SAPT2+(3)/aug-cc-pVTZ including δE_{MP2} (a MAE of 0.15 kcal/mol) and SAPT2+/aug-cc-pVTZ including δE_{MP2} and the $E_{\text{disp}}^{(2)}$ [CCD+ST(CCD)] dispersion in place of $E_{\text{disp}}^{(20)} + E_{\text{disp}}^{(21)} + E_{\text{disp}}^{(22)}$ (a MAE of 0.12 kcal/mol). Thus, different many-body SAPT flavors are suitable for different purposes, from cheap qualitative assessment of the interaction character to computing total interaction energies with quantitative accuracy and physical insights into the binding in the complex.

2.3 | SAPT(DFT)

In the previous section, the effects of intramolecular electron correlation on the interaction energy were included by means of a second, MP-type perturbation expansion, or its selective infinite-order summation using CC techniques. While these approaches can give very accurate energy decompositions, they are expensive: the triples part of $E_{\text{disp}}^{(22)}$ (or $E_{\text{disp}}^{(2)}$ [CCD+ST(CCD)]) scales like N^7 with the system size, and $E_{\text{disp}}^{(2)}$ [CCD] scales like N^6 with a large prefactor due to the iterative solution of three coupled sets of amplitude equations. Thus, it is worthwhile to explore more efficient options for including intramolecular correlation, and density functional theory (DFT) appears the most sensible choice due to its proven capability of producing accurate correlated ground-state structures and energies while its computational efficiency matches or exceeds that of the HF approach. However, it is well known that semilocal DFT functionals, applied in the supermolecular framework, are incapable of even a qualitatively accurate reproduction of dispersion energy^{114,115}: for this reason, many extensions to DFT that provide some approximate account of dispersion have been proposed—see References 19 and 26 for recent reviews. However, the SAPT formalism provides an attractive alternative which relies on *using DFT for what it does well* (intramolecular correlation) *but not for what it does poorly* (intermolecular correlation or dispersion).

The combination of SAPT0 expressions and Kohn-Sham (KS) orbitals and orbital energies in place of the HF ones, commonly denoted SAPT(KS), was first proposed by Williams and Chabalowski.¹¹⁶ Formally, SAPT(KS) replaces the double perturbation theory of Equation (17), with the monomer Fock operators in the zeroth order, with a new one involving the sum of monomer KS operators K_A and K_B as the zeroth-order Hamiltonian:

$$H = K_A + K_B + \xi(H_A - K_A + H_B - K_B) + \lambda V, \quad (35)$$

and then considers only the terms of zeroth-order in ξ just like SAPT0. It is expected that, as the monomer KS determinants already contain a reasonable account of intramolecular correlation, SAPT(KS) should be much more accurate than SAPT0 but not more costly. However, this was not the case in the original investigation of Williams and Chabalowski¹¹⁶—the first-order SAPT(KS) energies were far from perfect and the second-order ones were badly overestimated. The evolution of SAPT(KS) into an accurate and broadly applicable approach, which occurred in a series of parallel developments by Misquitta et al.^{70,117–119} and by Hesselmann and Jansen,^{120–123} required correcting for two deficiencies of the original framework:

Asymptotic correction: The exchange correlation potential in DFT, the functional derivative of the exchange correlation energy, should formally behave at large distances r like $-1/r + (I + \epsilon_{\text{HOMO}})$, where I is the ionization potential and ϵ_{HOMO} is the KS orbital energy for the highest occupied molecular orbital.^{124,125} However, typical exchange correlation

potentials decay to zero at long range, very often exponentially. Such potentials need to be replaced at long range by ones that behave like $-1/r$, shifted by a constant amount $I + \epsilon_{\text{HOMO}}$, and spliced with the short-range potential to avoid the charge density leaking into the asymptotic region. Such a shift and splice can be performed in several ways, including the Fermi-Amaldi-Tozer-Handy (FA) scheme^{124,126} and the gradient-regulated asymptotic correction (GRAC)¹²⁷ splicing the exchange correlation potential with that of the van Leeuwen-Baerends functional¹²⁸ (which decays like $-1/r$ in the long range limit but is not competitive at short range). Alternatively, range separated hybrids (RSH),¹²⁹ also called long-range corrected (LC)^{130,131} functionals, can be used to alleviate the asymptotic incorrectness.^{132–134} Note that the asymptotic correction occurs at the level of the exchange correlation potential and cannot be traced back to the exchange correlation energy,¹³⁵ that is, total energies cannot be computed and the asymptotic correction is of no help to supermolecular DFT. After enforcing the correct asymptotic behavior of the exchange correlation potential, the electrostatic, first-order exchange, and induction components of SAPT(KS) are reasonable and accurate, however, the dispersion energies are still overestimated.¹¹⁷

Coupled KS dispersion: The $E_{\text{disp}}^{(20)}$ expression, evaluated with either HF or KS orbitals and orbital energies, corresponds to the evaluation of Equation (9) with the monomer FDDSSs, Equation (10), approximated at the *uncoupled* HF/KS level of theory, neglecting the orbital relaxation. While this might often be a reasonable approximation for the HF variant, the uncoupled KS dispersion energies are strongly inaccurate.¹²² The alternative, known as the coupled Kohn-Sham (CKS) approach to dispersion energy, is to obtain FDDSSs in a proper linear response fashion, that is, from time-dependent DFT (TDDFT).¹³⁶ Note that the corresponding coupled HF expression, coming from time-dependent HF linear response, is often referred to as the random-phase approximation (RPA) dispersion energy.^{137,138} The Hessian matrices needed for TDDFT contain the *exchange correlation kernel*, the functional derivative of the exchange correlation potential or second functional derivative of the exchange correlation energy.¹³⁹ This kernel does not necessarily need to be evaluated with the actual density functional used for SAPT(KS): a popular approximation consists of the use of the adiabatic local density approximation (ALDA) kernel¹⁴⁰ for all nonhybrid functionals and a properly weighted average of the ALDA and time-dependent Hartree-Fock (TDHF) Hessians for hybrid functionals.¹²² It has been shown that while uncoupled KS dispersion does not improve over the SAPT0 one, the accuracy of the CKS dispersion rivals that of high-level wavefunction-based SAPT such as $E_{\text{disp}}^{(20)} + E_{\text{disp}}^{(21)} + E_{\text{disp}}^{(22)}$.^{70,122}

When the exchange correlation potential in SAPT(KS) is asymptotically corrected and the uncoupled KS dispersion (and induction) energies are replaced by their CKS counterparts, the resulting approach is called SAPT(DFT)¹¹⁹ or DFT-SAPT.¹²³ Here, I will stick to the SAPT(DFT) name as it fits within the general SAPT(...) notation that specifies the method used to treat intramonomer correlation.

I will present some illustrative applications of SAPT(DFT), showcasing its impressive combination of accuracy and computational efficiency, in Section 2.4. First, however, it is worth asking what one can expect from SAPT(DFT) if an exact density functional, which is unknown but guaranteed to exist, is applied. As this hypothetical functional produces exact monomer densities $\rho_A^{(0)}$ and $\rho_B^{(0)}$, the electrostatic energy will be exact because of Equation (8). Note, however, that Equation (8) is sensitive to the overlap of monomer density tails and thus it is important to enforce the correct asymptotics for an approximate exchange correlation potential. The first-order exchange energy requires monomer one- and two-particle density matrices,⁷⁹ not just the electron density, and is not guaranteed to be exact even for an exact density functional. However, the analysis of Reference 118 proved that the leading asymptotic term of the true first-order exchange energy is exactly recovered from the monomer KS determinants obtained with an exact functional. Obviously, an exact electron density for a monomer generates an exact electrostatic potential, and the density of the other monomer should also respond to this potential in an exact way. Thus, the induction energy is potentially exact in SAPT(DFT), that is, it is exact provided that (a) the exchange correlation functional is exact, (b) the kernel in TDDFT linear response calculations is exact, and (c) the coupled KS approach is employed.^{118,122} The same is true for the dispersion energy. Note that the CKS approach has been highly successful in accurately computing response functions related to FDDSSs, such as static¹⁴¹ and dynamic¹⁴² polarizabilities as well as the leading van der Waals coefficients in the asymptotic expansion of the interaction energy.¹⁴³

SAPT(KS) scales with the system size the same as SAPT0, that is, as N^5 . The computation of dispersion energy from FDDSSs, Equation (9), scales like N^6 . However, the latter scaling can be reduced by density fitting,¹⁴⁴ that is, by expanding products of occupied and virtual orbitals as linear combinations of auxiliary basis functions. As the number N_{aux} of such functions is significantly smaller than the number n_{ov} of the required products, significant reduction in the time and storage requirements might be achieved. SAPT(DFT) with density fitting scales like N^5 and the errors due to an incomplete auxiliary basis are minimal.^{123,145,146}

2.4 | Applications of SAPT and SAPT(DFT)

I will now provide some illustrative applications of the well-established SAPT and SAPT(DFT) approaches presented in the preceding sections. The initial applications of other, emerging variants of SAPT will be presented later as those new developments are discussed. It should be stressed that the primary focus of this review is on the further development of the SAPT methodology and the set of applications below is far from complete. Some other applications of SAPT have been reviewed, for example, in References 5 and 7.

At the turn of the century, probably the most important application of SAPT was the construction of potential energy surfaces (PESs) that were in turn applied to predict spectra, scattering cross sections, and properties of bulk matter.¹⁴⁷ Since then, the hardware and software progress has made supermolecular CCSD(T) calculations of accurate PESs feasible for many complexes of experimental interest, but SAPT(DFT) surfaces are still useful as lower-cost alternatives that provide the additional benefit of energy decomposition.^{148,149} Moreover, there exists a class of medium-sized complexes where a calculation of a sufficient number of CCSD(T)/CBS interaction energies to construct a complete PES is still a formidable task and SAPT(DFT) remains the best practical approach to provide data for an accurate PES. The most important example is the benzene dimer, for which a complete six-dimensional SAPT(DFT) PES has been constructed in Reference 150 and refined in Reference 151, enabling an elucidation of the complicated pattern of intermolecular vibration-rotation-tunneling levels. It should also be noted that a recently proposed framework for an automated PES generation¹⁵² was built upon SAPT(DFT) interaction energies at suitable autogenerated grid points, even though a supermolecular approach such as CCSD(T) can easily be substituted for SAPT. Eight illustrative SAPT(DFT) surfaces were produced in Reference 152 for systems ranging from the $\text{H}_2\text{O}\cdots\text{Cl}^-$ complex to the homodimer of the energetic molecule cyclotrimethylene trinitramine (RDX).¹⁵³

In the context of a PES generation, the defining feature of SAPT(DFT) is its ability to produce accurate total interaction energies at a modest N^5 computational cost, with the energy decomposition being of secondary importance. In fact, SAPT(DFT) is typically one of the most accurate N^5 approaches to intermolecular interactions (another strong performer, the “MP2 coupled” (MP2C) approach of Hesselmann,^{154,155} shares the CKS treatment of dispersion energy with SAPT(DFT)) and is usually a much better choice than standard MP2 or its spin component scaled variants.^{36,92} As a result, SAPT(DFT) is quite often the method of choice when computing interaction energies for large complexes for which CCSD(T) is not feasible. An important example of such a benchmark SAPT(DFT) study is the calculation¹⁵⁶ of interaction energies for the S12L database of large complexes.¹⁵⁷ For systems of this size, a computation of unambiguous benchmark values exceeds our current algorithmic and computational capabilities, and the original S12L benchmark data (obtained by back-correcting experimental association free energies¹⁵⁷) as well as high-level local CC¹⁵⁸ and quantum Monte Carlo¹⁵⁹ interaction energies differ by up to several kcal/mol.³⁰ In this case, it is highly advantageous to have other data available that combine reasonable accuracy with physical insight via the SAPT(DFT) energy decomposition. Another class of systems featuring SAPT(DFT) interaction energy benchmarks (but, to my knowledge, no CCSD(T) ones) are endohedral complexes of fullerenes with H_2 ,¹⁶⁰ rare gas atoms,¹⁶¹ rare gas dimers,¹⁶² and a host of small molecules ranging from diatomics to formaldehyde and methanol.¹⁶³ Perhaps the most inspiring study of this kind is the SAPT(DFT) investigation of the chiral host-guest recognition, that is, the interaction of a chiral CHFCI_{Br} molecule with its chiral C₈₂ fullerene cage.¹⁶⁴

Let me now move on to applications where the individual SAPT or SAPT(DFT) components are required rather than the overall interaction energy. For many purposes, it is sufficient to have just a qualitative assessment of the importance of various SAPT terms and the decomposition can be performed at a low level of theory. In this case, the SAPT0/jun-cc-pVDZ and sSAPT0/jun-cc-pVDZ combinations have emerged as the optimal theory level and basis set choices that facilitate error cancellation.⁹² The primary application of such an approximate energy decomposition is classifying different complexes according to their interaction types. While chemical experience allows one to recognize many different types of interactions such as hydrogen bonding, $\pi - \pi$ stacking, $\text{CH}\cdots\pi$ contact, halogen bonding, etc., according to SAPT, intermolecular bonding arises from any combination of electrostatics, induction, and dispersion (the exchange energy is always destabilizing for closed-shell complexes). The relative weight of these three bonding factors, defined as in Figure 1 (that is, the induction and dispersion values include their exchange and HF delta counterparts), quantifies the type of the noncovalent interaction and, as first proposed by Kim and coworkers,⁹⁰ can be conveniently represented by a point on a ternary diagram. As the electrostatic interaction can be attractive or repulsive, a double ternary diagram, taking on the shape of a rhombus, is needed to represent it.¹⁶⁵ Ternary diagrams are particularly useful when evaluating the degree of diversity in a benchmark database of intermolecular interaction energies⁹¹—if the points corresponding to different systems cluster at one particular location in the diagram, the database clearly

favors one particular interaction type and might not be diverse enough for, for example, fitting a new approximate dispersion expression for DFT. The ternary diagram analysis performed in Reference 91 and illustrated in Figure 2 indicates that even the extensive and very popular S66x8 database,¹⁶⁶ widely regarded as “well balanced,” actually covers quite a small section of the ternary diagram and thus represents only some particular interaction types. On the other hand, the configurations sampled from a complete PES of a given complex, for example, 2,510 water dimer geometries selected in Reference 147, or the configurations attained in real systems, such as the set of 3,380 amino acid sidechain-sidechain interactions (SSI) extracted from the entire Protein Data Bank,¹⁶⁷ cover a significantly larger area of the ternary diagram (though not the entire diagram) and thus can be viewed as more diverse.

The SAPT energy decomposition has been highly useful in elucidating the physical origins of different types of noncovalent bonding. Overall, the picture emerging from SAPT is more nuanced than the chemical intuition might suggest. Even in an “electrostatically bound,” dipole–dipole complex such as the water dimer, dispersion amounts to about 50% of the interaction energy at the van der Waals minimum. On the other hand, in nonpolar systems such as the substituted sandwich benzene dimers, while electrostatic energy is minuscule at large separations, the short-range electrostatics (charge penetration) is an important and unexpected source of binding.⁶⁵ It should be kept in mind that the interaction energy at the van der Waals minimum always stems from a delicate balance of the attractive and repulsive contributions: when the intermolecular separation is decreased, the magnitude of the repulsive exchange effects grows faster than that of the attractive terms, leading to a net increase of the interaction energy. On the other hand, when the separation is increased, the magnitude of the attractive effects initially decays faster than for the repulsive terms, leading to an increase of the interaction energy as well. However, when one is mindful of this balance, SAPT and SAPT(DFT) energy decompositions can provide valuable insight into the nature of different kinds of bonding. A particularly important example is the interactions stemming from the so-called σ -hole, a region of positive electrostatic potential directly opposite a σ bond.^{9,168} The σ -holes were first discovered on halogen atoms, leading to the highly popular concept of halogen bonding. The origins of this type of interaction have been extensively studied by diverse methodology, with SAPT (especially SAPT(DFT)) being the typical method of choice, providing a reference decomposition of binding energy into physical terms.^{169–175} The SAPT description of halogen bonds has been extensively compared to that of conventional hydrogen bonds,^{176–178} revealing a very different interaction character despite often similar total interaction energies. While electrostatics is the leading binding force in hydrogen-bonded complexes, the halogen-bonded systems are characterized by a much larger role of dispersion, which directly results from the presence of two highly polarizable atoms, the halogen and the electron donor, in close contact. In fact, the weaker halogen bonds are primarily held together by dispersion forces and only the particularly strong ones are dominated by electrostatics and induction¹⁶⁸ (the effects ascribed to induction by the SAPT decomposition are in this case attributable to a donor-acceptor interaction, that is, charge transfer). Perhaps even more surprisingly, the directionality of the halogen bond is not a consequence of the electrostatic interaction, but the linear arrangement minimizes the density overlap and drives down the exchange repulsion¹⁷⁰ due to the nonspherical character (polar flattening) of a σ -bonded halogen atom.¹⁷⁴ Halogens are not the only atoms to possess a σ -hole, and a whole class of other related bonding patterns has been subjected to the SAPT(DFT) (or many-body SAPT) energy decomposition, including chalcogen,¹⁷⁹ pnicogen,^{180–182} and tetrel bonding.¹⁸³

Another phenomenon whose understanding has been significantly advanced using SAPT and SAPT(DFT) energy decompositions are interactions involving aromatic systems, in particular, the $\pi - \pi$ stacking interactions and their

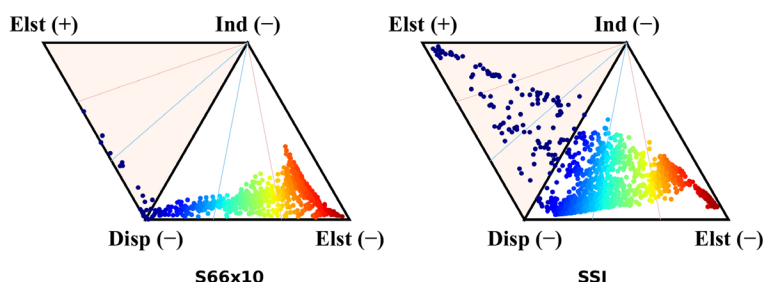


FIGURE 2 Ternary diagrams illustrating the relative magnitudes of electrostatics, induction, and dispersion in the SAPT0/jun-cc-pVDZ energy decompositions for the S66x10 database of noncovalent complexes (the S66x8 set¹⁶⁶ extended to short range in Reference 91) and the SSI database of sidechain-sidechain interactions in proteins.¹⁶⁷ (Reprinted with permission from the Supporting Information to Reference 91. Copyright 2016 American Chemical Society)

variation upon substitution. The classical explanation of substituent effects via a donation or withdrawal of π -electron density was challenged by Wheeler and Houk¹⁸⁴ who provided evidence that those effects stem from a direct interaction of the substituent with the aromatic ring of the other molecule, showing a strong correlation between the interaction energies of benzene with the substituted benzene C_6H_5-X and with the substituent alone, H-X. In subsequent studies,^{185,186} Wheeler et al. used SAPT to explain this correlation in terms of the electrostatic contribution (note that the SAPT decomposition for various structures of aromatic complexes was earlier studied by Kim and coworkers^{187,188}). SAPT energy decompositions have continued to facilitate our understanding of the interactions between various substituted aromatic compounds,¹⁸⁹ and the typical conclusion has been summarized best by the title of Reference 190: “dispersion dominates and electrostatics commands,” that is, while dispersion energy provides the bulk of attraction in an aromatic dimer, it is the electrostatic energy that dictates the optimal structures and controls the substituent effect.

Interactions involving polycyclic aromatic hydrocarbons (PAHs), both flat and curved, are important both in their own right and as models of interactions involving fullerenes, carbon nanotubes, and graphene. The pioneering application of SAPT(DFT) to PAHs comes from the works of Podeszwa et al.^{191,192} concerning homodimers of hydrocarbons ranging in size from naphthalene to coronene. The latter complex belongs to the realm where SAPT(DFT) is a useful source of both energy decomposition and benchmark total energies, as an unambiguous CCSD(T)-level reference value has not yet been established for this system.^{193,194} Podeszwa went on to extrapolate the SAPT(DFT) results to the graphene-graphene limit and estimate the effect of subsequent layers on the exfoliation energy of graphite.¹⁹² Later, Kennedy et al.¹⁹⁵ employed SAPT0 to investigate how the interaction energies in the coronene and corannulene dimers change with the curvature, in an attempt to compare the stacking interactions involving flat graphene and curved carbon forms such as fullerenes and carbon nanotubes. Other large PAHs whose dimers have been investigated using SAPT and/or SAPT(DFT) include derivatives of rubrene¹⁹⁶ and sumanene.^{197,198} Moreover, Cabaleiro-Lago and Rodríguez-Otero compared the SAPT(DFT) stacking energies for complexes involving PAHs and their fully hydrogenated analogues (with cyclohexane-like rings), identifying enhanced dispersion energy as the main factor behind the superior stability of large $\pi - \pi$ stacked complexes compared to the $\sigma - \sigma$ and $\sigma - \pi$ ones.¹⁹⁹ Besides the stacked PAH dimers, understanding physisorption processes requires studying interactions between a single PAH representing the surface and a small adsorbate molecule. Using models of a graphene surface ranging in size from four (pyrene) to 14 (circumpyrene) aromatic rings, SAPT(DFT) has been used to gain insight into the adsorption of water,²⁰⁰ methane,²⁰¹ hydrogen,²⁰² Cl₂,²⁰³ and tetracyanoquinodimethane (TCNQ) and its derivatives.²⁰⁴ The largest calculations of this kind involve a SAPT0 analysis of the interaction between benzene (or its fluorinated derivatives) and a graphene nanoflake as large as C₁₅₀H₃₀.^{205,206} In addition to adsorption on carbon nanostructures, interactions between small molecules and cluster models of other surfaces such as MgO,²⁰⁷ TiO₂,²⁰⁸ or a metal organic framework²⁰⁹ have also been subjected to the SAPT and/or SAPT(DFT) decompositions.

The unique ability of SAPT to provide both an energy decomposition and accurate total interaction energies means that its important job is to serve as a term-by-term reference when more approximate approaches are constructed, refined, and validated. The prime example, and a very hot topic in the current literature, is the development of physically justified force fields for the treatment of systems beyond the reach of ab initio electronic structure theory. The design of new force field expressions, in particular of the terms responsible for noncovalent inter- and intramolecular interactions, is a formidable task that combines physical knowledge, chemical intuition, and a great deal of numerical testing and validation. While a force-field energy expression that accounts for all interaction contributions at once might benefit from an error cancellation when fitted to the right collection of ab initio data, separate expressions for distinct contributions are easier to establish, better grounded in the underlying physics, and seamlessly connected to the known asymptotic expansion of interaction energy in terms of multipole moments and polarizabilities.⁶⁴ Thus, starting from the early attempts by Piquemal, Szalewicz, and coworkers,^{210,211} ab initio force fields are developed term by term, and the reference data for individual noncovalent energy contributions are best provided by SAPT and/or SAPT(DFT). The long-range form of different force field terms uses the multipole moments and polarizabilities distributed into contributions centered on individual atoms^{74,212,213}; however, it is much harder to come up with an accurate force-field description of the charge-overlap effects absent in the multipole approximation, such as charge penetration, exchange repulsion, and charge transfer. It should be noted that the short-range terms produced by common force fields may have little in common with the SAPT(DFT) reference values even though total interaction energies at equilibrium distances are similar.²¹⁴ Various forms of the short-range terms have been proposed in the literature, with their adjustable parameters fitted to SAPT or SAPT(DFT) data, and earlier ab initio force fields for specific systems^{215,216} were later generalized to provide force fields that are transferable at least within a class of similar compounds.^{217–222} In the last few years, an enhanced force-field description of short-range interactions has been brought about by considering the

asymptotic form of the intermolecular density overlap and using novel algorithms to partition molecular density into atomic contributions.^{223,224} Moreover, a further improvement in the recovery of reference SAPT(DFT) contributions came from considering the anisotropy of the short-range terms arising from the nonspherical character of the atomic densities.²²⁵ Besides the development of first-principles force fields, the dispersion (more precisely, dispersion plus exchange dispersion) energies from SAPT(DFT) are highly useful in constructing empirical expressions to augment ab initio methods that do not contain dispersion energy on their own, such as HF,^{88,226} DFT variants made dispersionless by fitting,^{227,228} or SAPT approximations with the dispersion terms removed.^{229–231} However, the SAPT(DFT) reference data might not be directly suitable for optimizing a damped atom–atom dispersion expression to augment an arbitrary density functional in the DFT+D method²³²; the damping in such an expression²³³ has to both account for physical charge overlap effects (present in SAPT(DFT)) and eliminate double counting of dispersion at short range (which has to be done in a functional-dependent way, and SAPT(DFT) is obviously of no help in this regard). Moreover, the interaction energy contributions missing in approximate supermolecular DFT are not rigorously dispersion-related, and the “+D” correction might be thought of as representing an effective dispersion potential with other effects mixed in.²³⁴ As the last application of SAPT of this type, let me mention the spin-network-scaled MP2 approach of Reference 235, where the system-dependent scaling coefficients for the same-spin and opposite-spin parts of the MP2 interaction energy are learned by a neural network, taking as inputs various easily calculated energy expressions including the terms in the SAPTO decomposition.

I conclude this section by showcasing the amazing creativity of researchers applying SAPT and SAPT(DFT) to current chemical problems. The pair potentials generated with SAPT(DFT), combined with a proper treatment of nonadditive many-body interactions, are a viable route to predicting molecular crystal structures,²³⁶ and the SAPT(DFT) potentials performed well in a recent blind test of crystal structure prediction methods²³⁷ (as well as in another blind test of the recovery of CCSD(T)/CBS interaction energies²³⁸). As far as cluster models of the liquid phase are concerned, SAPT has been applied to elucidate the origins of interactions involving ionic liquids^{50,239–242} and to understand the $\pi - \pi$ stacking occurring in an organic solvent.²⁴³ Besides the endohedral fullerenes mentioned earlier, the SAPT and SAPT(DFT) energy decompositions have been applied to other supramolecular complexes including catenanes,²⁴⁴ porphyrins and metalloporphyrins,²⁴⁵ and the cucurbit[7]uril macrocycle.²⁴⁶ SAPTO has been used to decompose interaction energies of dimers relevant to organic electronics²⁴⁷; in particular, it has been proposed to improve electronic couplings via an enhancement of charge penetration brought about by incorporating large heteroatoms in π -conjugated cores.⁶⁶ The interaction of C₆₀ with large conjugated oligomers relevant to organic solar cells has been investigated by SAPTO,²⁴⁸ while SAPT(DFT) was employed to elucidate another interaction of interest to photovoltaics, the binding of C₆₀ to various concave receptors.²⁴⁹ Finally, the applications of SAPT decompositions to biologically relevant complexes span an impressive range from the stacking of DNA and RNA base pairs^{250,251} to the active center of the algal light harvesting complex.²⁵²

3 | EXTENDING THE APPLICABILITY OF SAPT

3.1 | Open-shell complexes and multiplet splittings

The closed-shell SAPT and SAPT(DFT) approaches have developed into popular general-purpose techniques, with several efficient implementations available and numerous successful applications, some of them mentioned in Section 2.4. The SAPT treatment of complexes composed of open-shell monomers is somewhat more complicated, in particular, the coupling of angular momenta for the two monomers may lead to several spin states of the weakly interacting system. For example, the interaction of two ground-state ($^3\Sigma_g^-$) O₂ molecules, in accordance with the rules of adding angular momenta, leads to a singlet state, a triplet state, and a quintet state of the complex. The three multiplets are *asymptotically degenerate*, that is, the energy of each state approaches twice the ground-state energy of O₂ at large intermolecular separations. Within the SRS-based SAPT formalism, all RS corrections are computed without any account of the spin coupling and are identical for all asymptotically degenerate states. Therefore, the entire splittings between different multiplets of the complex arise out of the different exchange energies.

The first applications and convergence assessments of open-shell SAPT were the system-specific developments for model few-electron complexes: H–H⁺,²⁵³ H–H,²⁵⁴ He–H,⁵⁴ and Li–H.^{56,62} As far as the general-purpose theory is concerned, Żuchowski et al. developed the first SAPTO and SAPT(DFT) variant based on restricted open-shell Hartree-Fock or Kohn-Sham (ROHF/ROKS) description of monomers.²⁵⁵ An analogous development based on spin-unrestricted

determinants (UHF/UKS) was carried out by Hapka et al.,²⁵⁶ followed by an efficient density-fitted implementation of SAPT0(UHF) by Gonthier and Sherrill²⁵⁷ (see also Reference 258). The approaches of References 255–257 share two limitations. First, they require each monomer to be qualitatively described by a single reference determinant, so they are appropriate only for interactions involving high-spin open-shell monomers. Second, all unpaired spins in the zeroth-order wavefunction of References 255–257 point in the same direction, that is, the quantum number M_S for the complex, describing the projection of the total spin angular momentum on the z axis, equals the sum of the respective quantum numbers for the monomers, $M_S = M_{S_A} + M_{S_B}$. Thus, the zeroth-order wavefunction is a pure, uncontaminated high-spin state, and the exchange corrections of References 255–257 are appropriate for the high-spin state of the dimer, but not for the low-spin states or for the calculation of spin splittings. For the oxygen dimer example mentioned above, SAPT(ROHF)/SAPT(UHF)/... are capable of describing the interaction in the quintet state, which happened to be one of the first applications of SAPT(ROKS).²⁵⁹ Another atmospherically relevant interaction is the O₂–N₂ one, for which a ground-state PES was constructed using SAPT(DFT)²⁶⁰ and used to accurately reproduce experimental second virial coefficient data and integral cross sections. Several interactions involving nitrogen oxides, important atmospheric pollutants, have also been thoroughly investigated using open-shell SAPT and/or SAPT(DFT): NO–H₂O²⁶¹ and NO₂–H₂O.²⁶² For the former system, the single-reference calculations are restricted to symmetric C_s configurations, for which the degeneracy in the ground-state, ² Π NO molecule is lifted to form two separate states of the complex, ² A' and ² A'' , both of which are amenable to the SAPT(ROKS) treatment. The existence of multiple states that may or may not be accessible to single-reference methods depending on geometry is a common complication in the computation of open-shell PESs,²⁶³ and even the long-range asymptotic form of potentials involving ² Π molecules is not trivial.²⁶⁴ In another study, open-shell SAPT(UHF) has been used for a comparative analysis of the O₂–H₂O and SO–H₂O complexes, explaining the differences in the positions and depths of different local minima.²⁶⁵

A particularly prevalent and feature-rich class of open-shell systems are transition metal atoms, ions, and complexes, and open-shell SAPT and SAPT(DFT) can shed some light on the interactions involving such difficult systems as long as the states in question are single reference. To this end, one of the earlier studies examined the aurophilic interactions using the SAPT and SAPT(DFT) energy decompositions for small closed- and open-shell complexes involving close contacts between two gold atoms.²⁶⁶ Kłos et al., motivated by the buffer-gas cooling and magnetic trapping experiments, examined the SAPT(UKS) decomposition of the interaction energy between the helium atom and the ground, ⁶ Σ^+ state of the CrH molecule, making comparisons to a somewhat similar He–MnH(⁷ Σ^+) complex.²⁶⁷ Sládeček and Tvaroška²⁶⁸ compared, at the SAPT0 and SAPT(DFT) levels, the interactions between the closed-shell (Mg^{2+} , Zn^{2+}) and open-shell (Mn^{2+}) cations and several ligands representing the active site of a metalloenzyme to investigate the influence of the metal ion on the enzyme's catalytic activity. Malenov and Zarić studied stacking interactions involving chelated complexes of Ni^{2+} , Zn^{2+} , and Cu^{2+} , using closed-shell configurations for systems involving the first two ions but open-shell SAPT0 for the copper complexes.²⁶⁹ Last but not least, the open-shell SAPT approaches of References 255–257 open up an avenue of studying interactions involving monomers in some specific (high-spin) excited states. Accordingly, SAPT(UHF) and SAPT(UKS) have been applied to complexes that are capable of undergoing Penning ionization, such as the complexes of He(³S) and Ne(³P) with hydrogen, helium, and argon,²⁷⁰ as well as the Ne(³P)–NH₃ complex and its isotopologues.²⁷¹

Interactions between genuinely multireference molecules require capturing a delicate balance between intermonomer dynamical correlation and intramonomer static correlation and are subject of intense research. For example, the stretching of a covalent bond in one of the interacting molecules has been shown to first enhance and then suppress the noncovalent binding, and single-reference SAPT provides useful insight into this behavior up to a certain point on the stretching curve.²⁷² Beyond that point, a truly multireference SAPT formalism is required, a goal that has not been fully accomplished yet. The first attempt at such a theory was the work of Reinhardt²⁷³ who proposed a method to calculate $E_{\text{elst}}^{(10)}$ and $E_{\text{disp}}^{(20)}$ between two systems described by multideterminantal wavefunctions of the valence bond (VB) approach. While $E_{\text{elst}}^{(10)}$ was computed exactly from the monomer electron densities (cf. Equation (8)), $E_{\text{disp}}^{(20)}$ was approximated by a weighted average of the asymptotic dipole–dipole terms corresponding to pairs of individual determinants. More recently, Hapka et al.²⁷⁴ proposed a multireference approach to dispersion energy based on the extended RPA (ERPA) linear response formalism²⁷⁵ that can utilize monomer one- and two-particle reduced density matrices (RDMs) from any multireference approach (in Reference 274, complete active space self-consistent field [CASSCF]²⁷⁶ and the generalized VB theory were used for this purpose). The ERPA treatment approximates the full CASSCF linear response by freezing the CI coefficients of different determinants in the CASSCF wavefunction; only the orbital response is taken into account including active-active orbital rotations. While the ERPA-based dispersion energy was,

predictably, unsuccessful at accounting for intramonomer dynamical correlation, the results for simple multireference systems such as H₂-stretched H₂ and Be–Be were highly encouraging.²⁷⁴ It appears that ERPA provides a viable route to developing a complete multireference analog of SAPTO.

The topic of computing exchange energies for high-spin open-shell systems combining into a low-spin state of the complex is the subject of ongoing research in my group. In the first development,²⁷⁷ we have modified the spin-restricted open-shell SAPT approach of Reference 255, introducing a new zeroth-order wavefunction in which the unpaired spins on two monomers point in different directions (say, up for A and down for B), so that $M_S = M_{S_A} - M_{S_B}$ for the overall complex. Such a wavefunction obviously does not correspond to a pure spin state, but appropriate zeroth-order functions for all spin states of the complex, $S = |S_A - S_B|, \dots, S_A + S_B$, can be extracted from it using suitable spin projections. In this fashion, we have derived²⁷⁷ the expressions for the leading-order exchange correction $E_{\text{exch}}^{(10)}$ within the S^2 approximation, valid for an arbitrary spin state. These expressions are linear combinations of two matrix elements: the *diagonal exchange term* representing the spin-averaged exchange energy and the *spin-flip term* solely responsible for the spin splittings. The matrix elements for the latter term involve a wavefunction where one unpaired spin on A has been lowered and one unpaired spin on B has been raised; therefore, we have called the new method spin-flip SAPT (SF-SAPT), in analogy to the spin-flip electronic structure theory developed over the years by Krylov and coworkers.²⁷⁸ A common feature of Krylov's approach and of SF-SAPT is that they can access genuinely multireference, low-spin states of the system in an entirely single reference calculation. The contributions to $E_{\text{exch}}^{(10)}$ from multiple spin flips vanish as a result of the single exchange approximation,²⁷⁷ in analogy to the Heisenberg Hamiltonian model with a single parameter describing all multiplet splittings.²⁷⁹ The $E_{\text{exch}}^{(10)}(S^2)$ estimates of these splittings, now available in the Psi4 electronic structure code,²⁸⁰ are inexpensive to compute and qualitatively correct; however, one cannot expect quantitative accuracy from a mere first-order perturbation treatment. An additional problem is the breakdown of the S^2 approximation at short range (see a detailed discussion in Section 4.2). To overcome this last issue, we have recently proposed²⁸¹ a new variant of SF-SAPT $E_{\text{exch}}^{(10)}$ in which the S^2 approximation has been replaced by a single spin-flip approximation. The latter one is exact for interactions involving a doublet state (as there is only one unpaired spin to flip) and much milder in general, as shown by comparisons to the existing nonapproximated high-spin $E_{\text{exch}}^{(10)}$ of Reference 255 (an example comparison for the N–N interaction is presented in Figure 3). The single spin-flip treatment removes the short-range artifacts of SF-SAPT(S^2) for model systems,²⁸¹ however, it does little to improve the splittings in important classes of complexes such as pancake-bonded dimers of aromatic radicals.²⁸² Clearly, one needs to go beyond first-order perturbation theory, and the extensions of SF-SAPT to the second-order exchange induction and exchange dispersion corrections, as well as an extension from ROHF to CASSCF monomer wavefunctions, are in progress in my group.

3.2 | Charge-transfer energy in SAPT

When I introduced various interaction energy terms in SAPT, I did not mention the energetic effects associated with a transfer of some amount of electronic density between the interacting subsystems. I did not do so because in SAPT, charge-transfer energy is not a separate term but it is folded into the induction contribution. The leading induction term in SAPT, $E_{\text{ind,resp}}^{(20)}$, involves single excitations from an occupied to a virtual orbital of one monomer (say, A) in the electric field coming from the other monomer. The SAPT corrections are usually computed in the full dimer-centered basis set (DCBS),¹⁰² which results in those single excitations accessing the virtual orbitals localized on both A and B. For an excitation to a virtual orbital located on molecule A, the electron density remains on A and such contributions can be attributed to an electronic polarization of A in the field of B, in accordance with the conventional understanding of the induction energy. In an excitation to a virtual orbital located on B, charge transfer from A to B occurs. On the other hand, if $E_{\text{ind,resp}}^{(20)}$ is computed in the monomer-centered basis set (MCBS) only, the virtual orbitals localized on B are not present in the basis set for A and the charge transfer is greatly diminished (note that MCBS is a perfectly valid basis set for SAPT as the method, unlike the supermolecular approach of Equation (1), is intrinsically free from the basis set superposition error). Therefore, it was proposed²⁸³ to isolate the charge-transfer energy in SAPT as the difference between the induction energies calculated within the DCBS and MCBS approaches. These induction energies can be taken from many-body SAPT or from SAPT(DFT), and an analogous separation is performed for the corresponding

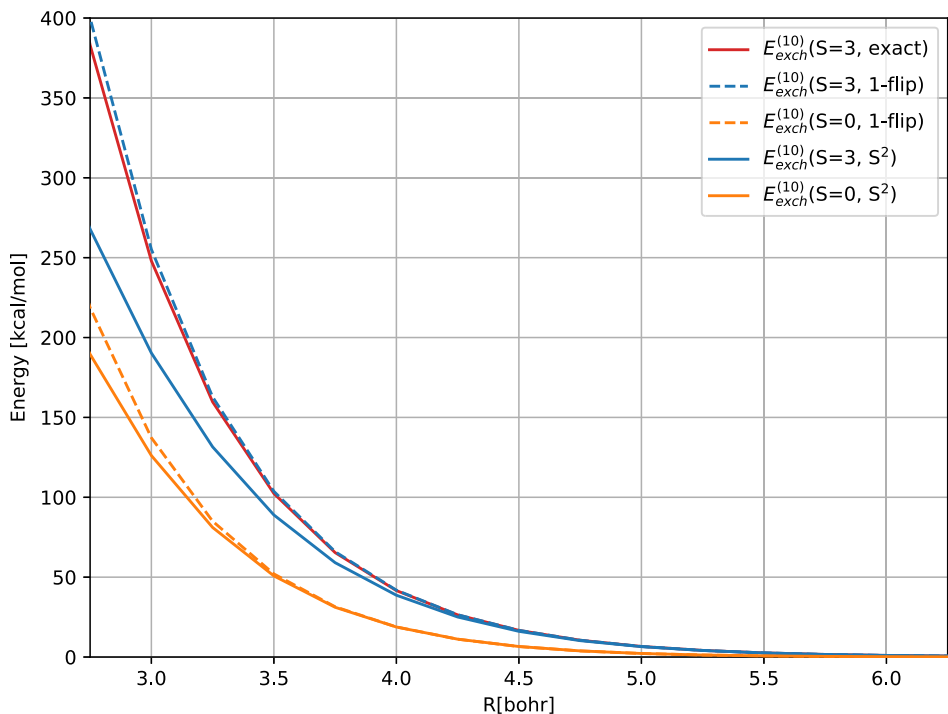
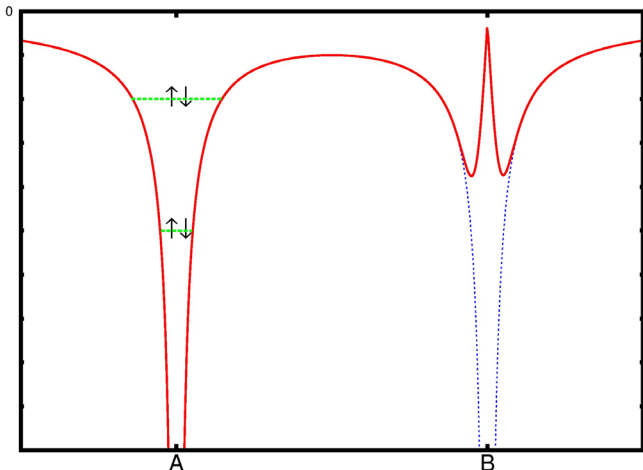


FIGURE 3 The values of the $E_{\text{exch}}^{(10)}$ SAPT correction for the singlet ($S = 0$) and septet ($S = 3$) states resulting from the interaction of two ground-state nitrogen atoms as functions of the interatomic separation. The “exact” results are nonapproximated corrections from the high-spin-only algorithm of Reference 255, and the “ S^2 ” and “1-flip” values are the spin-flip SAPT (SF-SAPT) arbitrary-spin exchange energies computed using the approximations of References 277 and 281, respectively. (Reprinted with permission from Reference 281. Copyright 2019 AIP Publishing LLC)

exchange correction $E_{\text{exch-ind,resp}}^{(20)}$ to properly attribute the exchange quenching to the polarization and charge-transfer phenomena.

The fundamental drawback of the approach of Reference 283 is its reliance on a particular one-electron basis set. At one extreme, let us imagine a helium atom in a very small basis containing only s functions, interacting with a polar water molecule. In the MCBS case, the electron density on helium is forced to be spherically symmetric and no polarization can occur. Thus, the (limited) polarization effects captured by the $E_{\text{ind,resp}}^{(20)}/\text{DCBS}$ calculation in this basis arise exclusively out of the use of the basis functions of the partner water molecule which are not exactly zero around the helium atom. At the other extreme, when the basis set on the helium atom is very large and contains many diffuse functions, the MCBS is by itself sufficient to reasonably describe the virtual orbitals of the water molecule, and thus capture the charge transfer energy without resorting to a DCBS calculation. Thus, the charge-transfer energy of Reference 283 lacks a meaningful CBS limit, which is a testament to the inherent imprecision in the definition of the charge transfer effect²⁸⁴ rather than a problem of the SAPT methodology. Nevertheless, for practical purposes, a designation of a meaningful and basis-set stable charge transfer term could significantly enhance the interpretive power of SAPT and facilitate the comparisons between SAPT and other energy decompositions.⁵⁰ One possible avenue²⁸⁵ of defining a charge transfer energy that has a meaningful CBS limit is the use of *regularized* SAPT, with the induction and exchange-induction energies computed using a modified electrostatic potential of the interacting partner molecule. In this regularized potential, the attractive singularity is removed from the nuclear-electron interaction by some form of range separation akin to the one ubiquitous in modern DFT.²⁸⁶ Regularization in SAPT has been introduced before^{58,287,288} to make the perturbation expansion in powers of V (Equation (2)) converge, as the reason for the divergence of the polarization approximation for many-electron systems has been traced down to the electrons on one monomer falling into the Coulomb wells around the other monomer’s nuclei^{56,62}—see Figure 4 for a schematic illustration. Note that the repulsive singularities in the perturbation operator are not a problem and only the nucleus-electron interactions are regularized. Reference 285 proposed to identify the sum of the regularized induction and exchange-induction energies as the true polarization energy so that the charge transfer term is obtained as the difference between the induction and exchange-induction effects computed using standard and regularized SAPT. Such a definition depends on a single parameter defining the range separation (which is typically called ω in the context of DFT²⁸⁹) whose value needs to be fixed using some additional constraint. Reference 285 proposed to obtain this parameter by requiring that all sufficiently large monomer-centered basis sets result in identical regularized induction energies, which are interpreted as quickly convergent polarization energies

FIGURE 4 A schematic illustration of the effects of regularization of the attractive singularities in the perturbation operator V . Without regularization (blue dashed curve), electrons from atom A tend to tunnel into the Coulomb well around the nucleus of atom B. The regularized Coulomb potential (red solid curve) has this well filled in to eliminate tunneling. As a result, regularization prevents the divergence of the polarization expansion^{58,287,288} and suppresses charge transfer in the second order²⁸⁵



with no contamination from charge transfer. It was shown²⁸⁵ that such a choice of a range separation parameter attributes (as it should) nearly all induction and exchange-induction energy of two noble gas atoms to charge transfer, and that the new approach, unlike the one of Reference 283, is virtually independent of the basis set. An alternative, hybrid approach proposed by Lao and Herbert²⁹⁰ carves out a basis-set stable charge-transfer energy obtained using constrained DFT^{291,292} from the induction and exchange-induction energy of standard SAPT, ascribing the remaining part to polarization and preserving all the other SAPT terms. I conclude this section by mentioning a recent application of the hybrid SAPT(DFT)/constrained DFT scheme to a diverse set of halogenated complexes, including halogen-bonded ones.²⁹³

The schemes described in this section attempt to extract the charge-transfer energy from the second-order SAPT induction and exchange-induction contributions. Both the higher-order induction and exchange-induction corrections such as $E_{\text{ind,resp}}^{(30)}$ and their $\delta E_{\text{HF}}^{(2)}$ approximation, Equation (20), contain charge transfer effects as well, however, to my knowledge, these effects have not been separated so far.

3.3 | Fine-graining SAPT energy terms: The A-SAPT and F-SAPT methods

The interpretive power of SAPT stems from its ability to split the overall noncovalent interaction energy into contributions that originate from different physical effects. In addition, it is often advantageous to distinguish interaction energy contributions originating from different atoms or functional groups in the monomers. Alternatively, interaction energy could be split into contributions from different locations in real space, in the spirit of the scalar fields used to visualize noncovalent interactions²⁸ such as the quantum theory of atoms in molecules (QTAIM),²⁹⁴ the noncovalent interaction (NCI) index,²⁹⁵ and the density overlap region indicator (DORI).²⁹⁶ In the context of SAPT, a fine-grained partitioning of each SAPT0-level correction has been accomplished by Parrish et al., who have formulated the atomic SAPT (A-SAPT)²⁹⁷ and functional group SAPT (F-SAPT)²⁹⁸ approaches.

Within these two theories, each SAPT0 energy term (referred to as order-0 decomposition in this context) is further partitioned into contributions arising from a given pair of atoms (A-SAPT) or functional groups (F-SAPT) on A and B, leading to an order-2 interaction energy decomposition that is rich in additional information. An intermediate step (order-1 decomposition) involves splittings over atoms/functional groups of one monomer only. Thus, order-1 A-SAPT can quantify, for example, the dispersion interaction of a given atom in A with the entire molecule B, while order-2 A-SAPT can quantify the dispersion interaction of a given atom in A with a given atom in B. The decompositions are complete and no interaction energy contribution is lost in the process:

$$E_{\text{term}}^{(n0)} = \sum_{A \in A} E_{\text{term}}^{(n0),A} = \sum_{A \in A} \sum_{B \in B} E_{\text{term}}^{(n0),AB}, \quad (36)$$

for any SAPT0-level contribution $E_{\text{term}}^{(n0)}$. Designing a suitable partitioning is nontrivial and the established A-SAPT and F-SAPT approaches are a result of extensive testing of different techniques of localizing the electron density and its

response, as well as resorting to scaled approximations for terms such as $\delta E_{\text{HF}}^{(2)}$ that elude an atomic assignment. While the order-1 A-SAPT partitioning is a useful visualization tool that provides insights in line with the chemical intuition,²⁹⁷ the electrostatic terms tend to show oscillations due to spurious partial charges on adjacent atoms. A coarse-graining of the partitioning from atoms to functional groups, compounded by a careful assignment of the contributions from the electron pair forming the interfragment σ bond, results in the F-SAPT method that is largely free of oscillations in the electrostatic term.²⁹⁸ The caveat is that the interfragment partitioning has to occur through a single σ bond, that is, F-SAPT will not produce meaningful results if double bonds, rings (aromatic or aliphatic), or pairs of atoms with significant charge transfer are cut through. One should bear in mind that, as the authors of Reference 298 stated, the partitions such as F-SAPT “are intended to aid our chemical understanding of noncovalent contacts but should not be mistaken for absolute physical realism”. This suggests that energy differences between F-SAPT contributions in related systems (for example, substituent effects) might be more meaningful than the F-SAPT results for any single system, as any nonuniqueness and/or artifacts of partitioning should exhibit at least some cancellation between similar complexes. For this reason, the F-SAPT difference analysis is a particularly appealing application of the fine-grained decomposition.

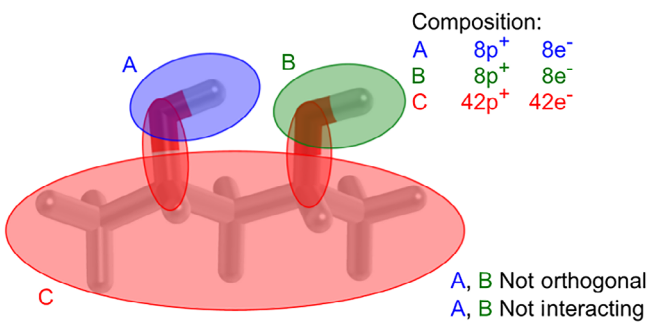
The first application of difference F-SAPT analysis²⁹⁹ revisited the influence of substituents on the $\pi - \pi$ stacking interactions, a topic that was already brought up when discussing the applications of conventional SAPT. By splitting the substituent effect, that is, the interaction energy difference between the benzene–substituted benzene complex and the plain benzene dimer, into the direct (interaction with the substituent versus interaction with the hydrogen atom) and indirect (interaction with the phenyl group) effects, Reference 299 was able to prove that the direct effect is stronger, confirming the Wheeler-Houk picture¹⁸⁴ mentioned in our earlier discussion. A similar analysis was recently performed for representative cation– π interactions, highlighting the importance of electrostatic effects and (mostly) confirming the Wheeler-Houk model.³⁰⁰ Another application of the difference F-SAPT analysis are the interactions between the enzyme pocket and substituted variations of a potential drug molecule,³⁰¹ revealing a multitude of intermediate-range electrostatic contacts that are crucial for the difference in binding energy. Beyond near-equilibrium intermolecular complexes, F-SAPT has also been applied to elucidate interactions in the transition states of some organocatalyzed reactions,^{302,303} attempting to explain their stereoselectivity and enantioselectivity. In my group, we have recently applied F-SAPT differences to elucidate the subtle noncovalent effects leading to chiral discrimination in the propylene oxide dimer.³⁰⁴

3.4 | Intramolecular noncovalent interactions

Noncovalent intermolecular interactions are no different in their origin from noncovalent intramolecular interactions occurring between functional groups of the same molecule that are not directly bonded to each other but might be spatially close. Intramolecular noncovalent forces, in particular dispersion, are implicated in a diverse range of phenomena; notable examples are the enhanced thermodynamic stability of branched alkanes over linear ones,³⁰⁵ the stability of highly sterically crowded molecules such as the all-*meta*-tert-butyl derivatives of hexaphenylethane,³⁰⁶ and the design and performance of molecular balances.³⁰⁷ However, the effects such as intramolecular dispersion are very difficult to quantify: where does one draw the line between short-range and long-range dynamical correlation? Despite the obvious need for energy decomposition, standard intermolecular SAPT cannot be directly applied to intramolecular complexes as one cannot define well separated monomers A and B. However, a SAPT description is possible (and highly useful) when the molecule is fragmented and the severed covalent bonds are capped with hydrogen atoms, so that the noncovalently interacting fragments reside on separate molecules.^{308,309} However, such a cut-and-cap procedure, no matter how careful, alters the chemical environment in the system, and it is advantageous to develop alternative SAPT-like energy decomposition techniques that do not require physical fragmentation of the molecule. In the last couple of years, two such techniques have been proposed.^{310–312}

The common feature of the two intramolecular SAPT (I-SAPT) approaches is the partitioning of the molecule of interest into two noncovalently interacting regions A and B that are covalently connected via a linker C—see Figure 5 for an example. Thus, I-SAPT seeks to compute the electrostatic, exchange, induction, and dispersion energies of A interacting with B in the presence of C. In the first approach,^{310,311} the zeroth-order wavefunction is a Slater determinant built of orbitals localized on the different regions, which are optimized using a non-Hermitian Fock matrix (adapted from the chemical Hamiltonian approach³¹³) in which the A–B interactions are artificially suppressed but

FIGURE 5 A schematic illustration of the intramolecular SAPT (I-SAPT) calculation of the intramolecular hydrogen bond energy in 2,4-pentanediol. The numbers of protons and electrons in each fragment are listed as well. (Reprinted with permission from Reference 312. Copyright 2015 AIP Publishing LLC)



the A–C and B–C ones are fully present. Initially, only the total A–B interaction energy was quantified as the difference between the HF energies of the fully interacting molecule and the artificial system without the A–B Fock matrix terms.³¹⁰ The zeroth-order wavefunction of Reference 310 was subsequently used³¹¹ to obtain an A–B interaction energy decomposition into the (electrostatics+exchange), polarization, delocalization (charge transfer), and dispersion contributions within a non-Hermitian (biorthogonal) perturbation theory framework. In the second approach,³¹² the zeroth-order wavefunctions for regions A and B are obtained in separate HF calculations embedded in the frozen HF wavefunction of the linker C. Subsequently, the standard SAPTO calculation is performed between A embedded in C and B embedded in C, which can be viewed as a generalization of the F-SAPT approach,²⁹⁸ described in Section 3.3, to fragments located on the same molecule. Both approaches give chemically sensible and useful descriptions of model weak intramolecular interactions, especially when coupled with a difference analysis to compare the I-SAPT decomposition of two related systems. The main weakness of both approaches is, in my opinion, associated with the designation of the linker C, which needs to fulfill two mutually exclusive goals of (1) separating A and B by a sufficient distance to eliminate their covalent interactions and (2) not having noncovalent interactions with A or B by itself, as such interactions will be missing from the I-SAPT analysis. The interfragment A–C and B–C σ bonds are also prone to a buildup of spurious multipoles. I expect further I-SAPT developments, addressing the weaknesses mentioned above while preserving the strengths of the methodology, to appear in the near future.

3.5 | SAPT for nonadditive three-body interactions

The properties of many molecular clusters, crystals, and liquids cannot be accurately described solely by the two-body interactions between pairs of molecules. What is missing in such a description are the nonadditive three-body, four-body, ... effects.²⁴ The most important correction beyond the pairwise additive interactions is provided by the three-body term, defined for three molecules A, B, C as

$$\Delta E_{\text{int}}^{\text{3-body}} = E_{ABC} - E_{AB} - E_{BC} - E_{AC} + E_A + E_B + E_C. \quad (37)$$

In addition to the supermolecular approach given by Equation (37), it is possible to evaluate and decompose $\Delta E_{\text{int}}^{\text{3-body}}$ by perturbation theory—see Reference 314 for a review. The resulting expressions for the most important three-body SAPT corrections were derived and implemented shortly after those of the two-body SAPT.^{315–317} While the electrostatic energy is strictly pairwise additive (which is a simple consequence of the two-electron character of the interaction operator V), and dispersion energy is strictly additive in the second order (where pair correlations are taken into account), the exchange and induction corrections, as well as the third- and higher-order dispersion, are not. Thus, the available SAPT contributions to $\Delta E_{\text{int}}^{\text{3-body}}$, labeled by two indices according to their orders in V (Equation (2)) and in $W_A + W_B + W_C$ (Equation (18)), are^{316,318}

$$\Delta E_{\text{int}}^{\text{3-body SAPT}} = \mathcal{E}_{\text{exch}}^{(10)} + \mathcal{E}_{\text{exch}}^{(11)} + \mathcal{E}_{\text{exch}}^{(12)} + \mathcal{E}_{\text{ind}}^{(20)} + \mathcal{E}_{\text{exch-ind}}^{(20)} + \mathcal{E}_{\text{exch-disp}}^{(20)} + \mathcal{E}_{\text{ind}}^{(30)} + \mathcal{E}_{\text{disp}}^{(30)} + \mathcal{E}_{\text{ind-disp}}^{(30)} + \mathcal{E}_{\text{disp}}^{(31)} + \mathcal{E}_{\text{disp}}^{(40)} + \delta \mathcal{E}_{\text{int}}^{\text{HF}}, \quad (38)$$

where I used the calligraphic notation to distinguish a three-body SAPT contribution $\mathcal{E}^{(kl)}$ from a two-body SAPT contribution $E^{(kl)}$. While a large scale benchmarking of three-body SAPT has not, to my knowledge, been performed yet, tests on model trimers show that the induction and first-order exchange corrections tend to exhibit the greatest nonadditivity, which is quite fortunate as the bulk of both corrections can be recovered in a supermolecular HF calculation.

The leading nonadditive dispersion term $\mathcal{E}_{\text{disp}}^{(30)}$ has attracted significant attention as it provides a generalization of the well-known asymptotic Axilrod-Teller-Muto (ATM) triple-dipole formula^{319,320} to complexes with nonzero intermolecular overlap. Moreover, this term is not present in the supermolecular MP2 calculation and is thus the primary reason why accurate three-body energies involving, for example, aromatic systems need to be computed at the CCSD(T) level.^{321,322} The most prominent early application of three-body SAPT was the PES for the water trimer,^{323,324} a key addition to the two-body water potential required for the reliable description of water clusters and liquid water.

An extension of the three-body SAPT methodology to SAPT(DFT) has been carried out by Podeszwa and Szalewicz.³²⁵ While most corrections require a simple replacement of the HF orbitals and orbital energies in the three-body SAPT expressions by the corresponding KS quantities, the $\mathcal{E}_{\text{ind}}^{(2)}$ and $\mathcal{E}_{\text{disp}}^{(3)}$ terms were computed from FDDSSs in the coupled KS formalism. Reference 325 also discovered an accurate and efficient hybrid approach denoted MP2+SDFT, where the supermolecular nonadditive MP2 energy was augmented by the CKS $\mathcal{E}_{\text{disp}}^{(3)}$ term (note that no double counting occurs in such an approach). The three-body SAPT(DFT) approach has found several applications, ranging from benchmarking an ab initio force field³²⁶ to incorporating three-body effects into a SAPT-derived force field for carbon dioxide.³²⁷ The MP2+SDFT algorithm, which can be viewed as a three-body generalization of the MP2C theory,^{154,155} was employed in a comparative study of several different three-body dispersion expressions,³²⁸ to refine the lattice energy prediction for the benzene crystal,²³⁶ to investigate the cooperativity effects in model tetrel- and triel-bonded trimers,¹⁸³ and to examine the interactions of azaborines with two water molecules at once.³²⁹ Finally, nonadditive SAPT(DFT) benchmarks can shed light on the performance of DFT-based methods for three-body interaction energies, enabling the partitioning of the supermolecular three-body DFT energy into exchange and deformation (polarization) terms.³³⁰

4 | ENHANCING THE ACCURACY OF SAPT

4.1 | CC-based SAPT for high-accuracy benchmarks

When discussing various flavors of the many-body SAPT, I mentioned that two of its terms are frequently enhanced by a partial infinite-order summation of intramolecular correlation effects using converged CC amplitudes, resulting in the $E_{\text{exch}}^{(1)}$ (CCSD)⁸⁰ and $E_{\text{disp}}^{(2)}$ [CCD + ST(CCD)]¹⁰⁴ expressions. These methods are, however, not fully equivalent to a rigorous CC treatment of first-order exchange and dispersion, respectively. The latter requires expressing each SAPT term by the appropriate monomer properties obtained with a truncated CC approach such as CCSD. For this purpose, monomer FDDSSs (Equation (10)) evaluated at imaginary frequencies are required for dispersion energy, and monomer one- and two-particle reduced density matrices are needed for first-order exchange. The development of a complete SAPT(CCSD) approach, with each SAPT0 correction enhanced with the intramonomer correlation effects computed using the appropriate properties from expectation-value CCSD theory,^{331,332} has been accomplished in a series of papers by Korona et al.^{333–341}—see Reference 342 for a review. The required CCSD quantities include one-particle densities and density matrices as well as the cumulant of the two-particle density matrix (which is the contribution beyond a simple antisymmetrized product of one-particle density matrices³⁴³), all evaluated for both unperturbed monomers and for those perturbed by the electrostatic potential of the interacting partner. In addition, the evaluation of dispersion energy requires monomer CCSD-level FDDSSs, and the exchange-dispersion correction makes use of a (slightly) generalized response function, the frequency-dependent density matrix susceptibility.³⁴¹ Both kinds of susceptibilities are particularly expensive to calculate, resulting in an iterative N^8 scaling of $E_{\text{disp}}^{(2)}$ (CCSD) and $E_{\text{exch-disp}}^{(2)}$ (CCSD), which can be reduced to a (still expensive) iterative N^7 by means of density fitting.³³⁷ Thus, the primary application of the SAPT(CCSD) theory of References 333–341 is in providing accurate benchmark values of individual SAPT contributions for the assessment of somewhat more approximate methods such as many-body SAPT or SAPT(DFT).

The most popular benchmark collection of accurate SAPT(CCSD) interaction energy terms, consisting of 21 small but diverse complexes, has been produced by Korona.³⁴⁴ Its original application³⁴⁴ concerned the performance assessment of SAPT(DFT) with a wide selection of underlying density functionals. Reference 344 confirmed that the SAPT(CCSD) total energies recover the supermolecular CCSD(T) interaction energies better than any SAPT(DFT) variant and much better than SAPT0. Among the functionals tested, it was confirmed that the asymptotically corrected PBE0 one,^{345,346} which is the most popular choice in practical SAPT(DFT) calculations, is indeed one of the best performers, together with (also asymptotically corrected) B3LYP^{347,348} and M05.³⁴⁹ The benchmark SAPT(CCSD) values from Reference 344 have been employed to assess the quality of several new SAPT variants presented throughout this review. A subsequent SAPT(CCSD) benchmark study³⁵⁰ specifically targeted rare gas dimers, investigating the residual inaccuracies remaining in the many-body SAPT and SAPT(DFT) contributions close to the CBS limit.

4.2 | Improved expressions for exchange energies

As it was already mentioned, the exchange corrections in many-body SAPT (and SAPT(DFT)) other than $E_{\text{exch}}^{(10)}$ are normally computed within the single exchange approximation (Equation (31)) which runs into trouble at short range.^{100,101}

This presents a potential problem especially for the induction corrections: the $E_{\text{ind},\text{resp}}^{(20)}$ and $E_{\text{exch-ind},\text{resp}}^{(20)}$ (or $E_{\text{ind},\text{resp}}^{(30)}$ and $E_{\text{exch-ind},\text{resp}}^{(30)}$) contributions tend to cancel each other to a large extent, and an approximation to the exchange contribution might adversely affect this cancellation. Therefore, in 2012 Schäffer and Jansen introduced a new approach¹⁰⁶ that allows for computing the full, nonapproximated $E_{\text{exch-ind},\text{resp}}^{(20)}$ correction. This approach, later extended to the complete nonapproximated $E_{\text{exch-disp}}^{(20)}$,¹⁰⁷ expresses the matrix elements involving the full antisymmetrizer A by the first and second cofactors of the determinant built of overlap integrals between spinorbitals occupied in $\Psi_A^{(0)}\Psi_B^{(0)}$ and those occupied in different parts of $\Psi_{\text{RS}}^{(1)}$ (Equations (12)–(15)). The nonapproximated $E_{\text{exch}}^{(10)}$ correction has been available for a long time⁹⁹ and it is well known that the S^2 approximation somewhat underestimates this correction at short range. In the second order, the relative effects of the post- S^2 contributions are more pronounced, leading to a more significant underestimation of $E_{\text{exch-ind},\text{resp}}^{(20)}$, while $E_{\text{exch-disp}}^{(20)}$ is usually overestimated.¹⁰⁷ As far as the total SAPT0 interaction energy is concerned, any inaccuracies in $E_{\text{exch-ind},\text{resp}}^{(20)}$ are counterbalanced by the $\delta E_{\text{HF}}^{(2)}$ term of Equation (20), and the only effect of the S^2 approximation on the total result comes from the (usually small in absolute terms) inaccuracy of the $E_{\text{exch-disp}}^{(20)}$ correction. On the other hand, the effect of neglecting multiple exchanges on nonhybrid SAPT results (i.e., those without a HF delta term) is significant at short range. The approach of References 106 and 107 is equally valid for the second-order exchange corrections in SAPT(DFT). However, the intramolecular correlation corrections (of first and higher orders in W , Equation (18)) to many-body SAPT exchange energies cannot yet be computed without the S^2 approximation, so that the validity of the scaling approximations to post- S^2 effects for these terms (see Equation (33)) cannot be assessed at this time. For the $E_{\text{exch-ind},\text{resp}}^{(20)}$ and $E_{\text{exch-disp}}^{(20)}$ corrections of SAPT0 and SAPT(DFT), a thorough assessment of the effects missing in the S^2 approximation has been carried out¹⁰¹ for model complexes involving ions, which present a particularly difficult case due to strong binding and short intermolecular distances. It was found that the absolute errors coming from the exchange-dispersion term are quite minor, while the large short-range errors of $E_{\text{exch-ind},\text{resp}}^{(20)}(S^2)$ can be alleviated by the scaling of Equation (33) with the exponent $\alpha = 2$. As the full second-order exchange corrections of References 106 and 107 have only recently been implemented in publicly available electronic structure codes (specifically, Psi4²⁸⁰ and Molpro³⁵¹), more extensive assessments of the accuracy of the S^2 approximation are likely to appear in the near future.

On a more fundamental level, Gniewek and Jeziorski proposed an alternative approach to the calculation of exchange corrections from the wavefunctions of the polarization approximation, $\Psi_{\text{RS}}^{(n)}$.^{352,353} Instead of the SRS expressions (which, for the two lowest orders, are given by Equations (11)–(12)), the exchange energy of References 352 and 353 is computed by a variational formula that contains the full Hamiltonian H in place of the perturbation V and the polarization functions $\Psi_{\text{RS}}^{(n)}$ in both the bra and the ket. The new approach, which could be termed variational SRS (VSRS), was numerically tested for the $\text{H} \cdots \text{H}^+$ interaction. VSRS greatly improves the convergence rate of the leading terms in the asymptotic series for the exchange energy with either the multipole³⁵² or polarization³⁵³ expansion of the

wavefunction. Moreover, the latter convergence was much faster than the former, indicating that the polarization expansion is highly successful at both selectively summing multipole contributions to infinite order and including charge-overlap terms missing in the multipole approximation. The VSRS expressions are equally valid for the exchange energy between many-electron systems and it is quite likely that VSRS can lead to general-purpose exchange expressions with improved properties compared to standard SRS, however, this avenue of research has not yet been pursued in the literature.

4.3 | Beyond standard SAPT(DFT): Hybrid kernels, ab initio densities, and FDDSSs from the Bethe-Salpeter equation

The “standard” approach to calculating SAPT(DFT) energy corrections, used in all applications discussed above, utilizes the monomer orbitals and orbital energies (and thus also densities and density matrices) from KS calculations with an asymptotically corrected exchange-correlation potential, and the density response functions computed using TDDFT with the ALDA (or a combination of ALDA and TDHF for hybrid functionals) exchange-correlation kernel. While this level of approximation has been immensely successful at producing accurate total interaction energies and energy decompositions, a formally higher-level treatment is an option for all aspects of this “standard” approach. The possibility of replacing the ALDA kernel by a full nonadiabatic and nonlocal exact-exchange kernel (TDEXX) was explored by Hesselmann.³⁵⁴ His tests concluded that there is only a slight improvement over the dispersion energies calculated with the ALDA response kernel, however, both results are highly accurate as evidenced by comparisons of dispersion energy to $E_{\text{disp}}^{(2)}$ [CCD+ST(CCD)]¹⁰⁴ and by comparisons of total interaction energy to supermolecular CCSD(T). Hesselmann attributed the observed high accuracy at least partly to a new form of asymptotically corrected exchange-correlation potential also proposed in Reference 354, concluding that the influence of the potential on the resulting accuracy is significant but the influence of the kernel is minor. Further tests of the TDEXX response kernel focused on an alternative to the Casimir-Polder integration of Equation (9), utilizing a complete diagonalization of the TDDFT Hessian matrix made block diagonal by decoupling and approximating excitations with low oscillator strengths.³⁵⁵

Seeking to improve upon a different aspect of “standard” SAPT(DFT), Holzer and Klopper proposed³⁵⁶ to compute the induction and dispersion energies starting from the Green’s function-based *GW* approach on top of DFT, computing the response properties from the Bethe-Salpeter equation (BSE). Comparing to the accurate SAPT(CCSD) benchmarks from Reference 344 and to the standard SAPT(DFT) values obtained using the asymptotically corrected PBE0 functional, Reference 356 observed quite a nuanced picture where the individual induction and dispersion energies agreed with SAPT(CCSD) somewhat worse than standard SAPT(DFT), however, the total interaction energies from *GW*-based SAPT agreed with the supermolecular CCSD(T) benchmark even better than SAPT(CCSD). Overall, the upgrade from TDDFT to BSE response seemed to be somewhat beneficial more often than not, however, more tests of the new method are needed to make definite conclusions. One undeniable advantage of the SAPT(BSE) approach is that an asymptotic correction is no longer needed as the *GW* quasiparticle energies are valid approximations to ionization energies for all occupied orbitals.

Last but not least, while in a regular KS calculation the density is determined from the exchange-correlation potential, this procedure can be inverted to reconstruct the potential from an ab initio density. Such a procedure was used in the early SAPT(DFT) work of Hesselmann and Jansen³⁵⁷ to derive an essentially exact exchange-correlation potential for use in SAPT(DFT) calculations for the helium dimer. In the more general case, SAPT(DFT) calculations employing an ab initio derived potential, computed from Brueckner doubles densities using the Zhao-Morrison-Parr (ZMP)³⁵⁸ method, and the ALDA exchange correlation kernel have been investigated by Boese and Jansen.³⁵⁹ The resulting SAPT(ZMP) approach showed an overall improved performance over SAPT(DFT), in particular, essentially removing the overbinding of the latter in the case of rare gas dimers.³⁶⁰

4.4 | Explicitly correlated SAPT

One often overlooked advantage of a perturbation expansion like SAPT over a single number provided by the supermolecular approach is that different perturbation corrections can be computed in different basis sets to satisfy their distinct CBS convergence requirements. While many SAPT corrections, especially those contributing to the supermolecular HF interaction energy (cf. Equation (20)), rapidly approach their CBS limits, dispersion energy is notoriously the slowest

converging contribution and approaching its CBS value in conventional SAPT0, SAPT2, ... calculations requires large correlation-consistent basis sets augmented with diffuse functions.^{108,109} The slow convergence of dispersion energy is alleviated by the addition of “midbond” basis functions centered in the region where “dispersion happens,” that is, in between the interacting monomers.^{102,361,362} The (closely related) slow convergence of supermolecular interaction energies, computed, for example, with MP2 or CCSD(T), can be significantly improved by the addition of midbond functions, by the explicitly correlated approaches such as MP2-F12^{363,364} or CCSD(T)-F12b,^{365,366} or by a combination of both.^{367,368} Thus, it is worthwhile to examine if a similar explicitly correlated “SAPT-F12” approach can speed up the basis set convergence of standard SAPT, and the most important candidate for designing an improved -F12 counterpart is the second-order dispersion energy. The exchange-dispersion correction $E_{\text{exch-disp}}^{(20)}$, while usually small, converges in relative terms no better than $E_{\text{disp}}^{(20)}$, and it is also a valid target for improvement via an F12 *Ansatz*.

The first explicitly correlated SAPT calculations were performed for the helium dimer^{52,369,370} using a Gaussian-type geminal (GTG) basis³⁷¹ and an algorithm specific to two interacting two-electron systems. In addition to the complete first-order correction $E_{\text{elst}}^{(1)} + E_{\text{exch}}^{(1)}$, with the intramolecular correlation included at the exact (FCI) level, the GTG calculations of References 52 and 370 included $E_{\text{disp}}^{(20)}$, $E_{\text{disp}}^{(21)}$, and $E_{\text{exch-disp}}^{(20)}(S^2)$. The dispersion pair function needed for all three second-order corrections was obtained by minimizing a suitable Hylleraas functional. This pair function was sufficient for computing $E_{\text{disp}}^{(20)}$ and $E_{\text{exch-disp}}^{(20)}(S^2)$, while $E_{\text{disp}}^{(21)}$ requires also an MP2-like pair function describing intramolecular correlation in each monomer. All three corrections converge rapidly with the length of the GTG expansion³⁷⁰ and the accuracy of the CBS limits of the helium dimer SAPT corrections cannot be matched by conventional orbital basis sets.

Much more recently, Przybytek³⁷² generalized the Hylleraas functional of References 52 and 370 to an arbitrary closed-shell complex and proposed an explicitly correlated F12 *Ansatz* for the dispersion pair function in the spirit of the *Ansatz* for the MP2-F12 correlation energy.³⁶⁴ Przybytek went on to compute the leading-order dispersion correction, $E_{\text{disp}}^{(20)}\text{-F12}$, using the explicitly correlated dispersion amplitudes obtained by a full minimization of the Hylleraas functional, for a selection of model complexes including the entire A24 database.³⁷³ Reference 372 included a thorough investigation of the influence of the specific F12 *Ansatz*, and of the length-scale parameter of the exponential F12 correlation factor, on the quality of the results. Overall, $E_{\text{disp}}^{(20)}\text{-F12}$ was shown to converge substantially faster than ordinary $E_{\text{disp}}^{(20)}$, which is very encouraging and perhaps somewhat surprising as dispersion energy is a long-range effect depending on the dispersion pair functions delocalized over a large area rather than a short-range phenomenon highly sensitive to the interelectronic correlation cusp.

The development of SAPT-F12 is an ongoing research direction also in my group, and very recently our collaborators and we have performed³⁷⁴ the second step of this development by extending the work of Przybytek³⁷² in two directions. First, we have eliminated the bottlenecks of the full amplitude optimization, which leads to an N^8 scaling with the system size and often ill-conditioned numerical equations, by introducing two efficient approximations. The first one, the optimized diagonal *Ansatz* (ODA), sets all off-diagonal amplitudes to zero but computes the diagonal ones in an unrestricted optimization, and the second, the fixed-amplitude *Ansatz* (FIX), sets all these diagonal amplitudes to the same value obtained by a simple minimization of a quadratic function. Both approximations scale like N^5 with the system size similar to conventional $E_{\text{disp}}^{(20)}$ (albeit with a larger prefactor), are free from numerical instabilities, and lose very little accuracy³⁷⁴ compared to Przybytek’s *Ansatz* with fully optimized amplitudes. Even the simplest possible F12 correction to dispersion, the -F12(MP2) *Ansatz*²¹ utilizing a suitable partitioning of the local MP2-F12 pair functions, provides substantial improvement over conventional $E_{\text{disp}}^{(20)}$ although the individual results are a little more erratic.³⁷⁴ Second, we have employed the F12 amplitudes obtained from either *Ansatz* to derive and implement an F12 correction to $E_{\text{exch-disp}}^{(20)}(S^2)$, which was shown to significantly speed up the basis set convergence of the exchange-dispersion contribution, as illustrated in Figure 6 on the example of the CH₄–CH₄ complex. Our current implementation of $E_{\text{disp}}^{(20)}\text{-F12}$ and $E_{\text{exch-disp}}^{(20)}\text{-F12}$ avoids many-electron integrals with a suitable resolution of identity,^{375,376} however, the two-electron integrals are computed without any further approximations. In order to make the newly developed SAPT-F12 corrections competitive with conventional SAPT0, further speedup needs to be accomplished by a robust density fitting scheme³⁷⁷ for all two-electron quantities. Work in this direction is in progress in my group.

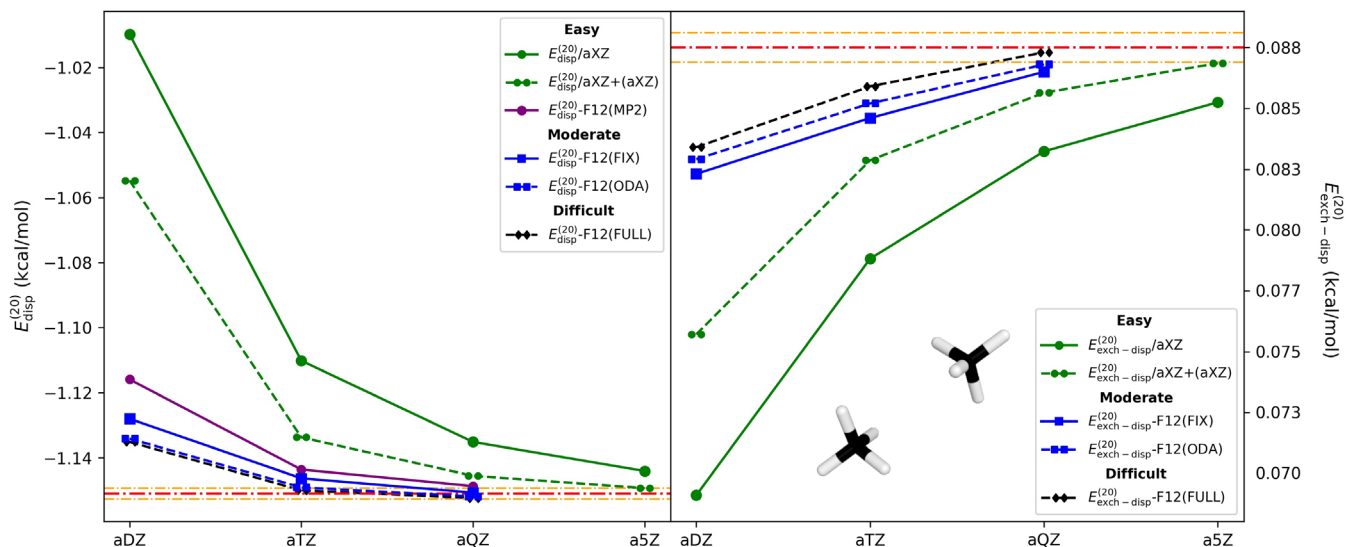


FIGURE 6 Convergence of the conventional and explicitly correlated $E_{\text{disp}}^{(20)}$ and $E_{\text{exch-disp}}^{(20)}$ SAPT corrections for the methane dimer with the orbital basis set aug-cc-pVXZ \equiv aXZ. The algorithm with full optimization of F12 dispersion amplitudes is denoted (FULL), and the approximate optimized diagonal Ansatz (ODA), fixed-amplitude Ansatz (FIX), and -F12(MP2) approaches are described in the text. The notation +(aXZ) signifies the addition of a hydrogenic aXZ set of midbond functions, with X the same as for the atom-centered part of the basis set. The rough grouping of different approaches according to their relative complexity has been illustrated by symbols used to rate the difficulty of North American ski trails. (Reprinted with permission from Reference 374. Copyright 2019 American Chemical Society)

4.5 | Relativistic effects in SAPT

Relativistic effects on the SAPT energy contributions can be included in a number of ways. If only scalar relativistic corrections are desired (which is normally sufficient for interactions between closed-shell molecules composed of atoms from the first four rows of the periodic table), one can use the second-order Douglas-Kroll-Hess Hamiltonian^{378,379} or, preferably, the exact two-component Hamiltonian transformed into the one-component basis (X2C-1c).^{380–382} In either case, only the one-electron integrals are altered by the relativistic approach, and any SAPT or SAPT(DFT) calculation proceeds as usual. Relativistic effective core potentials (ECPs)³⁸³ may also be used in SAPT, albeit with some caution. It has been observed³⁸⁴ that ECPs require a hybrid SAPT treatment, that is, the δE_{HF} correction of Equation (20) or (28) must be included. This observation was rationalized by the importance of intermolecular exchanges involving core electrons: core exchanges cannot be neglected in an accurate frozen-core approximation to SAPT³⁸⁴ and they might also be recovered insufficiently well by the common ECPs.

Beyond the scalar relativistic picture, Holzer and Klopper³⁸⁵ developed an algorithm, based on the two-component time-dependent DFT approach of Reference 386, to compute the SAPT(DFT) dispersion energy using two-component wavefunctions to account for the spin-orbit correction to dispersion. Numerical calculations for heavy rare gas dimers and a few other small complexes utilized both the X2C Hamiltonian, for which the difference between the two- and one-component results is entirely a consequence of spin-orbit coupling, and an ECP, for which some of the spin-orbit effects are likely missing and the corresponding difference is smaller. Overall, for closed-shell complexes studied in Reference 385, the spin-orbit effects were predictably small, but not negligible for the heaviest systems such as the radon dimer.

5 | BOOSTING THE EFFICIENCY OF SAPT

5.1 | Density fitting and related enhancements

In the last decade, the computational efficiency of the available SAPT and SAPT(DFT) computer implementations has greatly increased and it is now possible to apply SAPT energy decompositions to quite large complexes of chemical interest. This section presents the algorithmic developments, most notably the introduction of density fitting,^{387,388} that made this efficiency leap possible. First, I need to set the stage for the discussions that follow by comparing the MO and AO implementations of the SAPT corrections. At first, all many-body SAPT terms were derived and implemented using

the MO integrals, amplitudes, and intermediates—see References 77 and 79 for some representative examples. Such an approach requires transforming a variety of two-electron integrals from the AO basis to the MO one. A transformation of this kind normally scales like oN^4 with the number o of occupied orbitals on a given monomer and the size N of the AO basis set. It also requires a large amount of memory or disk to store intermediate quantities, and is hard to parallelize efficiently. An even more difficult case is presented by integrals with four virtual indices required for some higher-order SAPT corrections such as $E_{\text{elst,resp}}^{(13)}$, $E_{\text{exch}}^{(12)}$, and $E_{\text{disp}}^{(30)}$. The generation of a complete set of four-virtual MO integrals scales like vN^4 , with the number of virtual orbitals v typically much larger than o , and the matrices of all intermediates (as well as the final integrals) are also substantially larger. Similar four-virtual integrals constitute the most computationally demanding contribution to the CCSD doubles amplitudes, and modern CC codes tend to avoid a four-virtual AO→MO transformation by computing the respective diagram in the AO basis, transforming and back-transforming the (much less numerous) CCSD amplitudes as needed.³⁸⁹ Therefore, an AO-based algorithm has been introduced for the four-virtual terms in many-body SAPT quite some time ago⁹⁸ while continuing to evaluate all remaining terms in the MO basis. On a larger scale, the AO expressions for all SAPTO/SAPT(KS) terms other than dispersion and exchange dispersion have been introduced in Reference 123. The important advantage of computing the $E_{\text{elst}}^{(10)}$, $E_{\text{exch}}^{(10)}$, $E_{\text{ind,resp}}^{(20)}$, and $E_{\text{exch-ind,resp}}^{(20)}$ corrections in the AO basis is that the two-electron integrals

$$(KL|MN) = \iint \chi_K^*(\mathbf{r}_1) \chi_L(\mathbf{r}_1) \frac{1}{|\mathbf{r}_1 - \mathbf{r}_2|} \chi_M^*(\mathbf{r}_2) \chi_N(\mathbf{r}_2) d\mathbf{r}_1 d\mathbf{r}_2, \quad (39)$$

computed over the quadruplets of AO basis functions χ_P , are the only four-index terms that enter the working expressions, and they only do so in the form of *generalized Coulomb and exchange matrices*

$$\mathbf{J}[\mathbf{X}]_{KL} = \sum_{MN} (KL|MN) \mathbf{X}_{MN} \quad \mathbf{K}[\mathbf{X}]_{KL} = \sum_{MN} (KM|NL) \mathbf{X}_{MN}, \quad (40)$$

for some two-index quantity \mathbf{X} (note that Equation (40) reduces to the standard Coulomb and exchange matrices if \mathbf{X} is the HF density matrix). The task of computing generalized Coulomb and exchange matrices is a common bottleneck for one-electron electronic structure theories such as HF and extensive effort has been directed to improve its computational efficiency. Therefore, the common feature of all efficient $E_{\text{elst}}^{(10)}$, $E_{\text{exch}}^{(10)}$, $E_{\text{ind,resp}}^{(20)}$, and $E_{\text{exch-ind,resp}}^{(20)}$ computations^{256–258,277,281,390,391} is the use of an AO algorithm coupled with an efficient evaluation of generalized Coulomb and exchange matrices. The $E_{\text{exch-disp}}^{(20)}$ correction is not fully expressible through the matrices of Equation (40) and other techniques must be used to speed up its evaluation.

Density fitting is a way of expressing four-index quantities such as two-electron integrals and dispersion amplitudes via auxiliary three-index quantities.^{144,388} This significantly reduces time and storage requirements of electronic structure algorithms, and in many cases also improves the scaling with the system size. Density fitting has greatly enhanced the computational capabilities of many popular methods including MP2^{392,393} and CCSD(T).³⁹⁴ In the context of SAPT, density fitting was first applied to the evaluation of FDDSSs, Equation (10), in the CKS dispersion expression for SAPT(DFT),^{119,123,146} reducing the overall scaling of SAPT(DFT) from N^6 to N^5 .

The benefits of density fitting were brought to SAPTO³⁹⁵ and many-body SAPT³⁹⁶ by Hohenstein and Sherrill. In the SAPTO case, the formal scaling remains N^5 , but the scaling with the orbital (N_{AO}) and auxiliary (N_{aux}) basis set sizes for a particular complex is reduced from N_{AO}^4 to $N_{\text{AO}}^2 N_{\text{aux}}$. The memory and storage requirements of the SAPTO algorithm are also significantly reduced by density fitting as the four-index AO integrals do not need to be either computed or transformed to the molecular orbital basis. For intramonomer correlation corrections beyond SAPTO,³⁹⁶ density fitting alleviates the storage bottlenecks and improves the formal scaling of some energy terms. Unfortunately, this is not the case for the most expensive term at the SAPT2+ and SAPT2+(3) levels (Equations (23)–(24)), the triples contribution to $E_{\text{disp}}^{(22)}$. For this term, significant speedup is however possible by truncating the size of the virtual space, and the error of this truncation is made much smaller by the use of MP2 natural orbitals in place of the canonical HF orbitals, and by the scaling of the resulting truncated $E_{\text{disp}}^{(22)}$ triples contribution by the ratio of the full and truncated $E_{\text{disp}}^{(20)}$ values.³⁹⁷ Further speedup of the various levels of many-body SAPT is possible by factorizing energy denominators using the Laplace transformation³⁹⁸ and extending the natural orbital truncation technique to $E_{\text{disp}}^{(2)} [\text{CCD+ST(CCD)}]$.³⁹⁹ Thanks to the

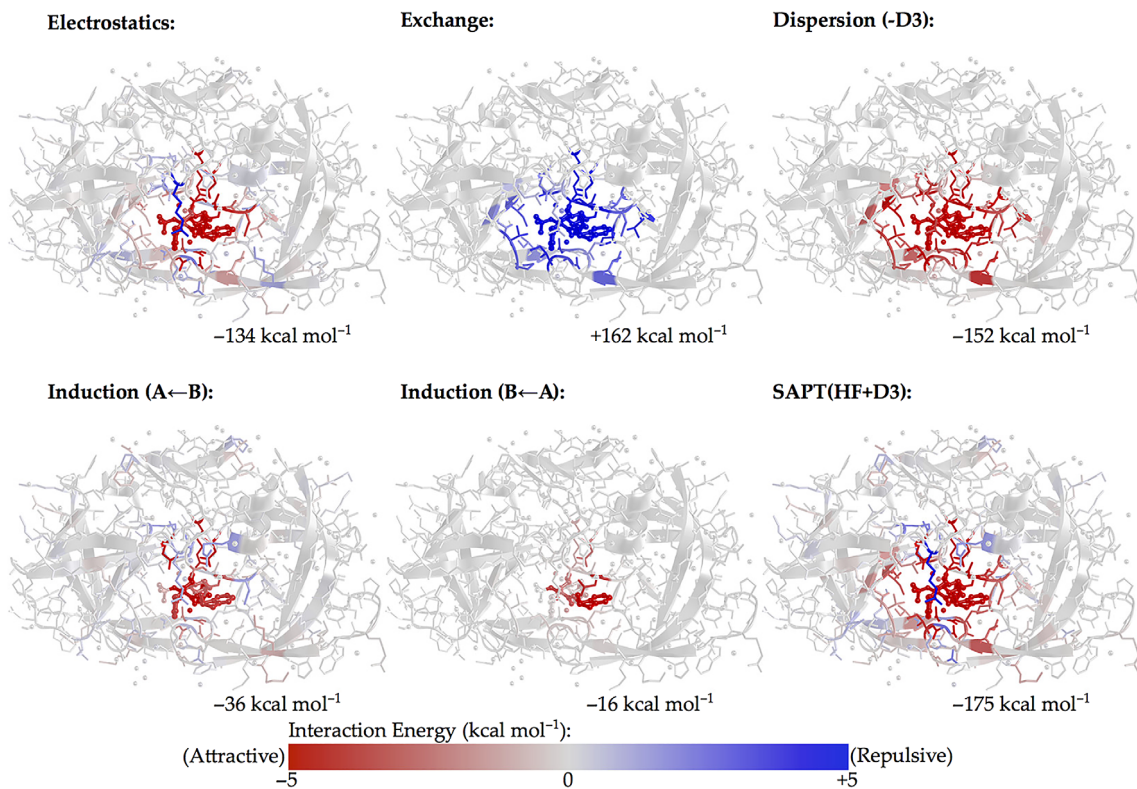


FIGURE 7 The order-1 F-SAPT/6-31G* interaction energy decomposition for the indinavir @ HIV-II protease complex, the largest system to date studied by any variant of SAPT. All atoms in each fragment are colored according to the contribution for the full fragment. (Reprinted with permission from Reference 391. Copyright 2018 American Chemical Society)

density fitting and other improvements, it has been possible to run both SAPTO³⁹⁸ and CKS dispersion⁴⁰⁰ for complexes with more than 200 atoms, and an F-SAPT analysis at an approximate SAPTO level³⁹¹ has been applied to the full indinavir @ HIV-II protease complex, with more than 3,000 atoms, as illustrated in Figure 7.

Density-fitted SAPT calculations typically use two auxiliary basis sets. The (aug-)cc-pVXZ-JKFIT family⁴⁰¹ is appropriate for fitting all generalized Coulomb and exchange matrices of Equation (40) while the (aug-)cc-pVXZ-RI sets^{402,403} are suitable for fitting occupied-virtual orbital products such as the ones entering the dispersion amplitudes. The default auxiliary bases with the cardinal number X the same as for the orbital basis are sufficient for most purposes. However, one needs to be extra careful when computing interaction energies in the asymptotic regime as the contributions from a given auxiliary function to a fitted orbital product decay very slowly with distance.⁴⁰⁴ In the extreme case, density fitting can lead to an unphysical long-range behavior of electrostatic energy⁴⁰⁵ in the form of a spurious charge-charge interaction when the fitted density does not exactly integrate out to the correct number of electrons.

5.2 | Efficient treatment of many-body induction: The XSAPT approach

Among the three-body SAPT contributions discussed in Section 3.5, induction energy is usually one of the most important. The source of the induction nonadditivity is the simple observation that the extent of the electronic polarization exerted on molecule A by molecule B changes when the latter molecule is itself polarized by molecule C. This observation makes it clear that all permutations of (A,B,C) in the above scheme of mutual polarization contribute to the nonadditive induction energy, and so do any chain processes of A₁ polarizing A₂ which then polarizes A₃ which then polarizes A₄ ..., irrespective of the chain length and the number of molecules in the system. Thus, induction energy exhibits both three-body and higher-body nonadditivity, and it might be advantageous to treat the chains of mutual polarization to self-consistency. A self-consistent treatment of electronic polarization is highly popular within the force-field community, where it is often modeled by a system of coupled classical Drude oscillators.⁴⁰⁶ However, applying self-consistent polarization within standard SAPT runs into the danger of mutual overpolarization, as the

intermolecular Pauli exclusion principle is not enforced in the polarization expansion (Equations (5)–(6)) and the electrons might fall into the Coulomb wells around the other monomer' nuclei (which is exactly the reason for the overall divergence of the RS expansion⁵⁸). Therefore, combining SAPT with self-consistent many-body induction is a delicate matter, but an efficient and practical approach for doing so has been developed by Herbert and coworkers^{230,231,407–409} under the name XSAPT.

XSAPT borrows the self-consistent treatment of many-body induction for a molecular cluster from the XPol method of Xie et al.^{410,411} The latter approach involves a doubly self-consistent procedure. At the inner level, the HF equations for one fragment at a time are solved in the presence of an electrostatic embedding, that is, a set of point charges representing the remaining fragments. At the outer level, the fragments are polarized, and their point charges adjusted, one by one, so that at convergence the cause (the point charges) matches the effect (the polarized electron density) for each fragment. Such an approach obviously ignores the effects of interfragment exchange and dispersion and in the original XPol method these effects were taken into account using empirical Lennard-Jones terms. In XSAPT, standard pairwise-additive corrections from SAPT0 or SAPT(KS) are used instead, with the one-electron embedding terms removed from the perturbation operator to avoid double counting.^{407,408} The keys to preventing overpolarization are the use of absolutely localized molecular orbitals (ALMO),⁴¹² expanded only in the basis functions centered on the same fragment, and the “CHarges from ELECTrostatic Potential using a Grid-based method” (CHELPG) algorithm to select embedding charges⁴¹³ rather than a simpler choice of Mulliken or Löwdin charges. It should be stressed that XPol provides the zeroth-order energy and wavefunction for XSAPT, where the many-body induction is already included to self-consistency. XSAPT does provide additional induction effects on top of the XPol picture, but it is assumed that these effects are limited to a pairwise additive term and a three-body induction and exchange-induction coupling term.⁴⁰⁸ The XSAPT approach has been thoroughly tested on both dimers and neutral and ionic clusters, and has done a respectable job on the difficult problem of the energetic ordering of different structures of the water hexamer.^{414,415} On the negative side, the quality of XSAPT data is highly sensitive (and fairly unsystematic) with respect to the one-electron basis set, an issue that is partly inherited from the SAPT0 dispersion employed, which is known to be overestimated at CBS for dispersion-bound systems.⁶ This is not a major problem as XSAPT is intended to be a fast, practical, and qualitatively correct method for estimating noncovalent interaction energies in large systems even if its success hinges on error cancellation. In accordance with this goal, further development of XSAPT proceeded in the direction of making the calculations even faster, at the price of replacing the SAPT(KS) dispersion and exchange dispersion terms by a suitable empirical atom-pairwise expression and neglecting three-body induction and exchange-induction couplings.^{230,231,409} The most recent enhancements to the XSAPT methodology include an efficient AO-based implementation²⁵⁸ that enables the study of large noncovalent complexes such as the S12L database,¹⁵⁷ a correction for dispersion nonadditivity based either on the comparison⁴¹⁶ of XSAPT dispersion (for monomers mutually polarized by the XPol embedding) and SAPT dispersion (for unperturbed monomers) or on the many-body dispersion (MBD)⁴¹⁷ model originally developed for DFT,⁴¹⁸ and a new, significantly faster charge embedding scheme to replace CHELPG.⁴¹⁹

5.3 | Local, linear scaling, and graphics processing unit implementations

The last class of recent SAPT enhancements discussed in this review are the approximations that can be made for very large complexes when even the SAPT0 level of theory is out of reach. The developments presented in this section are possible due to spatial locality of electron correlation, improvements in the computer implementation, and/or a replacement of the most expensive SAPT0 terms by their empirical approximations.

A linear scaling, localized approach to electrostatic⁴²⁰ and (FDDs-based) dispersion⁴²¹ energies was proposed by Szalewicz and coworkers. In this approach, each monomer is split into the “near-range” (NR) and “far-range” (FR) regions according to the proximity to the other monomer. Now, the SAPT contributions coming from the NR-NR intermolecular interactions are computed ab initio, with a full account of charge-overlap effects, while the NR-FR, FR-NR, and FR-FR contributions are approximated by inexpensive asymptotic formulas based on the distributed multipole expansion. It is worth noting that a reasonable reproduction of dispersion energies by a localized approach requires⁴²¹ a special form of density fitting for the FDDs with additional constraints to minimize the “charge-flow” terms on the edge of the NR and FR regions.

Among the SAPT0 and/or SAPT(DFT) terms, the most computationally demanding (up to N^5) ones are the dispersion and exchange dispersion contributions. Therefore, a possible replacement of $E_{\text{disp}}^{(2)} + E_{\text{exch-disp}}^{(2)}$ by a suitable empirical

expression will lead to a major improvement in computational efficiency. It should be noted that, as long as the $\delta E_{\text{HF}}^{(2)}$ correction of Equation (20) is included, the use of empirical dispersion makes SAPT0 interaction energies exactly equivalent to the long-standing “HF plus dispersion” (HFD) approach,⁸⁸ with the additional decomposition of the HF part of the HFD energy into distinct physical contributions. When SAPT0 is replaced by SAPT(DFT), the HFD interaction energy is augmented with the corrections for intramolecular correlation on the electrostatic, exchange, induction, and exchange-induction energies. It has been argued that the first two of these corrections (the first-order ones) are the most important, and their inclusion on top of HFD was proposed in Reference 226, leading to a method denoted HFDc⁽¹⁾ with the SAPT(DFT) dispersion and HFD_{as}c⁽¹⁾ with an empirical dispersion. Thus, Reference 226 was probably the first study combining a variant of SAPT with a force-field-like atom-pairwise dispersion expression. Shortly thereafter, Hesselmann²²⁹ developed a new atom-pairwise dispersion correction to be combined with all nondispersion terms from SAPT(DFT), leading to an efficient approximation termed SAPT+D. Another dispersion correction for the same purpose, constructed similarly to Grimme’s DFT-D3 method²³² but with a modified short-range damping function, was proposed by Sedlak and Řezáč.⁴²² As presented in Section 5.2, a similar strategy was adopted by Lao and Herbert to improve the efficiency of their XSAPT approach^{230,231,409}; in fact, the first two generations of dispersion expressions in XSAPT were taken from References 229 and 226. Note that, for reasons that were discussed earlier, the empirical dispersion expressions for SAPT+D and related methods might benefit from different damping functions than the analogous expressions for DFT+D,^{232,233} so that the physical, overlap-including dispersion is taken into account at short range instead of being switched off to eliminate double counting with DFT.

An approximate SAPT variant applicable to the largest systems was proposed recently by Martínez and collaborators.³⁹¹ This variant owes its impressive efficiency to the combination of empirical dispersion in place of $E_{\text{disp}}^{(20)} + E_{\text{exch-disp}}^{(20)}$, the use of nonaugmented basis sets to maximize the benefits of integral screening (note that diffuse basis functions are particularly important for dispersion, which is not computed anyway), and the interface to a highly efficient code that performs generalized Coulomb and exchange contractions of Equation (40) on graphics processing units (GPUs). The approximate SAPT0 and F-SAPT GPU-accelerated code of Reference 391 shattered all the records for the system sizes treatable by SAPT, enabling a calculation with over 3,000 atoms and over 25,000 basis functions (Figure 7). The -D3 dispersion expression with the Becke-Johnson damping²³³ and the parameters optimized for HF, employed in the study of Reference 391, does a respectable job recovering SAPT(DFT) dispersion and exchange dispersion energies.⁴²³ However, as the authors of Reference 391 stated themselves, the accuracy of the approximate approach might still benefit from a replacement of the DFT-derived atom–atom dispersion expression by one that is targeted for SAPT. I conclude this section by mentioning a variant proposed by Ochsenfeld and collaborators³⁹⁰ which is intermediate between SAPT0 and SAPT+D, that is, $E_{\text{disp}}^{(20)}$ is computed ab initio and only $E_{\text{exch-disp}}^{(20)}$ is approximated via an empirical scaling of $E_{\text{disp}}^{(20)}$. In this approach, all remaining SAPT0 terms (including $E_{\text{disp}}^{(20)}$) are efficiently computed from linear-scaling AO-based implementations with extensive integral prescreening, allowing for the applications of such an approximate SAPT0 variant to systems up to 1,100 atoms on conventional (non-GPU) computers.

6 | CONCLUSIONS

It has been a very successful decade for SAPT and SAPT(DFT). Thanks to the new and improved computer implementations, the size of systems to which these methods can be applied has increased significantly, and the quantity and breadth of applications keeps growing every year. In addition to a stand-alone SAPT/SAPT(DFT) code,⁴²⁴ various flavors of SAPT are now available in several general-purpose quantum chemistry packages, including Molpro,³⁵¹ Psi4,²⁸⁰ and Q-Chem.⁴²⁵ While approaches such as SAPT0, SAPT(DFT), or SAPT2+(3) have become the common method of choice for quantifying and analyzing intermolecular interactions, many novel SAPT-based techniques have been developed in recent years, and my main goal while writing this review has been to introduce the recent advances that have made SAPT more accurate, more efficient, and more robust. It is quite likely that 10 years from now some of these new SAPT variants will be as routine as SAPT0 and SAPT(DFT) are today.

The development of perturbative approaches to noncovalent interactions remains an active field of research, and there are many loose ends in the theory that still need to be tied. To name just a few examples, the computational chemistry community is looking forward to

- Further advances in the SAPT methodology for open-shell complexes, including systems with significant static correlation, spin splittings, and/or quasidegeneracy.
- Continued progress in the development of efficient SAPT approximations applicable to very large dimers and clusters.
- The development of SAPT analytical gradients and of new formalisms applicable to embedded systems, including noncovalent interactions in solution.
- Improved methods to quantify and describe intramolecular noncovalent interactions.

On a final note, my personal least favorite SAPT term is the $\delta E_{HF}^{(2)}$ correction of Equation (20) or (28). I consider its presence as an admission that pure SAPT has a difficulty that cannot be fully resolved from within, and it requires outside help in a form of supermolecular HF. However, the $\delta E_{HF}^{(2)}$ term brings about unphysical contributions in addition to physical high-order induction and exchange-induction effects, is cumbersome to calculate (especially on top of SAPT(DFT) where no part of the $\delta E_{HF}^{(2)}$ calculation can be reused for any other terms), and is inherently nonlocal and not amenable to, for example, a rigorous F-SAPT partition. Therefore, I am particularly fond of advances in the pure SAPT methodology that eliminate the need for including $\delta E_{HF}^{(2)}$ for more classes of interacting complexes, relegating this correction to a fairly limited class of highly polarizable systems where high-order induction effects are particularly important. These advances come in the form of more accurate descriptions of intramolecular correlation and improved exchange corrections that do not rely on the single-exchange approximation. Several such advances have been described in this review, and some others will hopefully appear soon.

ACKNOWLEDGMENTS

I thank Professor Bogumił Jeziorski and Professor Krzysztof Szalewicz for reading and commenting on the manuscript.

CONFLICT OF INTEREST

The author has declared no conflicts of interest for this article.

ORCID

Konrad Patkowski  <https://orcid.org/0000-0002-4468-207X>

RELATED WIREs ARTICLES

[Symmetry-adapted perturbation theory based on density functional theory for noncovalent interactions](#)

[Wavefunction methods for the accurate characterization of water clusters](#)

[Finding chemical concepts in the Hilbert space: Coupled cluster analyses of noncovalent interactions](#)

[Wavefunction methods for noncovalent interactions](#)

[Symmetry-adapted perturbation theory of intermolecular forces](#)

REFERENCES

1. Przybytek M, Cencek W, Jeziorski B, Szalewicz K. Pair potential with submillikelvin uncertainties and nonadiabatic treatment of the halo state of the helium dimer. *Phys Rev Lett.* 2017;119:123401.
2. Sure R, Grimme S. Comprehensive benchmark of association (free) energies of realistic host-guest complexes. *J Chem Theory Comput.* 2015;11:3785–3801.
3. Riley KE, Hobza P. Noncovalent interactions in biochemistry. *WIREs Comput Mol Sci.* 2011;1:3–17.
4. Grimme S. Density functional theory with London dispersion corrections. *WIREs Comput Mol Sci.* 2011;1:211–228.
5. Szalewicz K. Symmetry-adapted perturbation theory of intermolecular forces. *WIREs Comput Mol Sci.* 2012;2:254–272.
6. Hohenstein EG, Sherrill CD. Wavefunction methods for noncovalent interactions. *WIREs Comput Mol Sci.* 2012;2:304–326.
7. Jansen G. Symmetry-adapted perturbation theory based on density functional theory for noncovalent interactions. *WIREs Comput Mol Sci.* 2014;4:127–144.
8. Howard JC, Tschumper GS. Wavefunction methods for the accurate characterization of water clusters. *WIREs Comput Mol Sci.* 2014;4:199–224.
9. Wolters LP, Schyman P, Pavan MJ, Jorgensen WL, Bickelhaupt FM, Kozuch S. The many faces of halogen bonding: A review of theoretical models and methods. *WIREs Comput Mol Sci.* 2014;4:523–540.

10. Hoja J, Reilly AM, Tkatchenko A. First-principles modeling of molecular crystals: Structures and stabilities, temperature and pressure. *WIREs Comput Mol Sci.* 2017;7:e1294.
11. Fang T, Li Y, Li S. Generalized energy-based fragmentation approach for modeling condensed phase systems. *WIREs Comput Mol Sci.* 2017;7:e1297.
12. Murray JS, Politzer P. Molecular electrostatic potentials and noncovalent interactions. *WIREs Comput Mol Sci.* 2017;7:e1326.
13. Demerdash O, Wang LP, Head-Gordon T. Advanced models for water simulations. *WIREs Comput Mol Sci.* 2018;8:e1355.
14. Tang X, Du A, Kou L. Gas sensing and capturing based on two-dimensional layered materials: Overview from theoretical perspective. *WIREs Comput Mol Sci.* 2018;8:e1361.
15. Bistoni G. Finding chemical concepts in the Hilbert space: Coupled cluster analyses of noncovalent interactions. *WIREs Comput Mol Sci.* 2019;9:e1442.
16. Corminboeuf C. Minimizing density functional failures for non-covalent interactions beyond van der Waals complexes. *Acc Chem Res.* 2014;47:3217–3224.
17. Cho Y, Cho WJ, Youn IS, Lee G, Singh NJ, Kim KS. Density functional theory based study of molecular interactions, recognition, engineering, and quantum transport in π molecular systems. *Acc Chem Res.* 2014;47:3321–3330.
18. Phipps MJS, Fox T, Tautermann CS, Skylaris CK. Energy decomposition analysis approaches and their evaluation on prototypical protein-drug interaction patterns. *Chem Soc Rev.* 2015;44:3177–3211.
19. Grimme S, Hansen A, Brandenburg JG, Bannwarth C. Dispersion-corrected mean-field electronic structure methods. *Chem Rev.* 2016;116:5105–5154.
20. Řezáč J, Hobza P. Benchmark calculations of interaction energies in noncovalent complexes and their applications. *Chem Rev.* 2016;116:5038–5071.
21. Frey JA, Holzer C, Klopper W, Leutwyler S. Experimental and theoretical determination of dissociation energies of dispersion-dominated aromatic molecular complexes. *Chem Rev.* 2016;116:5614–5641.
22. Cisneros GA, Wikfeldt KT, Ojamäe L, et al. Modeling molecular interactions in water: From pairwise to many-body potential energy functions. *Chem Rev.* 2016;116:7501–7528.
23. Dubecý M, Mitas L, Jurečka P. Noncovalent interactions by quantum Monte Carlo. *Chem Rev.* 2016;116:5188–5215.
24. Beran GJO. Modeling polymorphic molecular crystals with electronic structure theory. *Chem Rev.* 2016;116:5567–5613.
25. McDaniel JG, Schmidt JR. Next-generation force fields from symmetry-adapted perturbation theory. *Annu Rev Phys Chem.* 2016;67:467–488.
26. Hermann J, DiStasio RA Jr, Tkatchenko A. First-principles models for van der Waals interactions in molecules and materials: Concepts, theory, and applications. *Chem Rev.* 2017;117:4714–4758.
27. Patkowski K. Benchmark databases of intermolecular interaction energies: Design, construction, and significance. In: Dixon DA, editor. *Annual reports in computational chemistry*. Volume 13. Amsterdam: Elsevier, 2017; p. 3–91.
28. Pastorczak E, Corminboeuf C. Perspective: Found in translation: Quantum chemical tools for grasping noncovalent interactions. *J Chem Phys.* 2017;146:120901.
29. Grynn'ova G, Lin KH, Corminboeuf C. Read between the molecules: Computational insights into organic semiconductors. *J Am Chem Soc.* 2018;140:16370–16386.
30. Al-Hamdani YS, Tkatchenko A. Understanding non-covalent interactions in larger molecular complexes from first principles. *J Chem Phys.* 2019;150:010901.
31. Kodrycka M, Patkowski K. Platinum, gold, and silver standards of intermolecular interaction energy calculations. *J Chem Phys.* 2019;151:070901.
32. Stöhr M, Van Voorhis T, Tkatchenko A. Theory and practice of modeling van der Waals interactions in electronic-structure calculations. *Chem Soc Rev.* 2019;48:4118–4154.
33. Chałasiński G, Szczęśniak MM. State of the art and challenges of the *ab initio* theory of intermolecular interactions. *Chem Rev.* 2000;100:4227–4252.
34. Bartlett RJ, Musiał M. Coupled-cluster theory in quantum chemistry. *Rev Mod Phys.* 2007;79:291–352.
35. Raghavachari K, Trucks GW, Pople JA, Head-Gordon M. A 5th-order perturbation comparison of electron correlation theories. *Chem Phys Lett.* 1989;157:479–483.
36. Burns LA, Marshall MS, Sherrill CD. Appointing silver and bronze standards for noncovalent interactions: A comparison of spin-component-scaled (SCS), explicitly correlated (F12), and specialized wavefunction approaches. *J Chem Phys.* 2014;141:234111.
37. Andrés J, Ayers PW, Boto RA, et al. Nine questions on energy decomposition analysis. *J Comput Chem.* 2019;40:2248–2283.
38. Kitaura K, Morokuma K. A new energy decomposition scheme for molecular interactions within the Hartree-Fock approximation. *Int J Quantum Chem.* 1976;10:325–340.
39. Chen W, Gordon MS. Energy decomposition analyses for many-body interaction and applications to water complexes. *J Phys Chem.* 1996;100:14316–14328.
40. Su P, Li H. Energy decomposition analysis of covalent bonds and intermolecular interactions. *J Chem Phys.* 2009;131:014102.
41. Glendening ED, Streitwieser A. Natural energy decomposition analysis: An energy partitioning procedure for molecular interactions with application to weak hydrogen bonding, strong ionic, and moderate donor-acceptor interactions. *J Chem Phys.* 1994;100:2900–2909.
42. Blanco MA, Pendás AM, Francisco E. Interacting quantum atoms: A correlated energy decomposition scheme based on the quantum theory of atoms in molecules. *J Chem Theory Comput.* 2005;1:1096–1109.

43. Ghosh D, Kosenkov D, Vanovschi V, et al. Noncovalent interactions in extended systems described by the effective fragment potential method: Theory and application to nucleobase oligomers. *J Phys Chem A.* 2010;114:12739–12754.
44. Gordon MS, Fedorov DG, Pruitt SR, Slipchenko LV. Fragmentation methods: A route to accurate calculations on large systems. *Chem Rev.* 2012;112:632–672.
45. Khalil RZ, Cobas EA, Lochan RC, Bell AT, Head-Gordon M. Unravelling the origin of intermolecular interactions using absolutely localized molecular orbitals. *J Phys Chem A.* 2007;111:8753–8765.
46. Thirman J, Head-Gordon M. An energy decomposition analysis for second-order Møller-Plesset perturbation theory based on absolutely localized molecular orbitals. *J Chem Phys.* 2015;143:084124.
47. Horn PR, Mao Y, Head-Gordon M. Probing non-covalent interactions with a second generation energy decomposition analysis using absolutely localized molecular orbitals. *Phys Chem Chem Phys.* 2016;18:23067–23079.
48. Schneider WB, Bistoni G, Sparta M, et al. Decomposition of intermolecular interaction energies within the local pair natural orbital coupled cluster framework. *J Chem Theory Comput.* 2016;12:4778–4792.
49. Flick JC, Kosenkov D, Hohenstein EG, Sherrill CD, Slipchenko LV. Accurate prediction of noncovalent interaction energies with the effective fragment potential method: Comparison of energy components to symmetry-adapted perturbation theory for the S22 test set. *J Chem Theory Comput.* 2012;8:2835–2843.
50. Tan SYS, Izgorodina EI. Comparison of the effective fragment potential method with symmetry-adapted perturbation theory in the calculation of intermolecular energies for ionic liquids. *J Chem Theory Comput.* 2016;12:2553–2568.
51. Stasyuk OA, Sedlak R, Fonseca Guerra C, Hobza P. Comparison of the DFT-SAPT and canonical EDA schemes for the energy decomposition of various types of noncovalent interactions. *J Chem Theory Comput.* 2018;14:3440–3450.
52. Korona T, Williams HL, Bukowski R, Jeziorski B, Szalewicz K. Helium dimer potential from symmetry-adapted perturbation theory calculations using large Gaussian geminal and orbital basis sets. *J Chem Phys.* 1997;106:5109–5122.
53. Korona T, Moszyński R, Jeziorski B. Convergence of symmetry-adapted perturbation theory for the interaction between helium atoms and between a hydrogen molecule and a helium atom. *Adv Quantum Chem.* 1997;28:171–188.
54. Korona T, Jeziorski B, Moszyński R, Diercksen GHF. Degenerate symmetry-adapted perturbation theory of weak interactions between closed- and open-shell monomers: Application to Rydberg states of helium hydride. *Theor Chem Acc.* 1999;101:282–291.
55. Przybytek M, Patkowski K, Jeziorski B. Convergence behavior of symmetry-adapted perturbation expansions for excited states. A model study of interactions involving a triplet helium atom. *Collect Czech Chem Commun.* 2004;69:141–176.
56. Patkowski K, Korona T, Jeziorski B. Convergence behavior of the symmetry-adapted perturbation theory for states submerged in Pauli forbidden continuum. *J Chem Phys.* 2001;115:1137–1152.
57. Patkowski K, Jeziorski B, Korona T, Szalewicz K. Symmetry-forcing procedure and convergence behavior of perturbation expansions for molecular interaction energies. *J Chem Phys.* 2002;117:5124–5134.
58. Patkowski K, Jeziorski B, Szalewicz K. Unified treatment of chemical and van der Waals forces via symmetry-adapted perturbation expansion. *J Chem Phys.* 2004;120:6849–6862.
59. Hirschfelder JO, Byers Brown W, Epstein ST. Recent developments in perturbation theory. *Adv Quantum Chem.* 1964;1:255–374.
60. Hirschfelder JO. Perturbation theory for exchange forces, I. *Chem Phys Lett.* 1967;1:325–329.
61. Kutzelnigg W. The ‘primitive’ wave function in the theory of intermolecular interactions. *J Chem Phys.* 1980;73:343–359.
62. Adams WH. On the limits of validity of the symmetrized Rayleigh-Schrödinger perturbation theory. *Int J Quantum Chem.* 1996;60:273–285.
63. Ahlrichs R. Convergence properties of the intermolecular force series (1/R-expansion). *Theor Chim Acta.* 1976;41:7–15.
64. Stone AJ. *The theory of intermolecular forces.* 2nd Edition: Oxford University Press, 2013.
65. Hohenstein EG, Duan J, Sherrill CD. Origin of the surprising enhancement of electrostatic energies by electron-donating substituents in substituted sandwich benzene dimers. *J Am Chem Soc.* 2011;133:13244–13247.
66. Gryn'ova G, Corminboeuf C. Implications of charge penetration for heteroatom-containing organic semiconductors. *J Phys Chem Lett.* 2016;7:5198–5204.
67. Eisenschitz R, London F. Über das Verhältnis der van der Waalsschen Kräfte zu den homöopolaren Bindungskräften. *Z Phys.* 1930;60:491–527.
68. Longuet-Higgins HC. Spiers memorial lecture: Intermolecular forces. *Disc Farad Soc.* 1965;40:7–18.
69. Jaszunski M, McWeeny R. Time-dependent Hartree-Fock calculations of dispersion energy. *Mol Phys.* 1985;55:1275–1286.
70. Misquitta AJ, Jeziorski B, Szalewicz K. Dispersion energy from density-functional theory description of monomers. *Phys Rev Lett.* 2003;91:033201.
71. Casimir HBG, Polder D. The influence of retardation on the London-van der Waals forces. *Phys Rev.* 1948;73:360–372.
72. Szalewicz K, Patkowski K, Jeziorski B. Intermolecular interactions via perturbation theory: From diatoms to biomolecules. *Struct Bonding.* 2005;116:43–117.
73. Jeziorski B, Szalewicz K, Chalański G. Symmetry forcing and convergence properties of perturbation expansions for molecular interaction energies. *Int J Quantum Chem.* 1978;14:271–287.
74. Stone AJ, Misquitta AJ. Atom-atom potentials from *ab initio* calculations. *Int Rev Phys Chem.* 2007;26:193–222.
75. Misquitta AJ, Stone AJ. Ab initio atom-atom potentials using CamCASP: Theory and application to many-body models for the pyridine dimer. *J Chem Theory Comput.* 2016;12:4184–4208.
76. Andreev EA. On asymptotic calculation of the exchange interaction. *Theor Chim Acta.* 1973;28:235–239.

77. Rybak S, Jeziorski B, Szalewicz K. Many-body symmetry-adapted perturbation theory of intermolecular interactions—H₂O and HF dimers. *J Chem Phys.* 1991;95:6579–6601.
78. Moszyński R, Jeziorski B, Ratkiewicz A, Rybak S. Many-body perturbation theory of electrostatic interactions between molecules: Comparison with full configuration interaction for four-electron dimers. *J Chem Phys.* 1993;99:8856–8869.
79. Moszyński R, Jeziorski B, Rybak S, Szalewicz K, Williams HL. Many-body theory of exchange effects in intermolecular interactions. Density matrix approach and applications to He-F[−], He-HF, H₂-HF, and Ar-H₂ dimers. *J Chem Phys.* 1994;100:5080–5093.
80. Moszyński R, Jeziorski B, Szalewicz K. Many-body theory of exchange effects in intermolecular interactions. Second-quantization approach and comparison with full configuration interaction results. *J Chem Phys.* 1994;100:1312–1325.
81. Jeziorski B, Moszynski R, Ratkiewicz A, Rybak S, Szalewicz K, Williams HL. SAPT: A program for many-body symmetry-adapted perturbation theory calculations of intermolecular interaction energies. In: Clementi E, editor. *Methods and techniques in computational chemistry: METECC-94*. Volume B. Cagliari: STEF, 1993; p. 79.
82. Jeziorski B, Moszyński R, Szalewicz K. Perturbation theory approach to intermolecular potential energy surfaces of van der Waals complexes. *Chem Rev.* 1994;94:1887–1930.
83. Szalewicz K, Jeziorski B. Symmetry-adapted perturbation theory of intermolecular interactions. In: Scheiner S, editor. *Molecular interactions—From van der Waals to strongly bound complexes*. Wiley: New York, 1997; p. 3–44.
84. Bukowski R, Cencek W, Patkowski K, et al. Portable parallel implementation of symmetry-adapted perturbation theory code. *Mol Phys.* 2006;104:2241–2262.
85. Caves TC, Karplus M. Perturbed Hartree-Fock theory. I. Diagrammatic double-perturbation analysis. *J Chem Phys.* 1969;50:3649–3661.
86. Jeziorska M, Jeziorski B, Cizek J. Direct calculation of the Hartree-Fock interaction energy via exchange perturbation expansion—The He = He interaction. *Int J Quantum Chem.* 1987;32:149–164.
87. Moszyński R, Heijmen TGA, Jeziorski B. Symmetry-adapted perturbation theory for the calculation of Hartree-Fock interaction energies. *Mol Phys.* 1996;88:741–758.
88. Hepburn J, Scoles G, Penco R. Simple but reliable method for prediction of intermolecular potentials. *Chem Phys Lett.* 1975;36:451–456.
89. Jurečka P, Šponer J, Černý J, Hobza P. Benchmark database of accurate (MP2 and CCSD(T) complete basis set limit) interaction energies of small model complexes, DNA base pairs, and amino acid pairs. *Phys Chem Chem Phys.* 2006;8:1985–1993.
90. Singh NJ, Min SK, Kim DY, Kim KS. Comprehensive energy analysis for various types of π -interaction. *J Chem Theory Comput.* 2009;5:515–529.
91. Smith DGA, Burns LA, Patkowski K, Sherrill CD. Revised damping parameters for the D3 dispersion correction to density functional Theory. *J Phys Chem Lett.* 2016;7:2197–2203.
92. Parker TM, Burns LA, Parrish RM, Ryno AG, Sherrill CD. Levels of symmetry adapted perturbation theory (SAPT). I Efficiency and performance for interaction energies. *J Chem Phys.* 2014;140:094106.
93. Misquitta AJ, Bukowski R, Szalewicz K. Spectra of Ar-CO₂ from *ab initio* potential energy surfaces. *J Chem Phys.* 2000;112:5308–5319.
94. Salter EA, Trucks GW, Bartlett RJ. Analytic energy derivatives in many-body methods. I First derivatives. *J Chem Phys.* 1989;90:1752–1766.
95. Patkowski K, Szalewicz K, Jeziorski B. Orbital relaxation and the third-order induction energy in symmetry-adapted perturbation theory. *Theor Chem Acc.* 2010;127:211–221.
96. Moszyński R, Cybulski SM, Chałasiński G. Many-body theory of intermolecular induction interactions. *J Chem Phys.* 1994;100:4998–5010.
97. Pernal K, Szalewicz K. Third-order dispersion energy from response functions. *J Chem Phys.* 2009;130:034103.
98. Patkowski K, Szalewicz K, Jeziorski B. Third-order interactions in symmetry-adapted perturbation theory. *J Chem Phys.* 2006;125:154107.
99. Jeziorski B, Bulski M, Piela L. First-order perturbation treatment of the short-range repulsion in a system of many closed-shell atoms or molecules. *Int J Quantum Chem.* 1976;10:281–297.
100. Lao KU, Herbert JM. Breakdown of the single-exchange approximation in third-order symmetry-adapted perturbation theory. *J Phys Chem A.* 2012;116:3042–3047.
101. Lao KU, Schäffer R, Jansen G, Herbert JM. Accurate description of intermolecular interactions involving ions using symmetry-adapted perturbation theory. *J Chem Theory Comput.* 2015;11:2473–2486.
102. Williams HL, Mas EM, Szalewicz K, Jeziorski B. On the effectiveness of monomer-, dimer-, and bond-centered basis functions in calculations of intermolecular interaction energies. *J Chem Phys.* 1995;103:7374–7391.
103. Rybak S, Szalewicz K, Jeziorski B, Jasunski M. Intraatomic correlation effects for the He-He dispersion and exchange dispersion energies using explicitly correlated Gaussian geminals. *J Chem Phys.* 1987;86:5652–5659.
104. Williams HL, Szalewicz K, Moszyński R, Jeziorski B. Dispersion energy in the coupled pair approximation with noniterative inclusion of single and triple excitations. *J Chem Phys.* 1995;103:4586–4599.
105. Patkowski K, Podeszwa R, Szalewicz K. Interactions in diatomic dimers involving closed-shell metals. *J Phys Chem A.* 2007;111:12822–12838.
106. Schäffer R, Jansen G. Intermolecular exchange-induction energies without overlap expansion. *Theor Chem Acc.* 2012;131:1235.
107. Schäffer R, Jansen G. Single-determinant-based symmetry-adapted perturbation theory without single-exchange approximation. *Mol Phys.* 2013;111:2570–2584.
108. Dunning TH Jr. Gaussian-basis sets for use in correlated molecular calculations. 1. The atoms boron through neon and hydrogen. *J Chem Phys.* 1989;90:1007–1023.

109. Kendall RA, Dunning TH Jr, Harrison RJ. Electron affinities of the 1st-row atoms revisited—Systematic basis sets and wave functions. *J Chem Phys.* 1992;96:6796–6806.
110. Papajak E, Zheng J, Xu X, Leverentz HR, Truhlar DG. Perspectives on basis sets beautiful: Seasonal plantings of diffuse basis functions. *J Chem Theory Comput.* 2011;7:3027–3034.
111. Chalasiński G, Szczęśniak MM. On the connection between the supermolecular Møller-Plesset treatment of the interaction energy and the perturbation theory of intermolecular forces. *Mol Phys.* 1988;63:205–224.
112. Chalasiński G, Szczęśniak MM. Origins of structure and energetics of van der Waals clusters from ab-initio calculations. *Chem Rev.* 1994;94:1723–1765.
113. Li A, Muddana HS, Gilson MK. Quantum mechanical calculation of noncovalent interactions: A large-scale evaluation of PMx, DFT, and SAPT approaches. *J Chem Theory Comput.* 2014;10:1563–1575.
114. Kristyán S, Pulay P. Can (semi)local density functional theory account for the London dispersion forces? *Chem Phys Lett.* 1994;229:175–180.
115. Peréz-Jordá JM, Becke AD. A density-functional study of van der Waals forces: Rare gas diatomics. *Chem Phys Lett.* 1995;233:134–137.
116. Williams HL, Chabalowski CF. Using Kohn-Sham orbitals in symmetry-adapted perturbation theory to investigate intermolecular interactions. *J Phys Chem A.* 2001;105:646–659.
117. Misquitta AJ, Szalewicz K. Intermolecular forces from asymptotically corrected density functional description of monomers. *Chem Phys Lett.* 2002;357:301–306.
118. Misquitta AJ, Szalewicz K. Symmetry-adapted perturbation theory calculations of intermolecular forces employing density functional description of monomers. *J Chem Phys.* 2005;122:214109.
119. Misquitta AJ, Podeszwa R, Jeziorski B, Szalewicz K. Intermolecular potentials based on symmetry-adapted perturbation theory including dispersion energies from time-dependent density functional calculations. *J Chem Phys.* 2005;123:214103.
120. Hesselmann A, Jansen G. First-order intermolecular interaction energies from Kohn-Sham orbitals. *Chem Phys Lett.* 2002;357:464–470.
121. Hesselmann A, Jansen G. Intermolecular induction and exchange-induction energies from coupled-perturbed Kohn-Sham density functional theory. *Chem Phys Lett.* 2002;362:319–325.
122. Hesselmann A, Jansen G. Intermolecular dispersion energies from time-dependent density functional theory. *Chem Phys Lett.* 2003;367:778–784.
123. Hesselmann A, Jansen G, Schütz M. Density-functional theory-symmetry-adapted intermolecular perturbation theory with density fitting: A new efficient method to study intermolecular interaction energies. *J Chem Phys.* 2005;122:014103.
124. Tozer DJ, Handy NC. Improving virtual Kohn-Sham orbitals and eigenvalues: Application to excitation energies and static polarizabilities. *J Chem Phys.* 1998;109:10180–10189.
125. Casida ME, Salahub DR. Asymptotic correction approach to improving approximate exchange-correlation potentials: Time-dependent density-functional theory calculations of molecular excitation spectra. *J Chem Phys.* 2000;113:8918–8935.
126. Fermi E, Amaldi G. Le orbite ∞ s degli elementi. *Mem Accad Italia.* 1934;6:117.
127. Grüning M, Gritsenko OV, van Gisbergen SJA, Baerends EJ. Shape corrections to exchange-correlation potentials by gradient-regulated seamless connection of model potentials for inner and outer region. *J Chem Phys.* 2001;114:652–660.
128. van Leeuwen R, Baerends EJ. Exchange-correlation potential with correct asymptotic behavior. *Phys Rev A.* 1994;49:2421–2431.
129. Gerber IC, Ángyán JG. Hybrid functional with separated range. *Chem Phys Lett.* 2005;415:100–105.
130. Iikura H, Tsuneda T, Yanai T, Hirao K. A long-range correction scheme for generalized-gradient-approximation exchange functionals. *J Chem Phys.* 2001;115:3540–3544.
131. Vydrov OA, Scuseria GE. Assessment of a long-range corrected hybrid functional. *J Chem Phys.* 2006;125:234109.
132. Rohrdanz MA, Herbert JM. Simultaneous benchmarking of ground- and excited-state properties with long-range-corrected density functional theory. *J Chem Phys.* 2008;129:034107.
133. Rohrdanz MA, Martins KM, Herbert JM. A long-range-corrected density functional that performs well for both ground-state properties and time-dependent density functional theory excitation energies, including charge-transfer excited states. *J Chem Phys.* 2009;130:054112.
134. Cencek W, Szalewicz K. On asymptotic behavior of density functional theory. *J Chem Phys.* 2013;139:024104.
135. Gaiduk AP, Staroverov VN. How to tell when a model Kohn-Sham potential is not a functional derivative. *J Chem Phys.* 2009;131:044107.
136. Runge E, Gross EKU. Density-functional theory for time-dependent systems. *Phys Rev Lett.* 1984;52:997–1000.
137. Moszyński R, Jeziorski B, Szalewicz K. Møller-Plesset expansion of the dispersion energy in the ring approximation. *Int J Quantum Chem.* 1993;45:409–431.
138. Żuchowski PS, Bussery-Honvault B, Moszyński R, Jeziorski B. Dispersion interaction of high-spin open-shell complexes in the random phase approximation. *J Chem Phys.* 2003;119:10497–10511.
139. Colwell SM, Handy NC, Lee AM. Determination of frequency-dependent polarizabilities using current density-functional theory. *Phys Rev A.* 1996;53:1316–1322.
140. Gross EKU, Dobson JF, Petersilka M. Density functional theory of time-dependent phenomena. In: Nalewajski RF, editor. *Density functional theory II. Topics in current chemistry.* Volume 181. Berlin and Heidelberg: Springer, 1996; p. 81–172.
141. Adamo C, Cossi M, Scalmani G, Barone V. Accurate static polarizabilities by density functional theory: Assessment of the PBE0 model. *Chem Phys Lett.* 1999;307:265–271.

142. Grüning M, Gritsenko OV, van Gisbergen SJA, Baerends EJ. On the required shape corrections to the local density and generalized gradient approximations to the Kohn-Sham potentials for molecular response calculations of (hyper)polarizabilities and excitation energies. *J Chem Phys.* 2002;116:9591–9601.
143. van Gisbergen SJA, Snijders JG, Baerends EJ. A density functional theory study of frequency-dependent polarizabilities and Van der Waals dispersion coefficients for polyatomic molecules. *J Chem Phys.* 1995;103:9347–9354.
144. Dunlap BI, Connolly JWD, Sabin JR. On first-row diatomic molecules and local density models. *J Chem Phys.* 1979;71:4993–4999.
145. Bukowski R, Podeszwa R, Szalewicz K. Efficient calculations of coupled Kohn-Sham dynamic susceptibility functions and dispersion energies with density fitting. *Chem Phys Lett.* 2005;414:111–116.
146. Podeszwa R, Bukowski R, Szalewicz K. Density-fitting method in symmetry-adapted perturbation theory based on Kohn-Sham description of monomers. *J Chem Theory Comput.* 2006;2:400–412.
147. Mas EM, Bukowski R, Szalewicz K, Groenenboom G, Wormer PES, van der Avoird A. Water pair potential of near spectroscopic accuracy. I. Analysis of potential surface and virial coefficients. *J Chem Phys.* 2000;113:6687–6701.
148. Leforestier C, Tekin A, Jansen G, Herman M. First principles potential for the acetylene dimer and refinement by fitting to experiments. *J Chem Phys.* 2011;135:234306.
149. Shirkov L, Makarewicz J. Theoretical study of the complexes of dichlorobenzene isomers with argon. II SAFT analysis of the intermolecular interaction. *J Chem Phys.* 2019;150:074302.
150. Podeszwa R, Bukowski R, Szalewicz K. Potential energy surface for the benzene dimer and perturbational analysis of $\pi-\pi$ interactions. *J Phys Chem A.* 2006;110:10345–10354.
151. van der Avoird A, Podeszwa R, Szalewicz K, et al. Vibration-rotation-tunneling states of the benzene dimer: An ab initio study. *Phys Chem Chem Phys.* 2010;12:8219–8240.
152. Metz MP, Piszczałkowski K, Szalewicz K. Automatic generation of intermolecular potential energy surfaces. *J Chem Theory Comput.* 2016;12:5895–5919.
153. Podeszwa R, Bukowski R, Rice BM, Szalewicz K. Potential energy surface for cyclotrimethylene trinitramine dimer from symmetry-adapted perturbation theory. *Phys Chem Chem Phys.* 2007;9:5561–5569.
154. Hesselmann A. Improved supermolecular second order Møller-Plesset intermolecular interaction energies using time-dependent density functional response theory. *J Chem Phys.* 2008;128:144112.
155. Pitoňák M, Hesselmann A. Accurate intermolecular interaction energies from a combination of MP2 and TDDFT response theory. *J Chem Theory Comput.* 2010;6:168–178.
156. Hesselmann A, Korona T. Intermolecular symmetry-adapted perturbation theory study of large organic complexes. *J Chem Phys.* 2014;141:094107.
157. Grimme S. Supramolecular binding thermodynamics by dispersion-corrected density functional theory. *Chem A Eur J.* 2012;18:9955–9964.
158. Calbo J, Ortí E, Sancho-García JC, Aragó J. Accurate treatment of large supramolecular complexes by double-hybrid density functionals coupled with nonlocal van der Waals corrections. *J Chem Theory Comput.* 2015;11:932–939.
159. Ambrosetti A, Alfè D, DiStasio RA Jr, Tkatchenko A. Hard numbers for large molecules: Toward exact energetics for supramolecular systems. *J Phys Chem Lett.* 2014;5:849–855.
160. Korona T, Hesselmann A, Dodziuk H. Symmetry-adapted perturbation theory applied to endohedral fullerene complexes: A stability study of $H_2@C_{60}$ and $2H_2@C_{60}$. *J Chem Theory Comput.* 2009;5:1585–1596.
161. Hesselmann A, Korona T. On the accuracy of DFT-SAPT, MP2, SCS-MP2, MP2C, and DFT+Disp methods for the interaction energies of endohedral complexes of the C_{60} fullerene with a rare gas atom. *Phys Chem Chem Phys.* 2011;13:732–743.
162. Gómez S, Restrepo A. Noble gas dimers confined inside C_{70} . *Phys Chem Chem Phys.* 2019;21:15815–15822.
163. Korona T, Dodziuk H. Small molecules in C_{60} and C_{70} : Which complexes could be stabilized? *J Chem Theory Comput.* 2011;7:1476–1483.
164. Dodziuk H, Ruud K, Korona T, Demissie TB. Chiral recognition by fullerenes: CHFClBr enantiomers in the C_{82} cage. *Phys Chem Chem Phys.* 2016;18:26057–26068.
165. Burns LA, Marshall MS, Sherrill CD. Comparing counterpoise-corrected, uncorrected, and averaged binding energies for benchmarking noncovalent interactions. *J Chem Theory Comput.* 2014;10:49–57.
166. Řezáč J, Riley KE, Hobza P. S66: A well-balanced database of benchmark interaction energies relevant to biomolecular structures. *J Chem Theory Comput.* 2011;7:2427–2438.
167. Burns LA, Faver JC, Zheng Z, et al. The BioFragment Database (BFDb): An open-data platform for computational chemistry analysis of noncovalent interactions. *J Chem Phys.* 2017;147:161727.
168. Kolář MH, Hobza P. Computer modeling of halogen bonds and other σ -hole interactions. *Chem Rev.* 2016;116:5155–5187.
169. Bernal-Uruchurtu MI, Hernández-Lamonedra R, Janda KC. On the unusual properties of halogen bonds: A detailed ab initio study of $X_2-(H_2O)_{1-5}$ clusters ($X = Cl$ and Br). *J Phys Chem A.* 2009;113:5496–5505.
170. Stone AJ. Are halogen bonded structures electrostatically driven? *J Am Chem Soc.* 2013;135:7005–7009.
171. Riley KE, Murray JS, Fanfrlík J, et al. Halogen bond tunability II: The varying roles of electrostatic and dispersion contributions to attraction in halogen bonds. *J Mol Model.* 2013;19:4651–4659.
172. Riley KE, Hobza P. The relative roles of electrostatics and dispersion in the stabilization of halogen bonds. *Phys Chem Chem Phys.* 2013;15:17742–17751.

173. Kolář M, Hostaš J, Hobza P. The strength and directionality of a halogen bond are co-determined by the magnitude and size of the σ -hole. *Phys Chem Chem Phys*. 2014;16:9987–9996.
174. Sedlak R, Kolář MH, Hobza P. Polar flattening and the strength of halogen bonding. *J Chem Theory Comput*. 2015;11:4727–4732.
175. Shaw RA, Hill JG, Legon AC. Halogen bonding with phosphine: Evidence for Mulliken inner complexes and the importance of relaxation energy. *J Phys Chem A*. 2016;120:8461–8468.
176. Domagała M, Matczak P, Palusiak M. Halogen bond, hydrogen bond and $N \cdots C$ interaction—On interrelation among these three noncovalent interactions. *Comp Theor Chem*. 2012;998:26–33.
177. Hill JG, Legon AC. On the directionality and non-linearity of halogen and hydrogen bonds. *Phys Chem Chem Phys*. 2015;17:858–867.
178. Wolf ME, Zhang B, Turney JM, Schaefer HF III. A comparison between hydrogen and halogen bonding: The hypohalous acid-water dimers, $HOX \cdots H_2O$ ($X = F, Cl, Br$). *Phys Chem Chem Phys*. 2019;21:6160–6170.
179. Pecina A, Lepšík M, Hnyk D, Hobza P, Fanfrlík J. Chalcogen and pnicogen bonds in complexes of neutral icosahedral and bicapped square-antiprismatic heteroboranes. *J Phys Chem A*. 2015;119:1388–1395.
180. Sánchez-Sanz G, Trujillo C, Solimannejad M, Alkorta I, Elguero J. Orthogonal interactions between nitril derivatives and electron donors: Pnictogen bonds. *Phys Chem Chem Phys*. 2013;15:14310–14318.
181. Grabowski SJ, Alkorta I, Elguero J. Complexes between dihydrogen and amine, phosphine, and arsine derivatives. Hydrogen bond versus pnictogen interaction. *J Phys Chem A*. 2013;117:3243–3251.
182. Li W, Spada L, Tasinato N, et al. Theory meets experiment for noncovalent complexes: The puzzling case of pnicogen interactions. *Angew Chem Int Ed*. 2018;57:13853–13857.
183. Yourdkhani S, Korona T, Hadipour NL. Interplay between tetrel and triel bonds in $RC_6H_4CN \cdots MF_3CN \cdots BX_3$ complexes: A combined symmetry-adapted perturbation theory, Møller-Plesset, and quantum theory of atoms-in-molecules study. *J Comput Chem*. 2015;36: 2412–2428.
184. Wheeler SE, Houk KN. Substituent effects in the benzene dimer are due to direct interactions of the substituents with the unsubstituted benzene. *J Am Chem Soc*. 2008;130:10854–10855.
185. Bloom JWG, Wheeler SE. Taking the aromaticity out of aromatic interactions. *Angew Chem Int Ed*. 2011;50:7847–7849.
186. Raju RK, Bloom JWG, Wheeler SE. Broad transferability of substituent effects in π -stacking interactions provides new insights into their origin. *J Chem Theory Comput*. 2013;9:3479–3490.
187. Geronimo I, Lee EC, Singh NJ, Kim KS. How different are electron-rich and electron-deficient π interactions? *J Chem Theory Comput*. 2010;6:1931–1934.
188. Geronimo I, Singh NJ, Kim KS. Can electron-rich π systems bind anions? *J Chem Theory Comput*. 2011;7:825–829.
189. Kumar S, Singh SK, Vaishnav JK, Hill JG, Das A. Interplay among electrostatic, dispersion, and steric interactions: Spectroscopy and quantum chemical calculations of π -hydrogen bonded complexes. *ChemPhysChem*. 2017;18:828–838.
190. Cabaleiro-Lago EM, Rodríguez-Otero J. $\sigma - \sigma$, $\sigma - \pi$, and $\pi - \pi$ stacking interactions between six-membered cyclic systems. Dispersion dominates and electrostatics commands. *ChemistrySelect*. 2017;2:5157–5166.
191. Podeszwa R, Szalewicz K. Physical origins of interactions in dimers of polycyclic aromatic hydrocarbons. *Phys Chem Chem Phys*. 2008; 10:2735–2746.
192. Podeszwa R. Interactions of graphene sheets deduced from properties of polycyclic aromatic hydrocarbons. *J Chem Phys*. 2010;132: 044704.
193. Sedlak R, Janowski T, Pitonák M, Řezáč J, Pulay P, Hobza P. Accuracy of quantum chemical methods for large noncovalent complexes. *J Chem Theory Comput*. 2013;9:3364–3374.
194. Pavošević F, Peng C, Pinski P, Riplinger C, Neese F, Valeev EF. SparseMaps—A systematic infrastructure for reduced scaling electronic structure methods. V Linear scaling explicitly correlated coupled-cluster method with pair natural orbitals. *J Chem Phys*. 2017;146: 174108.
195. Kennedy MR, Burns LA, Sherrill CD. Buckyplates and Buckybowls: Examining the effects of curvature on π - π interactions. *J Phys Chem A*. 2012;116:11920–11926.
196. Sutton C, Marshall MS, Sherrill CD, Risko C, Brédas JL. Rubrene: The interplay between intramolecular and intermolecular interactions determines the planarization of its tetracene core in the solid state. *J Am Chem Soc*. 2015;137:8775–8782.
197. Guan Y, Wheeler SE. Intercolumnar interactions control the local orientations within columnar stacks of sumanene and sumanene derivatives. *J Phys Chem C*. 2017;121:8541–8547.
198. Cabaleiro-Lago EM, Fernández B, Rodríguez-Otero J. Dissecting the concave-convex $\pi - \pi$ interaction in corannulene and sumanene dimers: SAPT(DFT) analysis and performance of DFT dispersion-corrected methods. *J Comput Chem*. 2018;39:93–104.
199. Cabaleiro-Lago EM, Rodríguez-Otero J. On the nature of $\sigma - \sigma$, $\sigma - \pi$, and $\pi - \pi$ stacking in extended systems. *ACS Omega*. 2018;3: 9348–9359.
200. Jenness GR, Karalti O, Al-Saidi WA, Jordan KD. Evaluation of theoretical approaches for describing the interaction of water with linear Acenes. *J Phys Chem A*. 2011;115:5955–5964.
201. Smith DGA, Patkowski K. Interactions between methane and polycyclic aromatic hydrocarbons: A high accuracy benchmark study. *J Chem Theory Comput*. 2013;9:370–389.
202. Kocman M, Jurečka P, Dubeký M, Otyepka M, Cho Y, Kim KS. Choosing a density functional for modeling adsorptive hydrogen storage: Reference quantum mechanical calculations and a comparison of dispersion-corrected density functionals. *Phys Chem Chem Phys*. 2015;17:6423–6432.

203. Kim DY, Madridejos JML, Ha M, et al. Size-dependent conformational change in halogen- π interaction: From benzene to graphene. *Chem Commun.* 2017;53:6140–6143.
204. Javadi N, Najafi M, Yourdkhani S. On the role of substituent in noncovalent functionalization of graphene and organophosphor recognition: IQA and SAPT perspective. *Int J Quantum Chem.* 2017;117:e25379.
205. Wang W, Zhang Y, Wang YB. Noncovalent $\pi \cdots \pi$ interaction between graphene and aromatic molecule: Structure, energy, and nature. *J Chem Phys.* 2014;140:094302.
206. Wang W, Sun T, Zhang Y, Wang YB. Benchmark calculations of the adsorption of aromatic molecules on graphene. *J Comput Chem.* 2015;36:1763–1771.
207. Karalti O, Alfè D, Gillan MJ, Jordan KD. Adsorption of a water molecule on the MgO(100) surface as described by cluster and slab models. *Phys Chem Chem Phys.* 2012;14:7846–7853.
208. de Lara-Castells MP, Stoll H, Mitrushchenkov AO. Assessing the performance of dispersionless and dispersion-accounting methods: Helium interaction with cluster models of the TiO₂(110) surface. *J Phys Chem A.* 2014;118:6367–6384.
209. Goings JJ, Ohlsen SM, Blaisdell KM, Schofield DP. Sorption of H₂ to open metal sites in a metal-organic framework: A symmetry-adapted perturbation theory analysis. *J Phys Chem A.* 2014;118:7411–7417.
210. Piquemal JP, Cisneros GA, Reinhardt P, Gresh N, Darden TA. Towards a force field based on density fitting. *J Chem Phys.* 2006;124:104101.
211. Li X, Volkov AV, Szalewicz K, Coppens P. Interaction energies between glycopeptide antibiotics and substrates in complexes determined by X-ray crystallography: Application of a theoretical databank of aspherical atoms and a symmetry-adapted perturbation theory-based set of interatomic potentials. *Acta Crystallogr.* 2006;D62:639–647.
212. Stone AJ. Distributed multipole analysis, or how to describe a molecular charge-distribution. *Chem Phys Lett.* 1981;83:233–239.
213. Williams GJ, Stone AJ. Distributed dispersion: A new approach. *J Chem Phys.* 2003;119:4620–4628.
214. Zgarbová M, Otyepka M, Šponer J, Hobza P, Jurečka P. Large-scale compensation of errors in pairwise-additive empirical force fields: Comparison of AMBER intermolecular terms with rigorous DFT-SAPT calculations. *Phys Chem Chem Phys.* 2010;12:10476–10493.
215. Kumar R, Wang FF, Jenness GR, Jordan KD. A second generation distributed point polarizable water model. *J Chem Phys.* 2010;132:014309.
216. McDaniel JG, Yu K, Schmidt JR. Ab initio, physically motivated force fields for CO₂ adsorption in zeolitic imidazolate frameworks. *J Phys Chem C.* 2012;116:1892–1903.
217. Tafipolsky M, Engels B. Accurate intermolecular potentials with physically grounded electrostatics. *J Chem Theory Comput.* 2011;7:1791–1803.
218. McDaniel JG, Schmidt JR. Robust, transferable, and physically motivated force fields for gas adsorption in functionalized zeolitic imidazolate frameworks. *J Phys Chem C.* 2012;116:14031–14039.
219. McDaniel JG, Schmidt JR. Physically-motivated force fields from symmetry-adapted perturbation theory. *J Phys Chem A.* 2013;117:2053–2066.
220. Wang Q, Rackers JA, He C, et al. General model for treating short-range electrostatic penetration in a molecular mechanics force field. *J Chem Theory Comput.* 2015;11:2609–2618.
221. McDaniel JG, Choi E, Son CY, Schmidt JR, Yethiraj A. Ab initio force fields for imidazolium-based ionic liquids. *J Phys Chem B.* 2016;120:7024–7036.
222. Rackers JA, Liu C, Ren P, Ponder JW. A physically grounded damped dispersion model with particle mesh Ewald summation. *J Chem Phys.* 2018;149:084115.
223. Van Vleet MJ, Misquitta AJ, Stone AJ, Schmidt JR. Beyond Born-Mayer: Improved models for short-range repulsion in ab initio force fields. *J Chem Theory Comput.* 2016;12:3851–3870.
224. Vandenbrande S, Waroquier M, Van Speybroeck V, Verstraelen T. The monomer electron density force field (MEDFF): A physically inspired model for noncovalent interactions. *J Chem Theory Comput.* 2017;13:161–179.
225. Van Vleet MJ, Misquitta AJ, Schmidt JR. New angles on standard force fields: Toward a general approach for treating atomic-level anisotropy. *J Chem Theory Comput.* 2018;14:739–758.
226. Podeszwa R, Pernal K, Patkowski K, Szalewicz K. Extension of the Hartree-Fock plus dispersion method by first-order correlation effects. *J Phys Chem Lett.* 2010;1:550–555.
227. Pernal K, Podeszwa R, Patkowski K, Szalewicz K. Dispersionless density functional theory. *Phys Rev Lett.* 2009;103:263201.
228. Austin A, Petersson GA, Frisch MJ, Dobek FJ, Scalmani G, Throssell K. A density functional with spherical atom dispersion terms. *J Chem Theory Comput.* 2012;8:4989–5007.
229. Hesselmann A. Comparison of intermolecular interaction energies from SAPT and DFT including empirical dispersion contributions. *J Phys Chem A.* 2011;115:11321–11330.
230. Lao KU, Herbert JM. Accurate intermolecular interactions at dramatically reduced cost: XPol+SAPT with empirical dispersion. *J Phys Chem Lett.* 2012;3:3241–3248.
231. Lao KU, Herbert JM. An improved treatment of empirical dispersion and a many-body energy decomposition scheme for the explicit polarization plus symmetry-adapted perturbation Theory (XSAPT) method. *J Chem Phys.* 2013;139:034107.
232. Grimme S, Antony J, Ehrlich S, Krieg H. A consistent and accurate ab initio parametrization of density functional dispersion correction (DFT-D) for the 94 elements H-Pu. *J Chem Phys.* 2010;132:154104.
233. Grimme S, Ehrlich S, Goerigk L. Effect of the damping function in dispersion corrected density functional theory. *J Comput Chem.* 2011;32:1456–1465.

234. Shahbaz M, Szalewicz K. Do semilocal density-functional approximations recover dispersion energies at small intermonomer separations? *Phys Rev Lett.* 2018;121:113402.
235. McGibbon RT, Taube AG, Donchev AG, et al. Improving the accuracy of Møller-Plesset perturbation theory with neural networks. *J Chem Phys.* 2017;147:161725.
236. Podeszwa R, Rice BM, Szalewicz K. Predicting structure of molecular crystals from first principles. *Phys Rev Lett.* 2008;101:115503.
237. Reilly AM, Cooper RI, Adjiman CS, et al. Report on the sixth blind test of organic crystal structure prediction methods. *Acta Crystallogr.* 2016;B72:439–459.
238. Taylor DE, Ángyán JG, Galli G, et al. Blind test of density-functional-based methods on intermolecular interaction energies. *J Chem Phys.* 2016;145:124105.
239. Izgorodina EI, MacFarlane DR. Nature of hydrogen bonding in charged hydrogen-bonded complexes and imidazolium-based ionic liquids. *J Phys Chem B.* 2011;115:14659–14667.
240. Izgorodina EI, Golze D, Maganti R, et al. Importance of dispersion forces for prediction of thermodynamic and transport properties of some common ionic liquids. *Phys Chem Chem Phys.* 2014;16:7209–7221.
241. Izgorodina EI, Hodgson JL, Weis DC, Pas SJ, MacFarlane DR. Physical absorption of CO₂ in protic and aprotic ionic liquids: An interaction perspective. *J Phys Chem B.* 2015;119:11748–11759.
242. Berquist EJ, Daly CA Jr, Brinzer T, et al. Modeling carbon dioxide vibrational frequencies in ionic liquids: I. Ab initio calculations. *J Phys Chem B.* 2017;121:208–220.
243. Yang L, Brazier JB, Hubbard TA, Rogers DM, Cockroft SL. Can dispersion forces govern aromatic stacking in an organic solvent? *Angew Chem Int Ed.* 2016;55:912–916.
244. Simeon TM, Ratner MA, Schatz GC. Nature of noncovalent interactions in catenane supramolecular complexes: Calibrating the MM3 force field with ab initio, DFT, and SAPT methods. *J Phys Chem A.* 2013;117:7918–7927.
245. Moreira L, Calbo J, Illescas BM, et al. Metal-atom impact on the self-assembly of cup-and-ball metalloporphyrin-fullerene conjugates. *Angew Chem Int Ed.* 2015;54:1255–1260.
246. Lambert H, Mohan N, Lee TC. Ultrahigh binding affinity of a hydrocarbon guest inside cucurbit[7]uril enhanced by strong host-guest charge matching. *Phys Chem Chem Phys.* 2019;21:14521–14529.
247. Sutton C, Risko C, Brédas JL. Noncovalent intermolecular interactions in organic electronic materials: Implications for the molecular packing vs electronic properties of acenes. *Chem Mater.* 2016;28:3–16.
248. Ravva MK, Wang T, Brédas JL. Nature of the binding interactions between conjugated polymer chains and fullerenes in bulk heterojunction organic solar cells. *Chem Mater.* 2016;28:8181–8189.
249. Cabaleiro-Lago EM, Rodríguez-Otero J, Carrazana-García JA. A theoretical study of complexes between fullerenes and concave receptors with interest in photovoltaics. *Phys Chem Chem Phys.* 2017;19:26787–26798.
250. Parker TM, Hohenstein EG, Parrish RM, Hud NV, Sherrill CD. Quantum-mechanical analysis of the energetic contributions to π stacking in nucleic acids versus rise, twist, and slide. *J Am Chem Soc.* 2013;135:1306–1316.
251. Parker TM, Sherrill CD. Assessment of empirical models versus high-accuracy ab initio methods for nucleobase stacking: Evaluating the importance of charge penetration. *J Chem Theory Comput.* 2015;11:4197–4204.
252. Toa ZSD, Dean JC, Scholes GD. Revealing structural involvement of chromophores in algal light harvesting complexes using symmetry-adapted perturbation theory. *J Photochem Photobiol B: Biol.* 2019;190:110–117.
253. Chałasiński G, Szalewicz K. Degenerate symmetry-adapted perturbation theory. Convergence properties of perturbation expansions for excited states of H₂⁺ ion. *Int J Quantum Chem.* 1980;18:1071–1089.
254. Ćwiok T, Jeziorski B, Kołos W, Moszyński R, Szalewicz K. On the convergence of the symmetrized Rayleigh-Schrödinger perturbation theory for molecular interaction energies. *J Chem Phys.* 1992;97:7555–7559.
255. Żuchowski PS, Podeszwa R, Moszyński R, Jeziorski B, Szalewicz K. Symmetry-adapted perturbation theory utilizing density functional description of monomers for high-spin open-shell complexes. *J Chem Phys.* 2008;129:084101.
256. Hapka M, Żuchowski PS, Szczeńiak MM, Chałasiński G. Symmetry-adapted perturbation theory based on unrestricted Kohn-Sham orbitals for high-spin open-shell van der Waals complexes. *J Chem Phys.* 2012;137:164104.
257. Gonthier JF, Sherrill CD. Density-fitted open-shell symmetry-adapted perturbation theory and application to π -stacking in benzene dimer cation and ionized DNA base pair steps. *J Chem Phys.* 2016;145:134106.
258. Lao KU, Herbert JM. Atomic orbital implementation of extended symmetry-adapted perturbation theory (XSAPT) and benchmark calculations for large supramolecular complexes. *J Chem Theory Comput.* 2018;14:2955–2978.
259. Żuchowski PS. Interaction potential for the quintet state of the O₂-O₂ dimer from symmetry-adapted perturbation theory based on DFT description of monomers. *Chem Phys Lett.* 2008;450:203–209.
260. Bartolomei M, Carmona-Novillo E, Hernández MI, Campos-Martínez J, Moszyński R. Global ab initio potential energy surface for the O₂(³S_g⁻) + N₂(¹S_g⁺) interaction. Applications to the collisional, spectroscopic, and thermodynamic properties of the complex. *J Phys Chem A.* 2014;118:6584–6594.
261. Cybulski H, Żuchowski PS, Fernández B, Sadlej J. The water-nitric oxide intermolecular potential-energy surface revisited. *J Chem Phys.* 2009;130:104303.
262. Murdachaew G, Varner ME, Phillips LF, Finlayson-Pitts BJ, Gerber RB. Nitrogen dioxide at the air-water interface: Trapping, absorption, and solvation in the bulk and at the surface. *Phys Chem Chem Phys.* 2013;15:204–212.
263. Ma Q, Kłos J, Alexander MH, van der Avoird A, Dagdigian PJ. The interaction of OH(X² Π) with H₂: *Ab initio* potential energy surfaces and bound states. *J Chem Phys.* 2014;141:174309.

264. Skomorowski W, Moszynski R. Long-range interactions between an atom in its ground S state and an open-shell linear molecule. *J Chem Phys.* 2011;134:124117.
265. Misiewicz JP, Noonan JA, Turney JM, Schaefer HF III. The non-covalently bound SO $\cdot\cdot$ H₂O system, including an interpretation of the differences between SO $\cdot\cdot$ H₂O and O₂ $\cdot\cdot$ H₂O. *Phys Chem Chem Phys.* 2018;20:28840–28847.
266. Liu R, Franzese CA, Malek R, et al. Auophilic interactions from wave function, symmetry-adapted perturbation theory, and rangehybrid approaches. *J Chem Theory Comput.* 2011;7:2399–2407.
267. Kłos J, Hapka M, Chałasiński G, Halwick P, Stoecklin T. Theoretical study of the buffer-gas cooling and trapping of CrH(X $^6\Sigma^+$) by ${}^3\text{He}$ atoms. *J Chem Phys.* 2016;145:214305.
268. Sladek V, Tvaroška I. First-principles interaction analysis assessment of the manganese cation in the catalytic activity of glycosyltransferases. *J Phys Chem B.* 2017;121:6148–6162.
269. Malenov DP, Zarić SD. Strong stacking interactions of metal-chelate rings are caused by substantial electrostatic component. *Dalton Trans.* 2019;48:6328–6332.
270. Hapka M, Chałasiński G, Kłos J, Żuchowski PS. First-principle interaction potentials for metastable He(${}^3\text{S}$) and Ne(${}^3\text{P}$) with closed-shell molecules: Application to Penning-ionizing systems. *J Chem Phys.* 2013;139:014307.
271. Jankunas J, Bertsche B, Jachymski K, Hapka M, Osterwalder A. Dynamics of gas phase Ne $^*+\text{NH}_3$ and Ne $^*+\text{ND}_3$ Penning ionisation at low temperatures. *J Chem Phys.* 2014;140:244302.
272. Pastorcza E, Shen J, Hapka M, Piecuch P, Pernal K. Intricacies of van der Waals interactions in systems with elongated bonds revealed by electron-groups embedding and high-level coupled-cluster approaches. *J Chem Theory Comput.* 2017;13:5404–5419.
273. Reinhardt P. A possible valence-bond approach to symmetry-adapted perturbation theory. *Comp Theor Chem.* 2017;1116:174–183.
274. Hapka M, Przybytek M, Pernal K. Second-order dispersion energy based on multireference description of monomers. *J Chem Theory Comput.* 2019;15:1016–1027.
275. Pernal K. Intergeminal correction to the antisymmetrized product of strongly orthogonal geminals derived from the extended random phase approximation. *J Chem Theory Comput.* 2014;10:4332–4341.
276. Siegbahn PEM, Almlöf J, Heiberg A, Roos BO. The complete active space SCF (CASSCF) method in a Newton-Raphson formulation with application to the HNO molecule. *J Chem Phys.* 1981;74:2384–2396.
277. Patkowski K, Żuchowski PS, Smith DGA. First-order symmetry-adapted perturbation theory for multiplet splittings. *J Chem Phys.* 2018;148:164110.
278. Krylov AI. Spin-flip equation-of-motion coupled-cluster electronic structure method for a description of excited states, bond breaking, diradicals, and triradicals. *Acc Chem Res.* 2006;39:83–91.
279. Wormer PES, van der Avoird A. (Heisenberg) exchange and electrostatic interactions between O₂ molecules: An ab initio study. *J Chem Phys.* 1984;81:1929–1939.
280. Parrish RM, Burns LA, Smith DGA, et al. Psi4 1.1: An open-source electronic structure program emphasizing automation, advanced libraries, and interoperability. *J Chem Theory Comput.* 2017;13:3185–3197.
281. Waldrop JM, Patkowski K. Spin splittings from first-order symmetry-adapted perturbation theory without single-exchange approximation. *J Chem Phys.* 2019;150:074109.
282. Kertesz M. Pancake bonding: An unusual Pi-stacking interaction. *Chem A Eur J.* 2019;25:400–416.
283. Stone AJ, Misquitta AJ. Charge-transfer in symmetry-adapted perturbation theory. *Chem Phys Lett.* 2009;473:201–205.
284. Stone AJ. Natural bond orbitals and the nature of the hydrogen bond. *J Phys Chem A.* 2017;121:1531–1534.
285. Misquitta AJ. Charge transfer from regularized symmetry-adapted perturbation theory. *J Chem Theory Comput.* 2013;9:5313–5326.
286. Toulouse J, Colonna F, Savin A. Long-range–short-range separation of the electron-electron interaction in density-functional theory. *Phys Rev A.* 2004;70:062505.
287. Patkowski K, Jeziorski B, Szalewicz K. Symmetry-adapted perturbation theory with regularized Coulomb potential. *J Mol Struct.* 2001;547:293–307.
288. Adams WH. Two new symmetry-adapted perturbation theories for the calculation of intermolecular interaction energies. *Theor Chem Acc.* 2002;108:225–231.
289. Chai JD, Head-Gordon M. Systematic optimization of long-range corrected hybrid density functionals. *J Chem Phys.* 2008;128:084106.
290. Lao KU, Herbert JM. Energy decomposition analysis with a stable charge-transfer term for interpreting intermolecular interactions. *J Chem Theory Comput.* 2016;12:2569–2582.
291. Kaduk B, Kowalczyk T, Van Voorhis T. Constrained density functional theory. *Chem Rev.* 2012;112:321–370.
292. Řezáč J, de la Lande A. Robust, basis-set independent method for the evaluation of charge-transfer energy in noncovalent complexes. *J Chem Theory Comput.* 2015;11:528–537.
293. Řezáč J, de la Lande A. On the role of charge transfer in halogen bonding. *Phys Chem Chem Phys.* 2017;19:791–803.
294. Bader RFW. A quantum theory of molecular structure and its applications. *Chem Rev.* 1991;91:893–928.
295. Johnson ER, Keinan S, Mori-Sánchez P, Contreras-García J, Cohen AJ, Yang W. Revealing noncovalent interactions. *J Am Chem Soc.* 2010;132:6498–6506.
296. de Silva P, Corminboeuf C. Simultaneous visualization of covalent and noncovalent interactions using regions of density overlap. *J Chem Theory Comput.* 2014;10:3745–3756.
297. Parrish RM, Sherrill CD. Spatial assignment of symmetry adapted perturbation theory interaction energy components: The atomic SAPT partition. *J Chem Phys.* 2014;141:044115.

298. Parrish RM, Parker TM, Sherrill CD. Chemical assignment of symmetry-adapted perturbation theory interaction energy components: The functional-group SAPT partition. *J Chem Theory Comput.* 2014;10:4417–4431.
299. Parrish RM, Sherrill CD. Quantum-mechanical evaluation of π - π versus substituent- π interactions in π stacking: Direct evidence for the Wheeler-Houk picture. *J Am Chem Soc.* 2014;136:17386–17389.
300. Yourdkhani S, Chojecki M, Korona T. Substituent effects in the so-called cation- \cdots π interaction of benzene and its boron-nitrogen doped analogues: Overlooked role of σ -skeleton. *Phys Chem Chem Phys.* 2019;21:6453–6466.
301. Parrish RM, Sitkoff DF, Cheney DL, Sherrill CD. The surprising importance of peptide bond contacts in drug-protein interactions. *Chem A Eur J.* 2017;23:7887–7890.
302. Bakr BW, Sherrill CD. Analysis of transition state stabilization by non-covalent interactions in the Houk-List model of organocatalyzed intermolecular aldol additions using functional-group symmetry-adapted perturbation theory. *Phys Chem Chem Phys.* 2016;18: 10297–10308.
303. Bakr BW, Sherrill CD. Analysis of transition state stabilization by non-covalent interactions in organocatalysis: Application of atomic and functional-group partitioned symmetry-adapted perturbation theory to the addition of organoboron reagents to fluoroketones. *Phys Chem Chem Phys.* 2018;20:18241–18251.
304. Hemmati R, Patkowski K. Chiral self recognition: Interactions in propylene oxide complexes. *J Phys Chem A.* 2019;123:8607–8618.
305. Wodrich MD, Wannere CS, Mo Y, Jarowski PD, Houk KN, von Ragué Schleyer P. The concept of protobranching and its many paradigm shifting implications for energy evaluations. *Chem A Eur J.* 2007;13:7731–7744.
306. Schreiner PR, Chernish LV, Gunchenko PA, et al. Overcoming lability of extremely long alkane carbon-carbon bonds through dispersion forces. *Nature.* 2011;477:308–311.
307. Maier JM, Li P, Vik EC, Yehl CJ, Strickland SMS, Shimizu KD. Measurement of solvent OH- π interactions using a molecular balance. *J Am Chem Soc.* 2017;139:6550–6553.
308. Meitei OR, Hesselmann A. On the stability of cyclophane derivates using a molecular fragmentation method. *ChemPhysChem.* 2016;17: 3863–3874.
309. Meitei OR, Hesselmann A. Intramolecular interactions in sterically crowded hydrocarbon molecules. *J Comput Chem.* 2017;38: 2500–2508.
310. Gonthier JF, Corminboeuf C. Exploration of zeroth-order wavefunctions and energies as a first step toward intramolecular symmetry-adapted perturbation theory. *J Chem Phys.* 2014;140:154107.
311. Pastorcak E, Prlj A, Gonthier JF, Corminboeuf C. Intramolecular symmetry-adapted perturbation theory with a single-determinant wavefunction. *J Chem Phys.* 2015;143:224107.
312. Parrish RM, Gonthier JF, Corminboeuf C, Sherrill CD. Communication: Practical intramolecular symmetry adapted perturbation theory via Hartree-Fock embedding. *J Chem Phys.* 2015;143:051103.
313. Mayer I. Towards a “chemical” Hamiltonian. *Int J Quantum Chem.* 1983;23:341–363.
314. Szalewicz K, Bukowski R, Jeziorski B. On the importance of many-body forces in clusters and condensed phase. In: Dykstra CE, Frenking G, Kim KS, Scuseria GE, editors. *Theory and applications of computational chemistry: The first 40 years. A volume of technical and historical perspectives.* Amsterdam: Elsevier, 2005; p. 919–962.
315. Moszynski R, Wormer PES, Jeziorski B, van der Avoird A. Symmetry-adapted perturbation-theory of nonadditive 3-body interactions in van-der-Waals molecules.1. General theory. *J Chem Phys.* 1995;103:8058–8074. Erratum: 107:672, 1997.
316. Lotrich VF, Szalewicz K. Symmetry-adapted perturbation theory of three-body nonadditivity of intermolecular interaction energy. *J Chem Phys.* 1997;106:9668–9687.
317. Wormer PES, Moszynski R, van der Avoird A. Intramonomer correlation contributions to first-order exchange nonadditivity in trimers. *J Chem Phys.* 2000;112:3159–3169.
318. Lotrich VF, Szalewicz K. Perturbation theory of three-body exchange nonadditivity and application to helium trimer. *J Chem Phys.* 2000;112:112–121.
319. Axilrod BM, Teller E. Interaction of the van der Waals type between three atoms. *J Chem Phys.* 1943;11:299–300.
320. Muto Y. Force between nonpolar molecules. *Proc Phys Math Soc Jpn.* 1943;17:629.
321. Kennedy MR, Ringer McDonald A, DePrince AE III, Marshall MS, Podeszwa R, Sherrill CD. Communication: Resolving the three-body contribution to the lattice energy of crystalline benzene: Benchmark results from coupled-cluster theory. *J Chem Phys.* 2014;140: 121104.
322. Yang J, Hu W, Usyat D, Matthews D, Schütz M, Chan GK. Ab initio determination of the crystalline benzene lattice energy to sub-kilojoule/mole accuracy. *Science.* 2014;345:640–643.
323. Groenenboom GC, Mas EM, Bukowski R, Szalewicz K, Wormer PES, van der Avoird A. Water pair and three-body potential of spectroscopic quality from *ab Initio* calculations. *Phys Rev Lett.* 2000;84:4072–4075.
324. Mas EM, Bukowski R, Szalewicz K. *Ab initio* three-body interactions for water. I. Potential and structure of water trimer. *J Chem Phys.* 2003;118:4386–4403.
325. Podeszwa R, Szalewicz K. Three-body symmetry-adapted perturbation theory based on Kohn-Sham description of the monomers. *J Chem Phys.* 2007;126:194101.
326. Wen S, Nanda K, Huang Y, Beran GJO. Practical quantum mechanics-based fragment methods for predicting molecular crystal properties. *Phys Chem Chem Phys.* 2012;14:7578–7590.
327. Yu K, Schmidt JR. Many-body effects are essential in a physically motivated CO₂ force field. *J Chem Phys.* 2012;136:034503.

328. Huang Y, Beran GJO. Reliable prediction of three-body intermolecular interactions using dispersion-corrected second-order Møller-Plesset perturbation theory. *J Chem Phys.* 2015;143:044113.
329. Yourdkhani S, Chojecki M, Hapka M, Korona T. Interaction of boron-nitrogen doped benzene isomers with water. *J Phys Chem A.* 2016;120:6287–6302.
330. Hapka M, Rajchel Ł, Modrzejewski M, Schäffer R, Chałasiński G, Szczęśniak MM. The nature of three-body interactions in DFT: Exchange and polarization effects. *J Chem Phys.* 2017;147:084106.
331. Jeziorski B, Moszynski R. Explicitly connected expansion for the average value of an observable in the coupled-cluster theory. *Int J Quantum Chem.* 1993;48:161–183.
332. Moszyński R, Żuchowski PS, Jeziorski B. Time-independent coupled-cluster theory of the polarization propagator. *Collect Czech Chem Commun.* 2005;70:1109–1132.
333. Korona T, Moszyński R, Jeziorski B. Electrostatic interactions between molecules from relaxed one-electron density matrices of the coupled cluster singles and doubles model. *Mol Phys.* 2002;100:1723–1734.
334. Korona T, Przybytek M, Jeziorski B. Time-independent coupled cluster theory of the polarization propagator. Implementation and application of the singles and doubles model to dynamic polarizabilities and van der Waals constants. *Mol Phys.* 2006;104:2303–2316.
335. Korona T, Jeziorski B. One-electron properties and electrostatic interaction energies from the expectation value expression and wave function of singles and doubles coupled cluster theory. *J Chem Phys.* 2006;125:184109.
336. Korona T. On the role of higher-order correlation effects on the induction interactions between closed-shell molecules. *Phys Chem Chem Phys.* 2007;9:6004–6011.
337. Korona T, Jeziorski B. Dispersion energy from density-fitted density susceptibilities of singles and doubles coupled cluster theory. *J Chem Phys.* 2008;128:144107.
338. Korona T. First-order exchange energy of intermolecular interactions from coupled cluster density matrices and their cumulants. *J Chem Phys.* 2008;128:224104.
339. Korona T. Two-particle density matrix cumulant of coupled cluster theory. *Phys Chem Chem Phys.* 2008;10:5698–5705.
340. Korona T. Second-order exchange-induction energy of intermolecular interactions from coupled cluster density matrices and their cumulants. *Phys Chem Chem Phys.* 2008;10:6509–6519.
341. Korona T. Exchange-dispersion energy: A formulation in terms of monomer properties and coupled cluster treatment of intramonomer correlation. *J Chem Theory Comput.* 2009;5:2663–2678.
342. Korona T. Coupled cluster treatment of intramonomer correlation effects in intermolecular interactions. In: Cársky P, Paldus J, Pittner J. *Recent progress in coupled cluster methods. Challenges and advances in computational chemistry and physics.* vol. 11. Springer, Dordrecht: Springer; 2010. p. 267–298.
343. Kutzelnigg W, Mukherjee D. Normal order and extended Wick theorem for a multiconfiguration reference wave function. *J Chem Phys.* 1997;107:432–449.
344. Korona T. A coupled cluster treatment of intramonomer electron correlation within symmetry-adapted perturbation theory: Benchmark calculations and a comparison with a density-functional theory description. *Mol Phys.* 2013;111:3705–3715.
345. Perdew JP, Burke K, Ernzerhof M. Generalized gradient approximation made simple. *Phys Rev Lett.* 1996;77:3865–3868.
346. Adamo C, Barone V. Toward reliable density functional methods without adjustable parameters: The PBE0 model. *J Chem Phys.* 1999;110:6158–6170.
347. Lee C, Yang W, Parr RG. Development of the Colle-Salvetti correlation-energy formula into a functional of the electron density. *Phys Rev B.* 1988;37:785–789.
348. Becke AD. Density-functional thermochemistry. 3. The role of exact exchange. *J Chem Phys.* 1993;98:5648–5652.
349. Zhao Y, Schultz NE, Truhlar DG. Exchange-correlation functional with broad accuracy for metallic and nonmetallic compounds, kinetics, and noncovalent interactions. *J Chem Phys.* 2005;123:161103.
350. Shirkov L, Sladek V. Benchmark CCSD-SAPT study of rare gas dimers with comparison to MP-SAPT and DFT-SAPT. *J Chem Phys.* 2017;147:174103.
351. Werner HJ, Knowles PJ, Knizia G, Manby FR, Schütz M. Molpro: A general-purpose quantum chemistry program package. *WIREs Comput Mol Sci.* 2012;2:242–253.
352. Gniewek P, Jeziorski B. Exchange splitting of the interaction energy and the multipole expansion of the wave function. *J Chem Phys.* 2015;143:154106.
353. Gniewek P, Jeziorski B. Determination of the exchange interaction energy from the polarization expansion of the wave function. *Phys Rev A.* 2016;94:042708.
354. Hesselmann A. DFT-SAPT intermolecular interaction energies employing exact-exchange Kohn-Sham response methods. *J Chem Theory Comput.* 2018;14:1943–1959.
355. Hesselmann A, Meitei OR. Intermolecular dispersion energies from coupled exact-exchange Kohn-Sham excitation energies and vectors. *Comput Theor Chem.* 2018;1129:57–69.
356. Holzer C, Klopper W. Communication: Symmetry-adapted perturbation theory with intermolecular induction and dispersion energies from the Bethe-Salpeter equation. *J Chem Phys.* 2017;147:181101.
357. Hesselmann A, Jansen G. The helium dimer potential from a combined density functional theory and symmetry-adapted perturbation theory approach using an exact exchange-correlation potential. *Phys Chem Chem Phys.* 2003;5:5010–5014.

358. Zhao Q, Morrison RC, Parr RG. From electron densities to Kohn-Sham kinetic energies, orbital energies, exchange-correlation potentials, and exchange-correlation energies. *Phys Rev A*. 1994;50:2138–2142.
359. Boese AD, Jansen G. ZMP-SAPT: DFT-SAPT using *ab initio* densities. *J Chem Phys*. 2019;150:154101.
360. Shirkov L, Makarewicz J. Does DFT-SAPT method provide spectroscopic accuracy? *J Chem Phys*. 2015;142:064102.
361. Tao FM. On the use of bond functions in molecular calculations. *J Chem Phys*. 1993;98:2481–2483.
362. Tao FM. Bond functions, basis set superposition errors and other practical issues with ab initio calculations of intermolecular potentials. *Int Rev Phys Chem*. 2001;20:617–643.
363. Klopper W, Samson CCM. Explicitly correlated second-order Møller-Plesset methods with auxiliary basis sets. *J Chem Phys*. 2002;116: 6397–6410.
364. Werner HJ, Adler TB, Manby FR. General orbital invariant MP2-F12 theory. *J Chem Phys*. 2007;126:164102.
365. Adler TB, Knizia G, Werner HJ. A simple and efficient CCSD(T)-F12 approximation. *J Chem Phys*. 2007;127:221106.
366. Knizia G, Adler TB, Werner HJ. Simplified CCSD(T)-F12 methods: Theory and benchmarks. *J Chem Phys*. 2009;130:054104.
367. Patkowski K. On the accuracy of explicitly correlated coupled-cluster interaction energies—Have orbital results been beaten yet? *J Chem Phys*. 2012;137:034103.
368. Patkowski K. Basis set converged weak interaction energies from conventional and explicitly correlated coupled-cluster approach. *J Chem Phys*. 2013;138:154101.
369. Szalewicz K, Jeziorski B. Symmetry-adapted double-perturbation analysis of intramolecular correlation effects in weak intermolecular interactions: The He-He interaction. *Mol Phys*. 1979;38:191–208.
370. Jeziorska M, Cencek W, Patkowski K, Jeziorski B, Szalewicz K. Pair potential for helium from symmetry-adapted perturbation theory calculations and from supermolecular data. *J Chem Phys*. 2007;127:124303.
371. Mitroy J, Babin S, Horiuchi W, et al. Theory and application of explicitly correlated Gaussians. *Rev Mod Phys*. 2013;85:693–749.
372. Przybytek M. Dispersion energy of symmetry-adapted perturbation theory from the explicitly correlated F12 approach. *J Chem Theory Comput*. 2018;14:5105–5117.
373. Řezáč J, Hobza P. Describing noncovalent interactions beyond the common approximations: How accurate is the ‘Gold Standard,’ CCSD(T) at the complete basis set limit? *J Chem Theory Comput*. 2013;9:2151–2155.
374. Kodrycka M, Holzer C, Klopper W, Patkowski K. Explicitly correlated dispersion and exchange dispersion energies in symmetry-adapted perturbation theory. *J Chem Theory Comput*. 2019;15:5965–5986.
375. Hättig C, Klopper W, Köhn A, Tew DP. Explicitly correlated electrons in molecules. *Chem Rev*. 2012;112:4–74.
376. Kong L, Bischoff FA, Valeev EF. Explicitly correlated R12/F12 methods for electronic structure. *Chem Rev*. 2012;112:75–107.
377. Manby FR. Density fitting in second-order linear-R12 Møller-Plesset perturbation theory. *J Chem Phys*. 2003;119:4607–4613.
378. Douglas M, Kroll NM. Quantum electrodynamical corrections to fine-structure of helium. *Ann Phys*. 1974;82:89–155.
379. Hess BA. Relativistic electronic-structure calculations employing a 2-component no-pair formalism with external-field projection operators. *Phys Rev A*. 1986;33:3742–3748.
380. Dyall KG. Interfacing relativistic and nonrelativistic methods. I. Normalized elimination of the small component in the modified Dirac equation. *J Chem Phys*. 1997;106:9618–9626.
381. Kutzelnigg W, Liu W. Quasirelativistic theory equivalent to fully relativistic theory. *J Chem Phys*. 2005;123:241102.
382. Cremer D, Zou W, Filatov M. Dirac-exact relativistic methods: The normalized elimination of the small component method. *WIREs Comput Mol Sci*. 2014;4:436–467.
383. Dolg M, Cao X. Relativistic pseudopotentials: Their development and scope of applications. *Chem Rev*. 2012;112:403–480.
384. Patkowski K, Szalewicz K. Frozen core and effective core potentials in symmetry-adapted perturbation theory. *J Chem Phys*. 2007;127: 164103.
385. Holzer C, Klopper W. Quasi-relativistic two-component computations of intermolecular dispersion energies. *Mol Phys*. 2017;115:2775–2781.
386. Wang F, Ziegler T, van Lenthe E, van Gisbergen S, Baerends EJ. The calculation of excitation energies based on the relativistic two-component zeroth-order regular approximation and time-dependent density-functional with full use of symmetry. *J Chem Phys*. 2005; 122:204103.
387. Baerends EJ, Ellis DE, Ros P. Self-consistent molecular Hartree-Fock-Slater calculations I. The computational procedure. *Chem Phys*. 1973;2:41–51.
388. Whitten JL. Coulombic potential energy integrals and approximations. *J Chem Phys*. 1973;58:4496–4501.
389. Schütz M, Lindh R, Werner HJ. Integral-direct electron correlation methods. *Mol Phys*. 1999;96:719–733.
390. Maurer SA, Beer M, Lambrecht DS, Ochsenfeld C. Linear-scaling symmetry-adapted perturbation theory with scaled dispersion. *J Chem Phys*. 2013;139:184104.
391. Parrish RM, Thompson KC, Martínez TJ. Large-scale functional group symmetry-adapted perturbation theory on graphical processing units. *J Chem Theory Comput*. 2018;14:1737–1753.
392. Feyereisen M, Fitzgerald G, Komornicki A. Use of approximate integrals in ab initio theory. An application in MP2 energy calculations. *Chem Phys Lett*. 1993;208:359–363.
393. Werner H, Manby FR, Knowles PJ. Fast linear scaling second-order Møller-Plesset perturbation theory (MP2) using local and density fitting approximations. *J Chem Phys*. 2003;118:8149–8160.
394. DePrince AE III, Sherrill CD. Accuracy and efficiency of coupled-cluster theory using density fitting/Cholesky decomposition, frozen natural orbitals, and a t_1 -transformed Hamiltonian. *J Chem Theory Comput*. 2013;9:2687–2696.

395. Hohenstein EG, Sherrill CD. Density fitting and Cholesky decomposition approximations in symmetry-adapted perturbation theory: Implementation and application to probe the nature of pi-pi interactions in linear acenes. *J Chem Phys.* 2010;132:184111.
396. Hohenstein EG, Sherrill CD. Density fitting of intramonomer correlation effects in symmetry-adapted perturbation theory. *J Chem Phys.* 2010;133:014101.
397. Hohenstein EG, Sherrill CD. Efficient evaluation of triple excitations in symmetry-adapted perturbation theory via second-order Moller-Plesset perturbation theory natural orbitals. *J Chem Phys.* 2010;133:104107.
398. Hohenstein EG, Parrish RM, Sherrill CD, Turney JM, Schaefer HF III. Large-scale symmetry-adapted perturbation theory computations via density fitting and Laplace transformation techniques: Investigating the fundamental forces of DNA-intercalator interactions. *J Chem Phys.* 2011;135:174107.
399. Parrish RM, Hohenstein EG, Sherrill CD. Tractability gains in symmetry-adapted perturbation theory including coupled double excitations: CCD+ST(CCD) dispersion with natural orbital truncations. *J Chem Phys.* 2013;139:174102.
400. Podeszwa R, Cencek W, Szalewicz K. Efficient calculations of dispersion energies for nanoscale systems from coupled density response functions. *J Chem Theory Comput.* 2012;8:1963–1969.
401. Weigend F. A fully direct RI-HF algorithm: Implementation, optimised auxiliary basis sets, demonstration of accuracy and efficiency. *Phys Chem Chem Phys.* 2002;4:4285–4291.
402. Weigend F, Köhn A, Hättig C. Efficient use of the correlation consistent basis sets in resolution of the identity MP2 calculations. *J Chem Phys.* 2002;116:3175–3183.
403. Hättig C. Optimization of auxiliary basis sets for RI-MP2 and RI-CC2 calculations: Core-valence and quintuple-zeta basis sets for H to Ar and QZVPP basis sets for Li to Kr. *Phys Chem Chem Phys.* 2005;7:59–66.
404. Jung Y, Sodt A, Gill PMW, Head-Gordon M. Auxiliary basis expansions for large-scale electronic structure calculations. *Proc Natl Acad Sci USA.* 2005;102:6692–6697.
405. Gubbels KB, van de Meerakker SYT, Groenenboom GC, Meijer G, van der Avoird A. Scattering resonances in slow NH₃-He collisions. *J Chem Phys.* 2012;136:074301.
406. Lamoureux G, Roux B. Modeling induced polarization with classical Drude oscillators: Theory and molecular dynamics simulation algorithm. *J Chem Phys.* 2003;119:3025–3039.
407. Jacobson LD, Herbert JM. An efficient, fragment-based electronic structure method for molecular systems: Self-consistent polarization with perturbative two-body exchange and dispersion. *J Chem Phys.* 2011;134:094118.
408. Herbert JM, Jacobson LD, Lao KU, Rohrdanz MA. Rapid computation of intermolecular interactions in molecular and ionic clusters: Self-consistent polarization plus symmetry-adapted perturbation theory. *Phys Chem Chem Phys.* 2012;14:7679–7699.
409. Lao KU, Herbert JM. Accurate and efficient quantum chemistry calculations for noncovalent interactions in many-body systems: The XSAPT family of methods. *J Phys Chem A.* 2015;119:235–252.
410. Xie W, Gao J. Design of a next generation force field: The X-POL potential. *J Chem Theory Comput.* 2007;3:1890–1900.
411. Xie W, Song L, Truhlar DG, Gao J. The variational explicit polarization potential and analytical first derivative of energy: Towards a next generation force field. *J Chem Phys.* 2008;128:234108.
412. Khalil RZ, Head-Gordon M, Bell AT. An efficient self-consistent field method for large systems of weakly interacting components. *J Chem Phys.* 2006;124:204105.
413. Breneman CM, Wiberg KB. Determining atom-centered monopoles from molecular electrostatic potentials. The need for high sampling density in formamide conformational analysis. *J Comput Chem.* 1990;11:361–373.
414. Bates DM, Tschumper GS. CCSD(T) complete basis set limit relative energies for low-lying water hexamer structures. *J Phys Chem A.* 2009;113:3555–3559.
415. Wang Y, Babin V, Bowman JM, Paesani F. The water hexamer: Cage, prism, or both. Full dimensional quantum simulations say both. *J Am Chem Soc.* 2012;134:11116–11119.
416. Lao KU, Herbert JM. A simple correction for nonadditive dispersion within extended symmetry-adapted perturbation theory (XSAPT). *J Chem Theory Comput.* 2018;14:5128–5142.
417. Carter-Fenk K, Lao KU, Liu KY, Herbert JM. Accurate and efficient *ab initio* calculations for supramolecular complexes: Symmetry-adapted perturbation theory with many-body dispersion. *J Phys Chem Lett.* 2019;10:2706–2714.
418. Tkatchenko A, DiStasio RA Jr, Car R, Scheffler M. Accurate and efficient method for many-body van der Waals interactions. *Phys Rev Lett.* 2012;108:236402.
419. Liu KY, Carter-Fenk K, Herbert JM. Self-consistent charge embedding at very low cost, with application to symmetry-adapted perturbation theory. *J Chem Phys.* 2019;151:031102.
420. Rob F, Podeszwa R, Szalewicz K. Electrostatic interaction energies with overlap effects from a localized approach. *Chem Phys Lett.* 2007;445:315–320.
421. Rob F, Misquitta AJ, Podeszwa R, Szalewicz K. Localized overlap algorithm for unexpanded dispersion energies. *J Chem Phys.* 2014;140:114304.
422. Sedlak R, Řezáč J. Empirical D3 dispersion as a replacement for ab initio dispersion terms in density functional theory-based symmetry-adapted perturbation theory. *J Chem Theory Comput.* 2017;13:1638–1646.
423. Shahbaz M, Szalewicz K. Evaluation of methods for obtaining dispersion energies used in density functional calculations of intermolecular interactions. *Theor Chem Acc.* 2019;138:25.

424. Bukowski R, Cencek W, Jankowski P, et al. *SAPT2016: An ab initio program for many-body symmetry-adapted perturbation theory calculations of intermolecular interaction energies*. Newark, Delaware: University of Delaware and University of Warsaw; 2016. Retrieved from <http://www.physics.udel.edu/~szalewic/SAPT/SAPT.html>.
425. Shao Y, Gan Z, Epifanovsky E, et al. Advances in molecular quantum chemistry contained in the Q-Chem 4 program package. *Mol Phys*. 2015;113:184–215.

How to cite this article: Patkowski K. Recent developments in symmetry-adapted perturbation theory. *WIREs Comput Mol Sci*. 2020;10:e1452. <https://doi.org/10.1002/wcms.1452>